"I am among those who think that science has great beauty. A scientist in his laboratory is not only a technician: he is also a child placed before natural phenomena which impress him like a fairy tale."

Marie Curie (1867-1934)

Gating kinetics of CNG channels studied with cyclic nucleotide-concentration jumps

Dissertation

zur Erlangung des akademischen Grades
doctor rerum naturalium
(Dr.rer.nat.)

vorgelegt dem Rat der Biologisch-Pharmazeutischen Fakultät
der Friedrich-Schiller-Universität Jena

von

Dipl.-Biochemikerin Vasilica Nache
geb. am 15.02.1978 in Bacau, Rumänien

Gutachter: 1. .....

2. .....

3. .....

Tag der öffentlichen Verteidigung: .....

Zusammenfassung

Durch zyklische Nukleotide gesteuerte Kanäle (CNG-Kanäle) (Kaupp et al., 1989) sind unspezifische Kationenkanäle, die u.a. die Lichttransduktion in Photorezeptoren und die chemische Transduktion in olfaktorischen Zellen vermitteln (Finn et al., 1995; Zimmerman, 1995; Kaupp und Seifert, 2002). Die Kanäle öffnen nach Bindung zyklischer Nukleotide (CN) an eine spezielle CN-Bindungsdomäne am C-Terminus (Kaupp und Seifert, 2002). CNG-Kanäle sind Heterotetramere, zusammengesetzt aus vier Untereinheiten, die sich um eine zentrale Pore anordnen. Jede Untereinheit besteht aus sechs Transmembrandomänen. N- und C-Terminus befinden sich intrazellulär und sind für zytosolische Modulatoren zugänglich (Matulef und Zagotta, 2003). Der native olfaktorische CNG-Kanal setzt sich aus drei Typen von Untereinheiten zusammen: CNGA2, CNGA4, CNGB1b (Bönigk et al., 1999, Bradley et al., 1994), die im Verhältnis 2 : 1 : 1 vorliegen (Zheng und Zagotta, 2004). Während die CNGA2-Untereinheit bei heterologer Expression allein in der Lage ist, funktionelle homotetramere Kanäle zu bilden, assemblieren CNGA4- und CNGB1b-Untereinheiten nur zusammen mit CNGA2-Untereinheiten. Die CNGA4- und CNGB1b-Untereinheiten sind für eine Reihe physiologischer Eigenschaften heterolog exprimierter Kanäle verantwortlich, die in ähnlicher Weise auch bei nativen olfaktorischen Kanälen beobachtet wurden (Bönigk et al., 1999; Bradley et al., 2001; Sautter et al., 1998).

Auf molekularer Ebene ist bisher nicht verstanden, in welcher Weise die Bindung der Liganden an die vier Untereinheiten zur Öffnung des Kanals führt und, im Falle der heteromeren Kanäle, welche Rolle den verschiedenen Untereinheiten im Aktivierungsmechanimus zukommt. Weiterhin ist unbekannt, ob die Aktivierung von unabhängigen Schaltvorgängen innerhalb der individuellen Untereinheiten verursacht wird oder von aufeinander abgestimmten kooperativen Interaktionen zwischen den Untereinheiten.

Um einen besseren Einblick in das Schalten olfaktorischer CNG-Kanäle zu erhalten, wurde die Aktivierung von CNGA1 bzw. CNGA2-Kanälen bei depolarisierenden Spannungssprüngen in Gegenwart verschiedener Ligandenkonzentrationen und bei sprunghaften Änderungen der Ligandenkonzentration bei konstanter Spannung untersucht.

Der Konzentrationssprung wurde durch die Photolyse „gecageter“ zyklischer Nukleosidmonophosphate (cNMPs) ermöglicht. Dabei wurden substituierte Coumarinyl-methylester von cGMP und cAMP verwendet (Hagen et al., 2001). Die Untersuchungen an

CNGA2-Kanälen zeigten, dass bei vergleichbarem Aktivierunsgrad der Aktivierungszeitverlauf homotetramerer Kanäle nach Applikation des Liganden cGMP bzw. cAMP keine Unterschiede aufweist. Auch zwischen homomeren und heteromeren Kanälen konnten nach Aktivierung mit dem gleichen zyklischen Nukleotid keine Unterschiede festgestellt werden. Anhand von Chimären aus CNGA1-Untereinheiten der Photorezeptoren und CNGA2-Untereinheiten der olfaktorischen Neurone des Rindes konnte gezeigt werden, dass sowohl Transmembranregionen als auch intrazelluläre Bestandteile des Kanals an der Kontrolle des Aktivierungszeitverlaufes beteiligt sind.

Das Schaltverhalten von CNG-Kanälen wurde bisher mit Hilfe verschiedener kinetischer Modelle beschrieben. Lineare Zustandsmodelle setzen vorraus, dass der Kanal zum öffnen voll ligandiert sein muss (Karpen et al., 1988; Gordon und Zagotta, 1995; Varnum et al., 1995). Allosterische Modelle dagegen erlauben Öffnungen auch im teilligandierten Kanal (Goulding et al., 1994; Varnum und Zagotta, 1996). Bei Analyse des Aktivierungszeitverlaufes homotetramerer Kanäle nach Ligandenkonzentrationssprüngen erwiesen sich Modelle mit äquivalenten Bindungsstellen für eine Beschreibung des Kanalverhaltens als nicht geeignet (Monod-Wyman-Changeaux-Modell, Coupled-Dimer-Modell). Das hier vorgestellte Modell schlägt eine hoch kooperative Bindung von drei Liganden vor: Sowohl bei cGMP als auch bei cAMP ist die Bindungssgeschwindigkeit des ersten und dritten Bindunggschrittes zwei bis drei Größenordnungen höher als die des zweiten Bindungsschrittes. Die geringere halbmaximale cGMP-Konzentration (EC_{50}) für cGMP im Vergleich zu cAMP wird vor allem durch eine schnellere Geschwindigkeit aller drei Bindunggsschritte verursacht.

Gating kinetics of CNG channels studied with cyclic nucleotide-concentration jumps

Dissertation

for acquiring a
Doctor rerum naturalium
academic degree

Presented to the Faculty of Biology and Pharmacy
Friedrich Schiller University Jena

by
Dipl.-Biochemist Vasilica Nache
born on 15.02.1978 in Bacau, Romania

Summary

Cyclic nucleotide-gated (CNG) channels (Kaupp et al., 1989) are non-specific cation channels, which mediate e.g. phototransduction in photoreceptors and chemotransduction in olfactory cells (Finn et al., 1995; Zimmerman, 1995; Kaupp and Seifert, 2002). The channels are opened when cyclic nucleotides bind to a domain in the C-terminus (Kaupp and Seifert, 2002). CNG channels are heterotetramers composed of four subunits distributed around a centrally located pore. Each subunit contains six transmembrane segments with intracellular amino- and carboxy-terminal domains that are accessible to cytosolic modulators (Matulef and Zagotta, 2003). Native olfactory CNG channels are composed of three types of subunits: CNGA2, CNGA4, CNGB1b (Bönigk et al., 1999; Bradley et al., 1994) in the ratio 2:1:1 (Zheng and Zagotta, 2004). Whereas the CNGA2 subunit can form functional homotetrameric channels when expressed in a heterologous system, the CNGA4 and CNGB1b subunits produce functional channels only together with CNGA2 as part of heterotetrameric channels. However, when expressed with CNGA2, CNGA4 and CNGB1b subunits confer a number of important physiological properties on the heterotetrameric channel which closely mirror the properties of native olfactory channels (Bönigk et al., 1999; Bradley et al., 2001; Sautter et al., 1998).

Presently it is not known how the binding of the ligands to the four subunits is translated to channel opening and, in the case of heterotetrameric channels, what is the role of the different subunits in the activation mechanism. Furthermore, it is still unclear whether activation depends on independent gating reactions within the individual subunits of the channel or on a concerted, cooperative interaction among the subunits.

To gain better insight into the conformational changes associated with the gating of ion channels, activation of CNGA1 and CNGA2 channels in response to a depolarizing voltage jump at different ligand concentrations and also in response to a ligand concentration jump at a constant voltage was studied.

The concentration jump was obtained by flash photolysis of caged cNMPs (cyclic nucleoside monophosphate). Using this method, we took advantage of the superior characteristics of the substituted coumarinylmethyl esters of cGMP and cAMP (Hagen et al., 2001).

For CNGA2 channels we showed that at equal degree of activation, the activation time course of homotetrameric channels was similar with cGMP and cAMP and it was also similar in homo- and heterotetrameric channels with the same cyclic nucleotide. Using

chimeric channels constructed between the CNGA1 subunit of the CNG channel from bovine retinal photoreceptors and the CNGA2 subunit of the CNG channel from olfactory sensory neurons, it was shown that both transmembrane and intracellular channel regions control the activation time course of the CNG channels.

Kinetic models used to describe the gating of CNG channels assume either that the channel has to be fully liganded to open (linear state models) (Karpen et al., 1988; Gordon and Zagotta, 1995; Varnum et al., 1995) or that opening may already occur in the partially liganded channel (allosteric models) (Goulding et al., 1994; Varnum and Zagotta, 1996).

Analysis of the activation time courses of homotetrameric channels in response to a ligand concentration jump with previously used kinetic schemes rules out the favored models with equivalent binding sites: the Monod-Wyman-Changeux model and the Coupled-Dimer model. Herein, a kinetic model is suggested, which assumes a highly cooperative binding of three ligands: With both cGMP and cAMP, the binding rate of the first and third binding event is two to three orders of magnitude faster than that of the second binding event. Moreover, the lower half maximum cGMP concentration (EC_{50}) for cGMP than cAMP is mainly caused by a faster rate of all three binding events. In addition, the three binding steps are significantly faster with cGMP than with cAMP.

Contents

1. Introduction

1.1. Cyclic nucleotide-gated channels

Many cellular processes rely upon the passive diffusion of ions through biological membranes. Cell membranes are constituted of a lipid bilayer that represents an enormous energy barrier for the movement of small ions across it. During evolution, a class of proteins, known as *ion channels*, has evolved in order to facilitate ion movements between the intracellular and extracellular aqueous compartments. These proteins are integrally embedded in the membrane, spanning the lipid bilayer to provide an expeditious and selective pathway for ions to cross down their electrochemical gradient. Despite their high selectivity, ion channels conduct ions at extremely high rates (10^6-10^9 ions per channel and second). Ion channels are not simply open holes of different diameter, since channels that allow the passage of one type of ion do not allow the passage of other types of ions, larger or smaller. Ion channels can be classified with respect to the best permeating ion.

Ion channels are widely distributed throughout the biological world appearing in membranes of excitable and non-excitable animal cells, prokaryotes, protozoa, and plant cells. Although ion channels share a common function allowing the passage of ions through the plasma membrane, they also specifically respond to stimuli that induce the opening (activation) of the permeation pathway in a process called “gating”. Gating can be regulated by various stimuli including the membrane voltage, the concentration of extracellular or intracellular ligands, or membrane stretch.

Cyclic nucleotide-gated (CNG) channels open by the direct binding of cyclic nucleotides, 3’,5’-cyclic guanosine monophosphate (cGMP) and 3’,5’-cyclic adenosine mono-phosphate (cAMP). Although their activity shows very little voltage dependence, CNG channels belong to the superfamily of voltage-gated ion channels along with so-called hyperpolarization-activated and cyclic nucleotide gated (HCN) pacemaker channels, the ether-a-gogo (EAG) and human eag-related gene (HERG) family of voltage-activated K^+ channels, and several plant K^+ channels (KAT, AKT, KST channels) (Kaupp and Seifert, 2002).

CNG channels are nonselective cation channels that do not discriminate well between alkali ions. They are also permeable for divalent cations, in particular Ca^{2+} (Menini et al.,

1988; Cervetto et al., 1988; Hodgkin et al., 1985). The Ca^{2+}permeability of CNG channels is a very important part of their cellular function.

CNG channels, unlike other ligand-gated channels, do not desensitize in the continued presence of the ligand. The activity of CNG channels is modulated by Ca^{2+}/calmodulin and by phosphorylation/dephosphorylation (Gordon et al., 1992).

CNG channels were first discovered in the plasma membrane of the outer segment of vertebrate rod photoreceptors (Fesenko et al., 1985). In short time similar channels were identified in cone photoreceptors (Haynes and Yau, 1985) and chemosensitive cilia of olfactory sensory neurons (OSNs) (Nakamura and Gold, 1987).

Molecular cloning of CNG channels became possible when the channel protein was purified and identified by functional reconstitution into artificial liposomes and lipid bilayers (Cook et al., 1986; Hanke et al., 1988). The first molecular identification of a CNG channel was a milestone in scientific progress. Within a few years, CNG channels have been identified in other tissues types, such as: aorta, heart (Biel et al., 1993, 1994), pineal gland (Dryer and Henderson, 1991; Distler et al., 1994), kidney (Biel et al., 1994), sperm (Biel et al., 1994; Weyand et al., 1994), and brain (Leinders-Zufall et al., 1995; Bradley et al., 1997).

In 1991, the first CNG channels in invertebrates were identified in ventral photoreceptors of *Limulus* (Bacigalupo et al.) and in insect antennae (Zufall and Hatt). In addition, in 1991, cAMP-specific channels are electrophysiologically observed in larval muscle of *Drosophila* (Delgado et al.). In 1994, Baumann et al., characterized a CNG channel present in eyes and antennae of *Drosphila* and in 1996, Komatsu et al. identified a CNG channel in *Caenorhabditis elegans.* In 1999, the first CNG channel from plants (*Arabidopsis*) was described by Leng et al..

1.2. Physiological importance of cyclic nucleotide-gated channels

CNG channels are highly specialized membrane proteins that open an ion-permeable pore across the membrane in response to the direct binding of intracellular cyclic nucleotides. By controlling the flow of specific ions across the lipid bilayer, CNG channels play important roles in the sensory transduction. In both, phototransduction and olfactory transduction, CNG channels transform the external sensory stimuli into electrical signals. CNG channels mediate the generation of an electrical response to light in rods and cones of

vertebrate retina. The rod photoreceptors contain the visual pigment - rhodopsin and are used for vision under dark-dim conditions at night. The cone photoreceptors contain opsins as their visual pigments and, are the basis of color perception in our visual image.

In the dark, the binding of cGMP to the CNG channels causes the channels to open, allowing Na^+ and Ca^{2+} to flow into the cell. This flow of inward current, the dark current, depolarizes the rod outer segment. When light hits the retina, it activates a phototransduction cascade (Figure 1a). The detection of light is carried out on the membrane disks in the outer segment of rod. These disks contain thousands of molecules of rhodopsin. Visual transduction begins with the absorption of a photon of light by 11-*cis* retinal. This absorption activates rhodopsin to bind and activate the G protein transducin, stimulating GTP-GDP exchange. Upon binding of GTP, transducin binds to and activates a phosphodiesterase that hydrolyzes cGMP to 5`-GMP. The CNG channels in the plasma membrane close in direct response to this decrease in cGMP, inhibiting the dark current, and hence hyperpolarizing the rod photoreceptors. This hyperpolarization causes a decrease in the tonic release of the neurotransmitter glutamate from the presynaptic terminals.

The sensitivity of the rod CNG channel has been optimized to detect and signal the drop in cGMP concentration resulting from the absorption of a single photon of light (Baylor et al., 1979). The channel's relatively low affinity for cGMP leads to a fast off rate for the ligand and allows the channel to close quickly in response to light (Cobbs and Pugh, 1987). In addition, the closure of CNG channels reduces the cytoplasmic Ca^{2+} concentration (Yau and Nakatani, 1985). This decrease in Ca^{2+} provides negative feedback in the phototransduction cascade by stimulating cGMP synthesis, increasing the channel affinity for cGMP, reducing the catalytic rhodopsin activity produced by light and accelerating rhodopsin deactivation by phosphorylation.

CNG channels play a similarly important role in the olfactory transduction, where they cause the cells to depolarize in response to increased concentration of cAMP (Figure 1b). Vertebrate olfactory receptors are cells that have sensory cilia projecting from the olfactory epithelium into the mucus of the nasal cavity, and extend axons to the olfactory bulb. The odorant molecules first activate a subset of receptor protein that couple via a G protein to the adenylyl cyclase. This causes an increase in intracellular cAMP in the olfactory cells, which activates cyclic nucleotide-gated channels from the olfactory cilia. In the presence of normal physiological extracellular Ca^{2+}, the second messengers (cAMP) elicit the opening of the channel, allowing Ca^{2+} to flow in. The increase in the intracellular Ca^{2+}

concentration appears to activate a Cl^- current that helps to depolarize the olfactory cell. Thus, the cyclic nucleotide-gated channels plus the Ca^{2+}-dependent Cl^- current results in the signal transduction (Lowe and Gold, 1993).

In addition to their role in primary sensory transduction, CNG channels are thought to be important in a variety of other physiological processes. In the retina, for example, CNG channels have been implicated in nitric oxide signaling (Ahmad et al., 1994). The *tax-2* and *tax-4* genes in the nematode *Caenorhabditis elegans*, which encode proteins that are closely related to the α and β subunits of CNG channels, where shown to be essential for formation of the appropriate synaptic connections between chemosensory neurons and the nerve ring (Coburn and Bargmann, 1996; Komatsu et al., 1996). In addition, Ca^{2+} imaging studies found that a rise in intracellular Ca^{2+} in hippocampal neurons could result from elevated intracellular cyclic nucleotide concentrations, suggesting that CNG channels play a role in the synaptic plasticity underlying learning and memory (Bradley et al., 1997).

Although the function of CNG channels has been firmly established in retinal photoreceptors and in OSNs, their role in other cells is not completely understood.

a

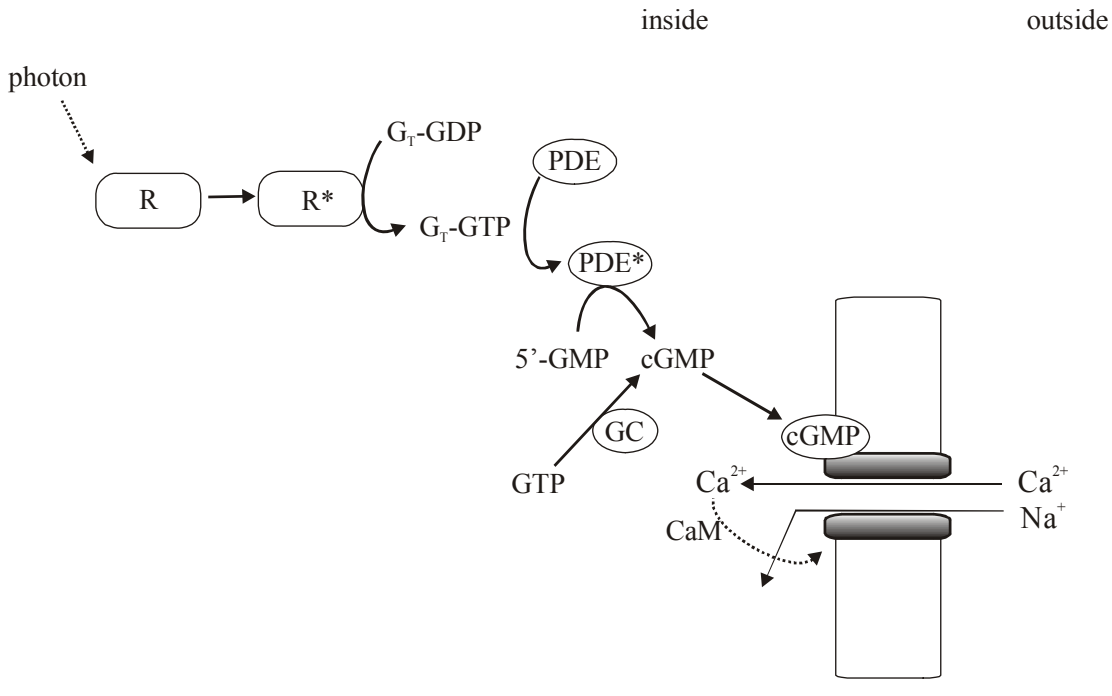

Rod CNG channel

b

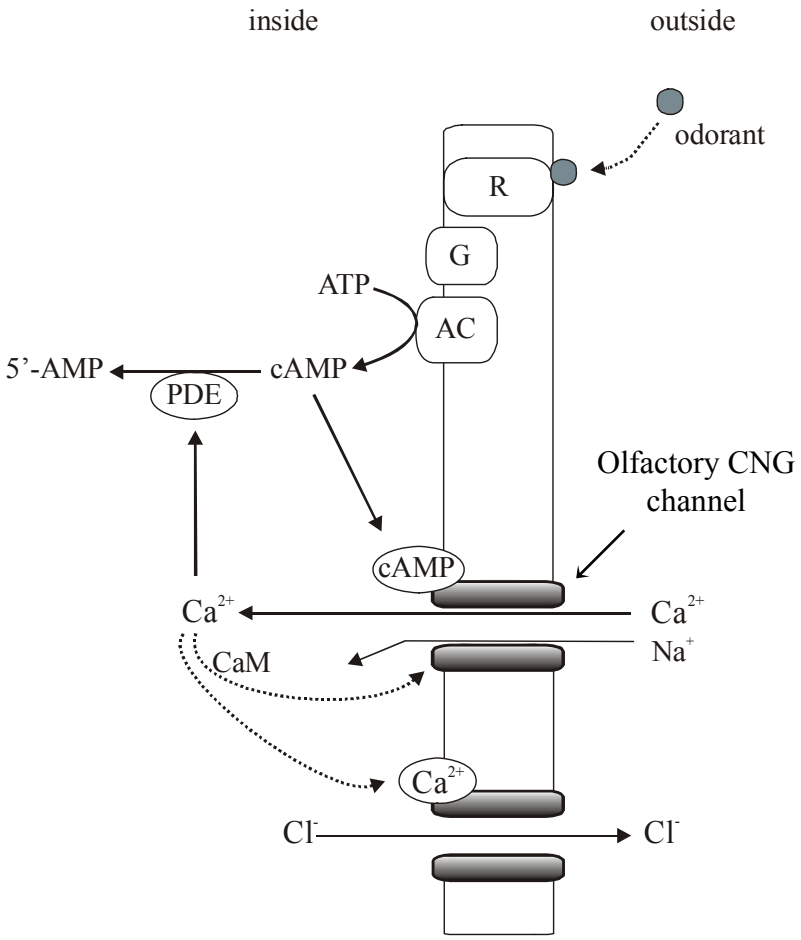

Figure 1. Signal transduction in sensory cells. (a) Top, the enzymatic cascade in rod photoreceptor cells operates through cGMP. Negative feedback is through Ca^{2+} ions via a Ca^{2+}/CaM-dependent component (dotted arrow). R and R*, resting and active receptor; G_T, transducin; GC, guanylate cyclase. (b) Bottom, the enzymatic cascade in olfactory sensory neurons that underlies olfactory transduction operates through cAMP. Ca^{2+} ions mediate negative feedback (dotted arrow) through calmodulin (CaM). R, olfactory receptor; G, G-protein; AC, adenylyl cyclase; PDE, phosphodiesterase.

1.3. Structure of cyclic nucleotide-gated channels

In vertebrates, six members of the CNG channel gene family have been identified. These genes are grouped according to sequence similarity into two subtypes, CNGA and CNGB (Bradley et al., 2001). Important functional features of these channels, such as ligand sensitivity and selectivity, ion permeation, and gating, are determined by the subunit composition of the respective channel complex.

The first cDNA clone for a subunit of a CNG channel (CNGA1) was isolated from bovine retina (Kaupp et al., 1989). CNGA1 was expressed in rod photoreceptors and produced functional channels that were gated by cGMP when expressed exogenously in *Xenopus* oocytes. Later, a second subunit of the rod CNG channel (CNGB1) was isolated and cloned (Chen et al., 1993). The CNGB1 subunit expressed alone does not produce functional CNG channels, but coexpression of CNGA1 and CNGB1 subunit yields heterotetrameric channels with characteristics similar to those of native channels (Chen et al. 1993; Körschen et al., 1995). In the last years, studies using a combination of different approaches show that native CNG channels from rod photoreceptors are composed of three CNGA1 subunits and one CNGB1 subunit (Weitz et al., 2002; Zheng et al., 2002).

Native olfactory channels are composed of three different subunits: CNGA2 (Dhallan et al., 1990), CNGA4 (Bradley et al., 1994; Liman and Buck, 1994) and CNGB1b (Bönigk et al., 1999; Picco et al., 2001; Sautter et al., 1998). The subunit stoichiometry (CNGA2: CNGA4: CNGB1b) is thought to be 2×CNGA2: 1×CNGA4: 1×CNGB1b (Zheng and Zagotta, 2004). CNGA4 and CNGB1b subunits do not form functional channels when expressed alone. The CNGA2 subunit forms functional homotetrameric CNG channels but lack some properties of the native channels (Bönigk et al., 1999).

CNG channel subunits share the same basic architectural plan, four subunits arranged around a centrally located pore (Gordon and Zagotta, 1995; Liu et al., 1996). Each subunit contains six transmembrane segments (S1-S6), a pore region situated between S5 and S6, and a cyclic nucleotide binding domain (cNBD) in the C-terminus that is connected via the C-linker region to the S6 segment (Figure 2) (Henn et al., 1995; Kaupp et al., 1989, Liu et al., 1996; Molday et al., 1991; Wohlfart et al., 1992).

These structural motifs are also seen in several voltage-dependent potassium channels including HCN channels (Ludwig et al., 1998).

The S4 segment in CNG channels resembles the voltage-sensor motif found in the S4 segment of voltage-gated K^+, Na^+, and Ca^{2+} channels. The significance of the S4 segment in CNG channels is still unknown, as the channels show very little voltage dependence.

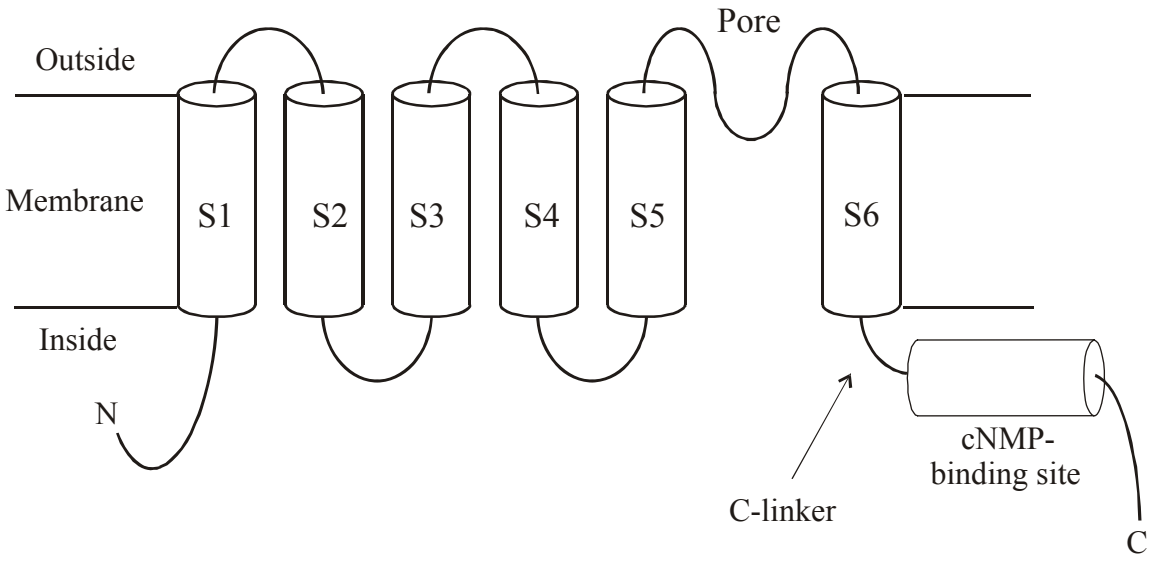

Figure 2. Structural cartoon of a CNG channel subunit. The N-terminal region, the C-linker, the cyclic nucleotide-binding domain and the C-terminal region are situated on the intracellular side of the membrane. The cylinders (S1-S6) indicate the transmembrane segments. The channel pore is situated between S5 and S6.

The CNG channel pore is thought to be structurally similar to those of other P-loop containing ion channels. The basic architectural plan for the pore of this family of channels was revealed by the crystal structure of a KcsA, a bacterial potassium channel from *Streptomyces lividans* (Doyle et al., 1998). To open the pore, a conformational change is thought to occur in its narrow part. An open channel conformation was revealed in 2002 by the crystal structure of another ion channel, the MthK channel (Jiang et al., 2002). MthK is structurally similar to KcsA in the P-loop but has a different conformation of the inner helix. Pore-lining 'inner' helices contain a 'gating hinge' that bends by approximately 30 degrees. In a straight conformation, four inner helices form a bundle, closing the pore near its intracellular surface. In a bent configuration, the inner helices stay open creating a wide (12Å) entryway. Aminoacid conservation among a wide range of P-loop containing channels suggests that the KcsA and MthK structures may serve as general models for the closed and open state conformations for this entire family of ion channels.

Studies on the structure of the CNG channel pore yielded heterogeneous results. Flynn and Zagotta (2001) suggest that the cytoplasmatic opening of the CNG channel pore is narrow when channels are closed and widens when channels open. Substituting a cysteine at the cytoplasmatic end of the S6 in a cysteine-free variant of CNGA1 channels promoted a channel closure by the spontaneous formation of an intersubunit disulfide bound (Flynn

and Zagotta, 2001). Because the disulfide bounds are formed between cysteine residues 5Å apart (Careaga and Falke, 1992), this result is consistent with a narrow cytoplasmatic opening and the occurrence of a helix bundle similar to the one in KcsA.

The study by Sun et al. (1996) suggested that the structure of the CNG channel pore is significantly different from that of the K^+ channels. The authors suggest that the P loop forms a thin blade that extends almost parallel to the surface of the membrane toward the central axis and that this irislike structure serves as both gate and selectivity filter. Using the substituted cysteine accessibility method, other studies (Becchetti et al., 1999) observed only slight differences in the accessibility map between pores of K^+ channels and CNG channels. There are several pieces of evidence for conformational changes in the pore of CNG channels associated with gating: (1) mutations in the selectivity filter have large effects on gating (Bucossi et al., 1996; Gavazzo et al., 2000); (2) CNG channels that are partially activated produce different single-channel currents compared to fully activated channels (Hackos and Korenbrot, 1999; Ruiz and Karpen, 1997; Kusch et al., 2004); (3) Cysteine-scanning mutagenesis studies suggest that the pore helix, near the selectivity filter, undergoes a conformational change during channel activation (Becchetti et al., 1999, Liu and Siegelbaum, 2000).

The cyclic nucleotide-binding domain (CNBD) of CNG channels shares sequence similarity with other cyclic nucleotide-binding proteins including cGMP- and cAMP-dependent protein kinases (PKG and PKA) and the *Escherichia coli* catabolite gene activator protein (CAP). The crystal structure of CAP, containing three α-helices and eight β-strands (McKay and Steitz, 1981), has been used as a model for the ligand-binding domains of CNG channels. Altenhofen et al. (1991) showed that in the CNBD of CNGA1 channels a threonine residue at position 560 plays an important role in determining the ligand specificity.

The C-linker appears to be important for the allosteric opening transition. Residues in the C-linker have been shown to be responsible for modulation of CNG channels by transition metals including: Ni^{2+}, Zn^{2+} (Gordon and Zagotta, 1995; Karpen et al., 1993). In addition, differences between gating of CNGA3 and CNGA2 channels have been attributed to three amino acids in the C-linker (Zong et al., 1998). On the other hand, the N-terminal region has also been found to affect the gating of CNG channels (Gordon and Zagotta, 1995; Gordon et al., 1997; Möttig et al., 2001). It has also been shown that N-terminal region of CNGA2 channels interacts via a CaM-binding site with the cNMP-binding domain in the C-terminal region (Varnum and Zagotta, 1997). This interaction lowers the change in free

energy between the unliganded open and closed states. Binding of CaM interferes with this interaction and thereby increases the EC_{50} of activation. This allosteric control seems to be less important for the CNGA1 channels (Bradley et al., 2001, 2004).
Further work is needed for describing how the movements of the cNMP-binding domain, the C-linker and of the pore helix interact.

1.4. Kinetic models

Two of the central questions concerning ion channel function are: what is the nature of the conformational changes that occur during channel activation and how do the individual subunits of a multi-subunit channel interact? These questions are not unique for ion channels. They are also relevant for other enzymes composed of multiple identical subunits.
The minimum gating model of CNG channels comprises the binding of *n* ligands, which promotes a conformational change, resulting in channel opening (Li et al., 1997). These processes can be described by kinetic models.
Sequential type models assume the binding of *n* molecules of a cyclic nucleotide to the closed channel (C), followed by a gating conformational change of the fully liganded channel to the open configuration (O). Because of the tetrameric structure of CNG channels, it seems to be reasonable to assume a four-site sequential model (Scheme 1). The binding of a ligand to each subunit is described by the binding rate constant k_1 and the reverse reaction by k_2. The gating transition to the open configuration is characterized by the rate constants k_3 and k_4.

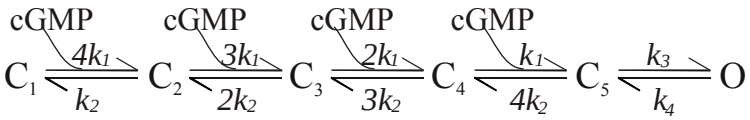

(Scheme 1)

This model predicts that a limiting slope of four will characterize the dose-response relationship. However, Ruiz et al. (1999) show that the dose-response relationship from single-channel recordings is considerably steeper than the one obtained from macroscopic currents suggesting that heterogeneous properties of individual single channel contribute to

the less steep dose-response relationship in macroscopic currents. Using jumps in cGMP concentration and voltage, Karpen et al. (1988) used a three-site sequential model to describe the kinetics of channel activation. In addition, a two-site sequential model was used by Gordon and Zagotta (1995) and Varnum et al. (1995) to describe some of the differences in CNG channel subfamilies related to ligand sensitivity and selectivity.

In the linear state models, the unliganded and partially liganded channels do not open. However, CNG channels were shown to open already in the absence of any activating ligand (Picones and Korenbrot, 1995; Tibbs et al., 1997). These results favor cyclic allosteric models, as originally proposed for allosteric enzymes (Monod et al., 1965). The Monod-Wyman-Changaux (MWC) model was first proposed by Stryer (1987) to describe the activation of CNG channels of retinal photoreceptors. The allosteric models assume that the binding sites of the four subunits are equivalent and that the ligand affinity is higher in the open than in the closed states by an allosteric factor *f* (Li et al., 1997). The stability of the open configuration is enhanced by a factor *f* each time an additional ligand molecule binds to the channel (Scheme 2).

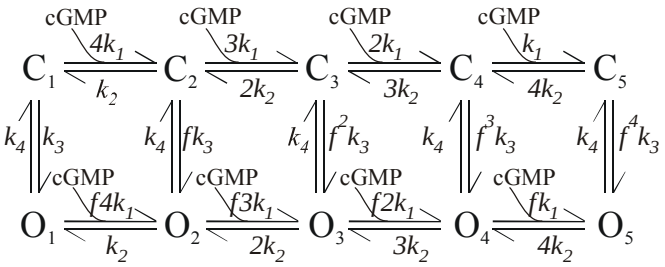

(Scheme 2)

k_1 and k_2 are the equilibrium constants for binding of the ligands to the open (O) and closed states (C). k_3 and k_4 represent the equilibrium constants between the closed and the open state.

However, when locking either one, two, three, or four cGMP molecules onto their binding sites to a CNGA1 channel by a photoaffinity technique (Ruiz and Karpen, 1997), the open probabilities for the partially liganded channels were not in the ratios predicted by the MWC model. Moreover, when coexpressing CNGA1 subunits and mutated CNGA1 subunits with disabled binding sites, the ratios of the open probabilities for the partially liganded channels were neither consistent with those determined with covalently locked cyclic nucleotides nor with the predictions of the MWC model (Liu et al., 1998). The

authors of this study proposed therefore a variation of the MWC model in which the channel is composed of a pair of dimers (Coupled-Dimer model).
In contrast to the assumption of binding to equivalent sites, the gating of single wild-type CNGA2 channels has been shown to support cooperative binding: One or two ligands bind to the closed channel and a further ligand can bind to the open channel (Li and Lester, 1999). Most noticeable is that, despite the assembly of four subunits in homotetrameric channels, only two or three ligands were needed to describe the single-channel activity.
These conflicting results reveal that fundamental issues upon the gating of CNG channels are still waiting to be discovered.

1.5. Flash photolysis of caged compounds

Better insight into the conformational changes associated with the activation of ion channels can be gained when studying current under non-steady state conditions, by changing a gating stimulus in a step like fashion and analyzing the relaxation kinetics of the current. The adequate gating stimulus for the activation of CNG channels is a step-like increase of the ligand concentration. This rapid increase of the cyclic nucleotide (CN) concentration is achieved in an elegant manner by using caged compounds. These compounds are molecules whose biological activity has been disabled by chemical modification. Photolysis cleaves the modifying group, thereby rapidly releasing the active cyclic nucleotide. The response induced by the instantaneous photolytic flash is more reliable in reflecting the kinetics of activation than from the single-channel analysis.
To be useful the caged cyclic nucleotides must meet specific requirements: they should be biologically inert, dissolve well in aqueous solutions, resistant toward solvolysis, display high photoefficiencies, and allow for a faster photochemical reaction releasing the cyclic nucleotide compared to the time course of channel activation (Kaplan and Somlyo, 1989). In addition, photolysis must not generate toxic side products. Suitable derivatives, which meet these criteria, are the substituted coumarinylmethyl esters of cNMPs (Hagen et al., 2001).
Caged cyclic nucleotides have been first synthesized and physiologically tested by Korth and Engels (1979) and successfully employed in photolysis experiments to study a cAMP-dependent slow Ca^{2+} current in the heart (Nargeot et al., 1983; Nerbonne et al., 1984).

In 1988, Karpen and coworkers were the first who studied the activation kinetics of the cGMP-gated channel from rod photoreceptor cells with the caged CN 4,5-dimethoxy-2-nitrosobenzaldehyde ester of cGMP. However, non-ideal physicochemical properties of this compound and great variability of the data prevented a more thorough quantitative analysis of the activation kinetics.

Over the last years, caged cNMP were used to study the signaling pathways in olfactory sensory neurons (OSNs) (Lowe and Gold, 1993), the Ca^{2+} permeability of CNG channels in intact rods and cones and OSNs (Dzeja, et al., 1999; Ohyama, et al., 2000), the desensitization of the olfactory CNG channel by Ca^{2+}/Calmodulin (Bradley, et al., 2001) and the cyclic nucleotide-stimulated Ca^{2+} entry in mammalian spermatozoa (Wiesner, et al., 1998).

2. Materials and Methods

2.1. Molecular biology

The experiments were performed on bovine CNGA1 (Kaupp et al., 1989) (accession number: X51604), CNGA2 channels (Dhallan et al., 1990; Ludwig et al., 1990) (accession numbers: 51604 and 55010) and on mixture of cRNAs from rat CNGA2 (Dhallan et al., 1990), CNGA4 (Bradley et al., 1994) and CNGB1b (Bönigk et al., 1999) of 2:1:1 (accession numbers: AF 126808, U 12623, and AF 068572). The rat CNG channel subunits used in this study were kindly provided by Prof. U. B. Kaupp (Forschungzentrum Jülich, Germany).

Also, a CNGA2 chimera with CNGA1 N-terminus (r1o; M_1-D_{157} from CNGA1, P_{135}-P_{663} from CNGA2), and a CNGA1 chimera with CNGA2 N-terminus (o1r; M_1-P_{134} from CNGA2, P_{158}-D_{690} from CNGA1; c.f. Möttig et al., 2001) were used.

The cRNA used in this study was prepared by Dr. Thomas Zimmer. After preparation, the cRNA specific for the respective channels was stored until use at -80°C.

2.2. Preparation of *Xenopus laevis* oocytes

In this study were used oocytes from the South African clawed frog *Xenopus laevis* (Figure 3). The preparation of the oocytes took place according to the method previously described by Goldin (1992). *Xenopus laevis* was anesthetized with 0.4% 3-aminobenzoic acid ethyl ester and the ovarian lobes were transferred in Barth medium with Ca^{2+}. Stage V oocytes (Dumont, 1972) were then incubated for 20-40 minutes in Barth medium Ca^{2+} free (see Table 1) containing 1 or 2 mg/ml collagenase Type I (Sigma). After this period, the oocytes are washed with Barth medium containing Ca^{2+} and then defolliculated manually under the microscope.

Within 2-7 hours after isolation, the cRNA was injected into oocytes through glass micropipettes (2.0 mm - outer diameter and 1.6 mm - inner diameter; Hilgenberg, Malsfeld). Until further use, the oocytes were stored up to 10 days in Barth medium with Ca^{2+} at 18°C. A change of the medium was performed every 48 hours. Before patching, the

oocytes are transferred to a hypertonic solution (Skinning solution, see Table 1) to manually remove the vitelline membrane, which was performed under the microscope. Freshly skinned oocytes were then transferred to the experimental chamber.

Figure 3. Oocytes from the South African clawed frog *Xenopus laevis*.

2.3. Chemicals

For activation of the CNG channels, we used cGMP and cAMP from Sigma. To obtain the desired concentrations of cyclic nucleotide, the appropriate dilutions were prepared using bath solution (Table 1). For the single-channel measurements, the dilutions were carried out with Aspartat solution. In this case, the pipette solution contains also 200 μM niflumic acid in order to block endogenous calcium-activated chloride currents.

For the flash-photolysis experiments, we used the following caged compounds, which were kindly provided by Dr. V. Hagen from the Institute of Molecular Pharmacology, Berlin (Figure 4):

- [7-(diethylamino)coumarin-4-yl]methyl ester of cGMP (DEACMcGMP),
- [7-(diethylamino)coumarin-4-yl]methyl ester of cAMP (DEACMcAMP),
- [6,7-bis(carboxymethoxy)coumarin-4-yl]methyl ester of cGMP (BCMCMcGMP),
- [7-bis(carboxymethylamino)coumarin-4-yl]methyl ester of cGMP (BCMACMcGMP).

These compounds dissolve well in aqueous solution, are resistant toward solvolysis, react quickly within a few nanoseconds, and have a high quantum yield (Hagen et al., 2001).

The caged cNMPs were first dissolved in dimethyl sulfoxide (Sigma) to a concentration of 10 mM and stored at -80°C in the dark. The stocks were diluted in bath solution to different concentrations, prior to each experiment. The final dimethyl sulfoxide concentration had no effect on the patches. When using high cyclic nucleotide concentrations (> 100 μM), the caged cNMP was dissolved in solution A (Table 1) and the mixture was treated with 3′,5′-cyclic-nucleotide-specific bovine brain phosphodiesterase

(Sigma), in order to hydrolyze the eventual existent free cGMP. Hydrolysis was stopped after 10-15 minutes by adding an equal volume of solution B that contained 1 mM EGTA (Table 1).

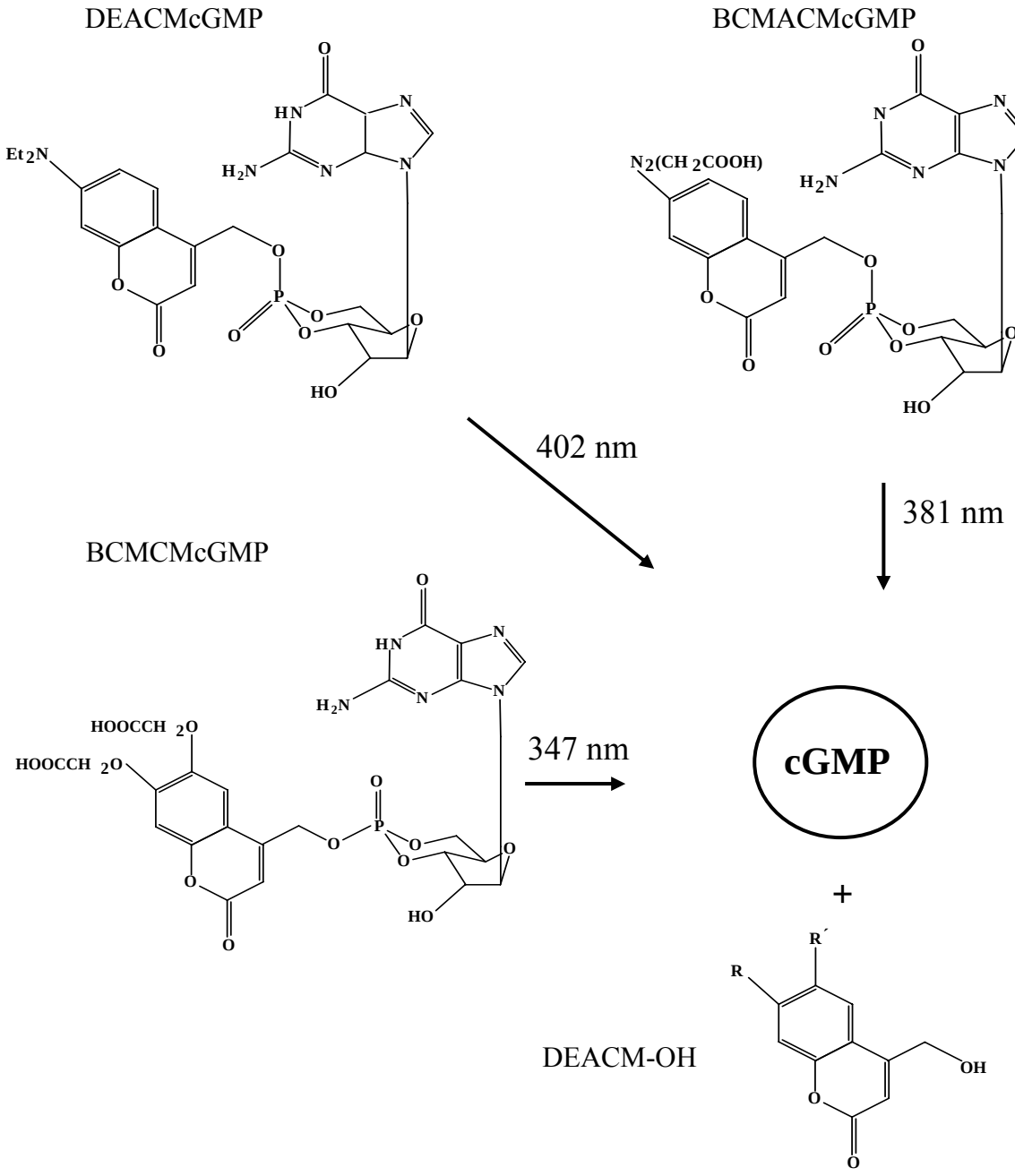

Figure 4. Structure of the used caged cGMPs and scheme of the flash photolysis.

In most of the experiments, DEACMcNMP compounds were used. Due to their superior property to release higher concentration of cyclic nucleotides, BCMCMcNMP and

BCMACMcNMP were also used for the activation of CNGA1 and CNGA2 channels. The wavelengths of the light necessary for photolysis were 320-480, 275-355, and 320-480 nm, respectively.

Table 1. Solutions

Solution	Ingredients	Concentration (mM)
Bath solution		
KCl (NaCl) solution	EGTA	1
	HEPES	5
	KCl (NaCl)	150
	pH 7.4 (KOH or NaOH)	
Aspartate solution	Aspartate	148
	KCl (NaCl)	2
	KOH (NaOH)	148
	EGTA	1
	HEPES	5
	pH 7.4 (KOH or NaOH)	
Pipette solution		
KCl (NaCl) solution	EGTA	1
	HEPES	5
	KCl (NaCl)	150
	pH 7.4 (KOH or NaOH)	
Aspartate solution	Aspartate	148
	KCl (NaCl)	2
	KOH (NaOH)	148
	EGTA	1
	HEPES	5
	Niflumic Acid	0.2
	pH 7.4 (KOH or NaOH)	

For caged cNMP		
Solution A	HEPES	5
	KCl (NaCl)	150
	pH 7.4 (KOH or NaOH)	
Solution B	EGTA	1
	HEPES	5
	KCl (NaCl)	150
	pH 7.4 (KOH or NaOH)	
For incubation of *Xenopus* oocytes	NaCl	84
	KCl	1
Barth medium, Ca^{2+} free	$NaHCO_3$	2.4
	$MgSO_4$	0.82
	Tris	7.5
	pH 7.4 (HCl)	
	NaCl	84
Barth medium with Ca^{2+}	KCl	1
	$NaHCO_3$	2.4
	$MgSO_4$	0.82
	Tris	7.5
	$Ca(NO_3)_2$	0.33
	$CaCl_2$	0.41
	Cefuroxin	1
	Penicillin/Streptomycin	1
	pH 7.4 (HCl)	
	Asparagine	200
Skinning solution	KCl	2
	$MgCl_2$	2
	EGTA	5
	HEPES	10
	pH 7.4 (KOH)	

2.4. Recording Technique

2.4.1. Preparing of patch pipettes

The patch pipettes were pulled from quartz tubing. For macroscopic currents, tubing either with an outer diameter of 1.2 mm, and an inner diameter of 0.8 mm (Hilgenberg, Malsfeld) or with an outer diameter of 1 mm, and inner diameter of 0.7 mm (BioMedical Instruments, Jena) were used. For single-channel experiments, quartz tubing with an outer diameter of 1 mm and an inner diameter of 0.4 mm (Hilgenberg, Malsfeld) or 0.5 mm (BioMedical Instruments, Jena) were used.
The pipettes were pulled using a laser puller (P-2000, Sutter Instrument Co., USA), visualized under microscope, and then used within 9 hours after fabrication. The solution used for filling the pipettes was filtered.

2.4.2. Electrophysiological recordings

Currents were recorded in inside-out patches (Figure 5b) with the patch-clamp technique (Hamill et al., 1981; Stühmer, 1992). The patch-clamp setup consisted of an inverted microscope (Axiovert 100, Carl-Zeiss-Jena GmbH, Germany) for cell visualization, placed on a vibration isolated table (Newport, USA), an Axopatch 200A amplifier (Axon Instruments, USA), a micromanipulator holding the amplifier headstage in conjunction with pipette holder and the pipette, a pump for bath perfusion, a videocamera plus monitor, a lamp, and a computer (Pentium III). The setup was positioned in a Faraday cage.
The experimental chamber was mounted on the stage of the microscope. It was composed of two compartments (Figure 5a). In the main compartment (width 8 mm) the oocyte was positioned, the sealing was performed and all free cyclic nucleotide concentrations were administered in a constant solution flow of 0.12 ml/min. Then the pipette was moved into the photolysis compartment (width 0.5 mm, height 1.0 mm). The solution containing the caged cyclic nucleotide was led to the main compartment in an angle of 90^{o}, thereby passing the photolysis compartment just before entering the main compartment. One wall of the photolysis compartment was formed by the end of the light guide (diameter 1.0 mm). The opposite wall consists of a mirror to intensify the light in the compartment. At the topside, the photolysis compartment was confined by a glass plate for light

transmission necessary at the visualization of the pipette. The bottom of the experimental chamber consisted of two parallel glass plates. Between these plates, thermostated water flew to control the temperature in both the main and the photolysis compartment. The experiments were viewed through the double-walled chamber bottom and the thermostated water. All experiments, if not mentioned otherwise, were made at 20.3°C. The chamber temperature was maintained with the help of a thermostat; model Haake DC1-K20 (USA). The bath and the pipette were filled with the same solution. The maximum current was then activated with a solution containing 100 μM cGMP or 1000 μM cAMP (for CNGA2 channels) and 700 μM cGMP (for CNGA1 channels). The pipette resistance was 0.6-2.5 MΩ for macroscopic currents and 5-25 MΩ for single-channel currents.

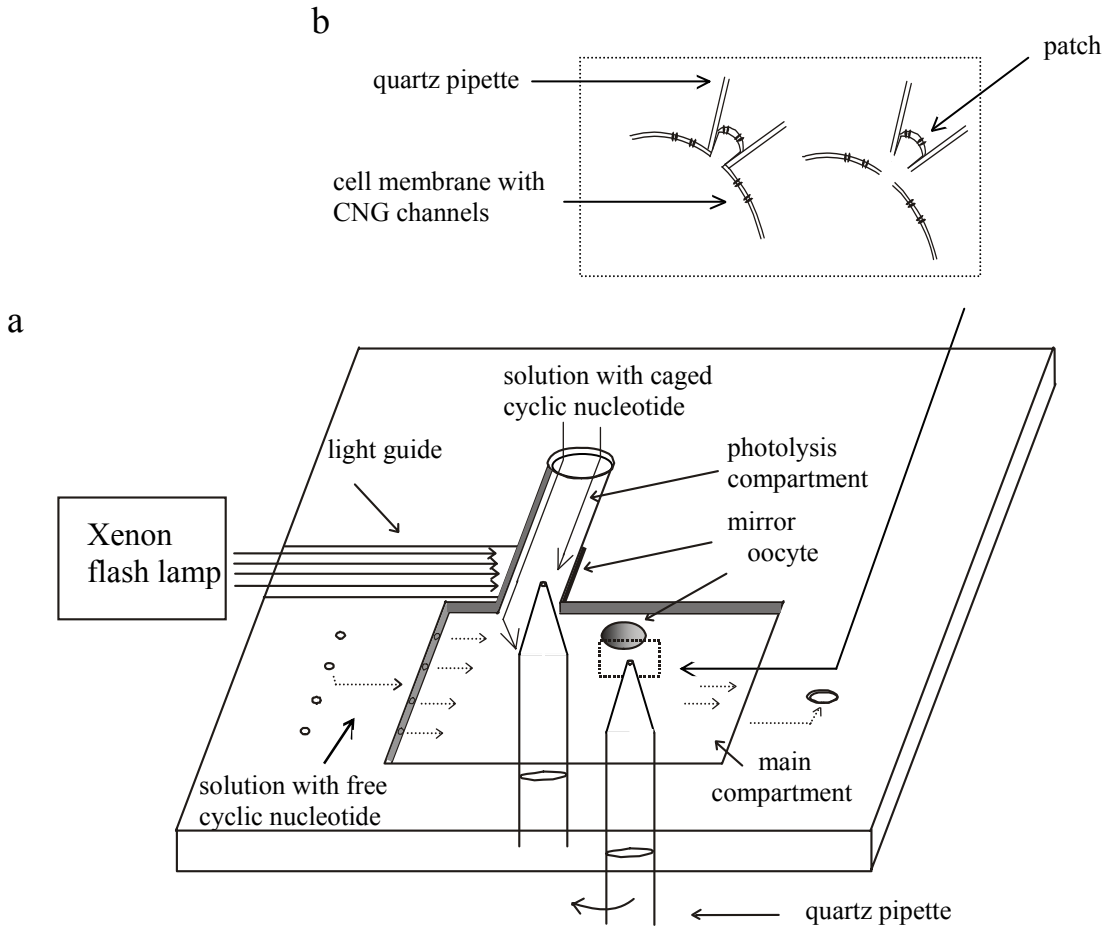

Figure 5. (a) Scheme of the experimental chamber.

(b) Inside-out configuration of the patch. The cytoplasmic face of the membrane is exposed to the bath solution.

If not otherwise stated, the currents were measured at a voltage of +100 mV. For macroscopic currents the sampling rate was generally 2 kHz (filter 1 kHz) except for CNGA1 channels where it was 20 kHz (filter 5 kHz). Single-channel activity of CNGA2 channels was recorded with a sampling rate of 20 kHz (filter 5 kHz).

2.4.3. Flash photolysis of caged cyclic nucleotides

Light flashes were generated by a flash-lamp system JML-C2 (Rapp OptoElectronic, Hamburg, Germany) and directed to the experimental chamber by a light guide (diameter 1.0 mm) fabricated of quartz glass. The flash lamp was controlled by the recording program. Photolysis was performed in a cylindrical volume of 390 nl. The energy of a light pulse was 0.45-1.47 mJ. Figure 6 describes the time course of the light pulse. The trace was recorded with a photodiode. The photolysis is completed within 150 μs. This time interval of photolysis was 40 times shorter than the time constant of the currents signals studied.

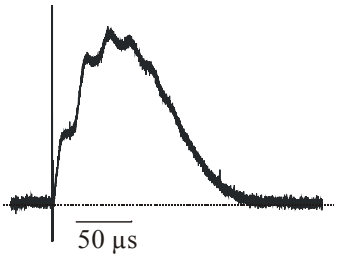

Figure 6. Time course of a light flash delivered by the xenon flash lamp.

The pipette tip was positioned in the middle of the photolysis chamber. The solution flow through the photolysis chamber was adjusted such that the concentration of the liberated cyclic nucleotide was constant for at least 1.5 seconds, as evaluated by the constant steady-state level of the CNGA2-channel current (Figure 7).
The next flash was applied after the current induced by the cyclic nucleotide had dropped to the current level in the absence of the cyclic nucleotide determined in the main chamber before the photolysis experiments. The time interval between the flashes ranged from 10 to 25 s depending on the concentration of the caged cyclic nucleotide used.

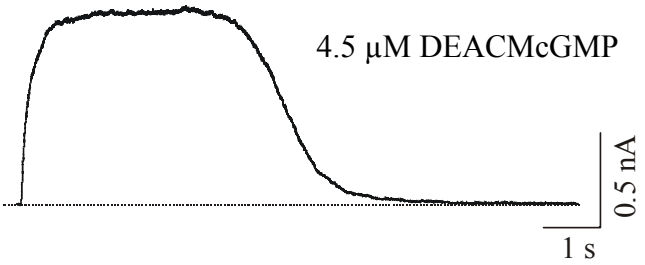

Figure 7. Representative experiment with DEACMcGMP. The CNGA2 current was activated by flash photolysis of 4.5 µM DEACMcGMP. After around 4 s the current started to decrease due to the wash-out of the liberated cGMP.

For some experiments, the intensity of the light flash was reduced in order to obtain a smaller concentration of free cyclic nucleotide from the caged compound.
Using the equation

$$[\text{cyclic nucleotide}] = EC_{50}\,[(I_{max}/I_{\infty})-1]^{(-1/H)} \qquad (1)$$

the concentration of the free cyclic nucleotide produced by flash photolysis was determined (Figure 8). I_{∞}/I_{max} represents the ratio of the steady-state current following a flash to the steady-state current at a saturating concentration of the free cyclic nucleotide. EC_{50} and H are the concentration of the cyclic nucleotide that causes half-maximal activation and the Hill coefficient determined from the dose-response relationship of the respective free cyclic nucleotide and channel.

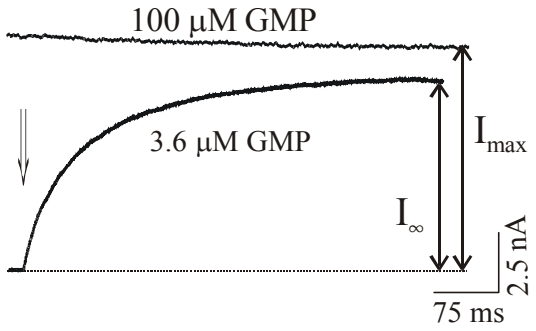

Figure 8. Method of determining the free cyclic nucleotide concentration liberated from the caged compound after flash photolysis. The maximal CNGA2 activation was recorded using a cGMP concentration of 100 µM (I_{max}). The channels in the same patch were activated by a cGMP jump generated by flash photolysis from the caged compound (I_{∞}). The fraction I_{∞}/I_{max} was inserted in equation (1).

For all channels included in this study, the following control experiments were performed:

1. To test whether the light flashes have any direct effects on the channels, CNGA2 channels were activated by free cGMP (10 μM) and the patches were exposed to 10 flashes as used for uncaging (Figure 9). The current amplitude was unaffected.

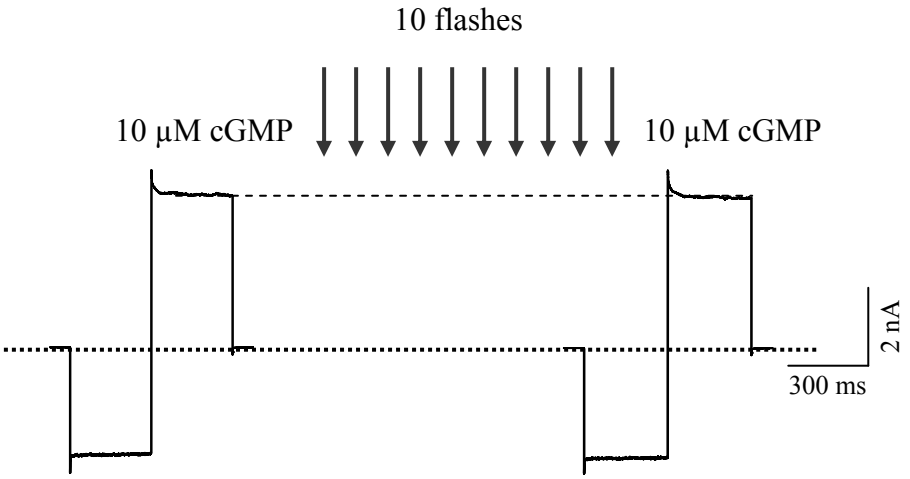

Figure 9. The CNGA2 current is activated by 10 μM cGMP. Onto the same patch, 10 light flashes were applied and the current was activated again by 10 μM cGMP. The conclusion is that the light flashes have no effect on the CNGA2 current amplitude.

2. To test whether the caged compounds had any effects on channels, experiments were performed on CNGA2 channnels using a mixture of caged cyclic nucleotide and a concentration of 2-3 times the EC_{50} value of free cyclic nucleotide (Figure 10). At high concentrations, the caged compounds slightly reduced the amplitude of the macroscopic current. This effect was reversible. The same experiment was repeated for all the channels included in this study and for the higher concentrations of all caged compounds used. For determination of the open probability, the measured currents were corrected by amplitude factors ranging from 1.002 to 1.21 (Table 2).

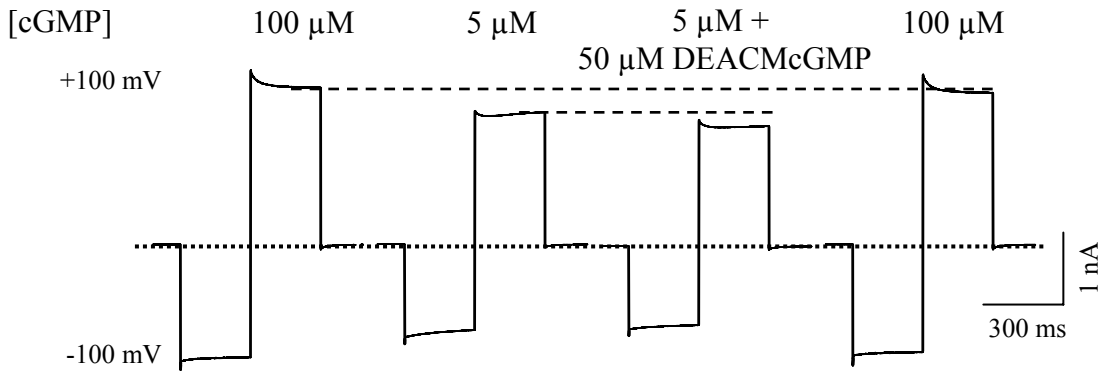

Figure 10. Effect of caged cGMP on CNGA2 current. The channels were first maximal activated by 100 µM cGMP. Comparing the amplitude of the current by 5µM cGMP with the amplitude determined with the same concentration of cGMP plus 50 µM DEACMcGMP allowed estimating the effect of the caged cNMP on CNGA2 channels.

Table 2. Block of caged cNMPs on different channels

[Caged compound]		Correction factor				
		CNGA1	CNGA2	CNGA2/A4/B1b	r1o	o1r
DEACMcGMP	50 µM		1.168		1.21	1.19
	30 µM	1.136	1.071			
	25 µM				1.148	1.145
	20 µM				1.124	
	15 µM				1.1	1.104
	10 µM	1.07	1.056		1.07	1.08
	6.5 µM					1.06
	4.5 µM		1.0126			
BCMCMcGMP	1 mM	1.1				
BCMACMcGMP	400 µM	1.137				
	200 µM	1.11				
DEACMcAMP	90 µM		1.066			
	50 µM		1.048			
	30 µM		1.037	1.052		
	20 µM		1.002	1.037		
	8 µM			1.008		

3. In the presence of high concentrations of caged cNMP, light flashes reduce the CNGA2 current amplitude by <7% per flash (Tabel 3). The decrease of the CNGA2 current is irreversible. The current amplitude at saturating concentrations of the cyclic nucleotide was therefore determined immediately after a light flash (Figure 11).

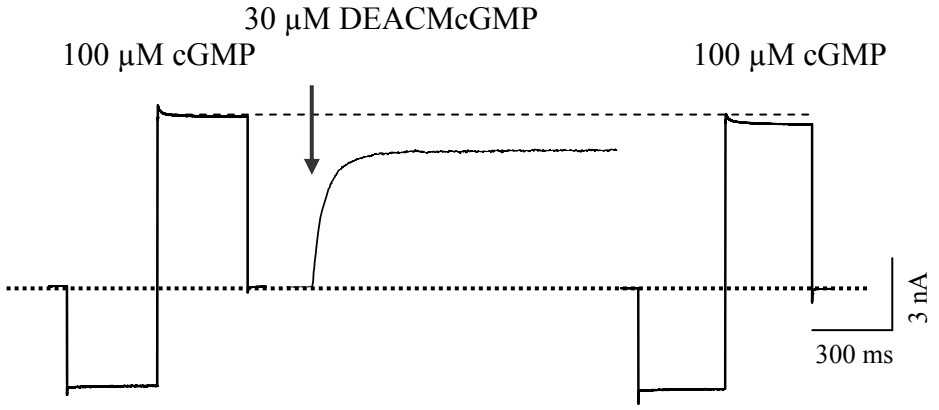

Figure 11. To estimate the cumulative effect of high concentrations of caged compound plus light flashes, we compared the maximal amplitude of a CNGA2 current recorded before and after a light flash (indicated by the black arrow). The experiment was performed with a saturating concentration of 100 µM cGMP and 30 µM DEACMcGMP.

Table 3. Estimation of the irreversible blocking effect of different caged compound concentrations and light flashes upon the channels.

[Caged cNMP]		% reduction of current per flash			
		CNGA1	CNGA2	r1o	o1r
DEACMcGMP	50 µM			1.64	1.6
	30 µM	3.0	2.5		
	25 µM			0.75	0.6
	20 µM			0.58	
	15 µM			0.42	0.3
	10 µM	0.7	2.2	0.2	0.12
	4.5 µM		1.2		
BCMCMcGMP	1 mM	7.0			
BCMACMcGMP	400 µM	3.94			
	200 µM	1.64			

4. To test whether the secondary product of photolysis (DEACM-OH) has any effects on the channels, the amplitude of the CNGA2 current at 50 μM cAMP was compared to that at a mixture of 50 μM cAMP with 30 μM DEACM-OH we. There was no significant difference. Therefore, the secondary product of photolysis has no effects on the channels.

2.5. Data acquisition

Measurements were controlled and data were collected with the ISO3 soft- and hardware (16-bit resolution; MFK Niedernhausen, Germany) on a Pentium PC.
To test for possible background channel activity, each excised patch was first exposed to a solution containing no cyclic nucleotide. Cyclic GMP- or AMP-activated currents were determined as the difference between currents measured in the presence and absence of cyclic nucleotide.

2.6. Data analysis

2.6.1. Macroscopic currents

2.6.1.1. Dose-response relationships

A common experiment that is done to study the activation of a CNG channels is to measure the dose-response relation for cAMP and cGMP. Steady-state currents were measured in response to different concentrations of activating ligand using the following pulse protocol:

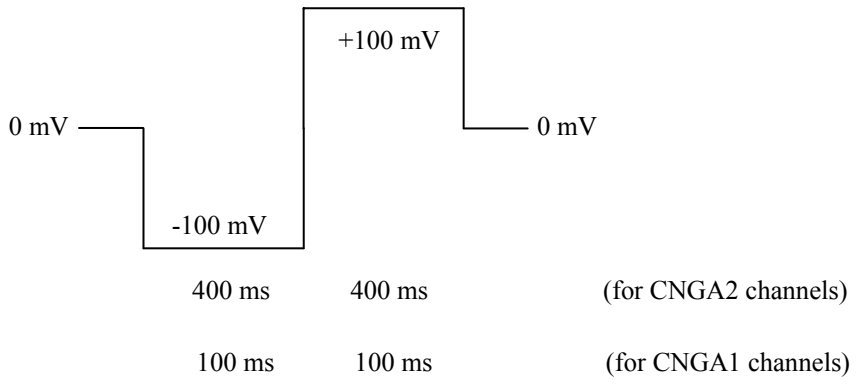

Each patch was first exposed to a saturating concentration of cGMP or cAMP. After testing the maximal current amplitude, the chamber was filled with different cyclic nucleotide concentrations and the current was recorded. The maximal currents and the leak currents (in the presence of a solution without any cyclic nucleotides) were measured two or three times during the same experiment.

The data were analyzed using the Origin 6.1® software. The dose-response relationships were fitted with the Hill equation (2). The fraction of maximal current, I/I_{max}, is the current at a given concentration divided by the maximal current measured at a saturating cyclic nucleotide (CN) concentration.

$$I/I_{max} = 1/(1 + (EC_{50}/[CN])^{H}) \quad (2)$$

H is the Hill coefficient and represents the minimum number of ligands required for a significant opening. EC_{50} represents the concentration that causes half-maximal activation of the current.

2.6.1.2. Voltage-jump experiments

Jumps in voltage perturb the CNG-channel gating (Karpen et al., 1988). The kinetics of activation were examined by switching the voltage from -100 to +100 mV.

For the voltage-jump experiments, we used the same voltages as for the dose-response relationship (see above). The pulse durations were variable, depending on the concentration of the cyclic nucleotide (short pulses for the smallest and the highest cyclic nucleotide concentrations and long pulses for intermediate cyclic nucleotide concentrations).

The relaxation in the current observed when the voltage was switched from -100 mV to +100 mV was fitted either with an exponential equation (3) or the sum of two exponentials equation (4) with the help of the ANA3 software.

$$y(t) = A \cdot e^{-x/\tau} + B \quad (3)$$

$$y(t) = A \cdot e^{-x/\tau_{fast}} + B \cdot e^{-x/\tau_{slow}} + C \quad (4)$$

A, B, and C are the amplitude of the activating and steady-state components, respectively.

2.6.1.3. Flash-photolysis induced currents

Most of the flash-photolysis induced currents were measured at +100 mV. For a small group of experiments four different voltage pulses: +50 mV, +100 mV, -50 mV, -100 mV were applied. Control experiments ascertained that these currents were activated by liberation of free cyclic nucleotide from the caged compound.

The activation time courses induced by jumps of a cyclic nucleotide were fitted with a sum of two exponentials equation (4) yielding the fats and the slow time constants τ_{fast} and τ_{slow}.

The temperature coefficient Q_{10} for the activation time constants τ_{fast} and τ_{slow} was calculated using:

$$Q_{10,\,\tau\,fast} = \tau_{fast}\,(10.3°C)/\,\tau_{fast}\,(20.3°C) \quad (5)$$

$$Q_{10,\,\tau\,slow} = \tau_{slow}\,(10.3°C)/\,\tau_{slow}\,(20.3°C) \quad (6)$$

Markov models were approximated to macroscopic currents following jumps of either cGMP or cAMP. Seven current traces covering a wide range of open probabilities were globally fitted. The respective systems of first-order differential equations were resolved by the Eigenvalue method, minimizing χ^2. The computations were performed by Prof. E. Schulz (Schmalkalden, Germany). Statistical data are given as mean±SEM.

2.6.2. Single-channel currents

Single-channel measurements were performed at +100 mV in order to obtain large amplitudes of the unitary currents. The currents were ON-line filtered at a cut-off frequency of 5 kHz. The measurements were performed at 20.3°C.

The patch was first exposed to a saturating concentration of 100 µM cGMP or 2 mM cAMP (for CNGA2 channels) and 700 µM cGMP (for CNGA1channels). At high ligand concentrations, patches containing only one channel were analyzed. For control, the patch was exposed also to solution containing no cyclic nucleotide. At zero and low ligand concentrations, multichannel patches were used.

The amplitude of single-channel currents was determined by forming all-point amplitude histograms and fitting the distributions with sums of two Gaussian functions. The single-

channel open time was evaluated by setting a threshold to the 50% level of the current amplitude. Open duration refers to the duration of individual excursions into the open state, terminated by closing, no matter how brief. Open-time histograms were formed and described by exponentials. For simplification of part of the analysis, the mean open time, τ_o, of two mean open times, τ_{o1} and τ_{o2} was calculated according to

$$\tau_o=(A_1\tau_{o1}^2+A_2\tau_{o2}^2)/(A_1\tau_{o1}+A_2\tau_{o2}) \quad (7)$$

where A_1 and A_2 are the respective amplitudes of the exponentials.

The open probabilities were determined from the amplitude histograms of single-channel recordings. In the absence of cyclic nucleotides, multichannel patches were used in which the channel number was such that amplitude histograms resolved single-channel events. The data were further analyzed using either the ANA3 or the Origin 6.1® software.

3. Results

3.1. Macroscopic currents

3.1.1. Dose-response relationships

Cyclic nucleotide-gated (CNG) channels respond to both, cAMP and cGMP, but lower concentration of cGMP than cAMP are required to open the channels. CNGA1 channels discriminate very well between cGMP and cAMP, whereas CNGA2 channels respond similarly well to both ligands, reflecting the importance of both messengers in olfaction.
The shape of the dose-response relationship and the limiting slope is interpreted to indicate that several CN molecules bind to the channel in a cooperative manner (Kaupp et al., 2002).
Dose-response relationships for CNGA1, CNGA2, CNGA2/A4/B1b, r1o and o1r channels were measured. The analysis of the dose-response relationships showed that channel activation depends steeply on the ligand concentration. Figures 12, 13, and 14 show double-logarithmic plots (log I/I_{max} vs. log [CN]) of the dose-response relationships that were used for the estimation of the free cyclic nucleotide concentration generated by the photolysis of the caged compounds. The CNG channel gating was quantified by fitting dose-response data with the Hill equation (2). For CNGA2 channels, the cGMP concentration producing half-maximum current (EC_{50}) was 1.76 µM whereas that for CNGA1 channels was 46.5 µM. The Hill coefficients were 2.35 and 1.98, respectively. These values agree with previously reported values (Bradley et al., 2001; Kaupp et al., 1989).
When changing the temperature from 20.3°C to 10.3°C (Figure 12c) the EC_{50} value of CNGA2 channels was unchanged (1.7 µM cGMP) whereas the Hill coefficient decreased (Table 4).

Table 4. EC_{50} values and Hill coefficient (H) for CNGA1 and CNGA2 channels activated with cGMP.

	EC_{50} (μM cGMP)	H
CNGA1 20.3°C	46.5	1.98
CNGA2 20.3°C	1.76	2.35
CNGA2 10.3°C	1.7	1.68

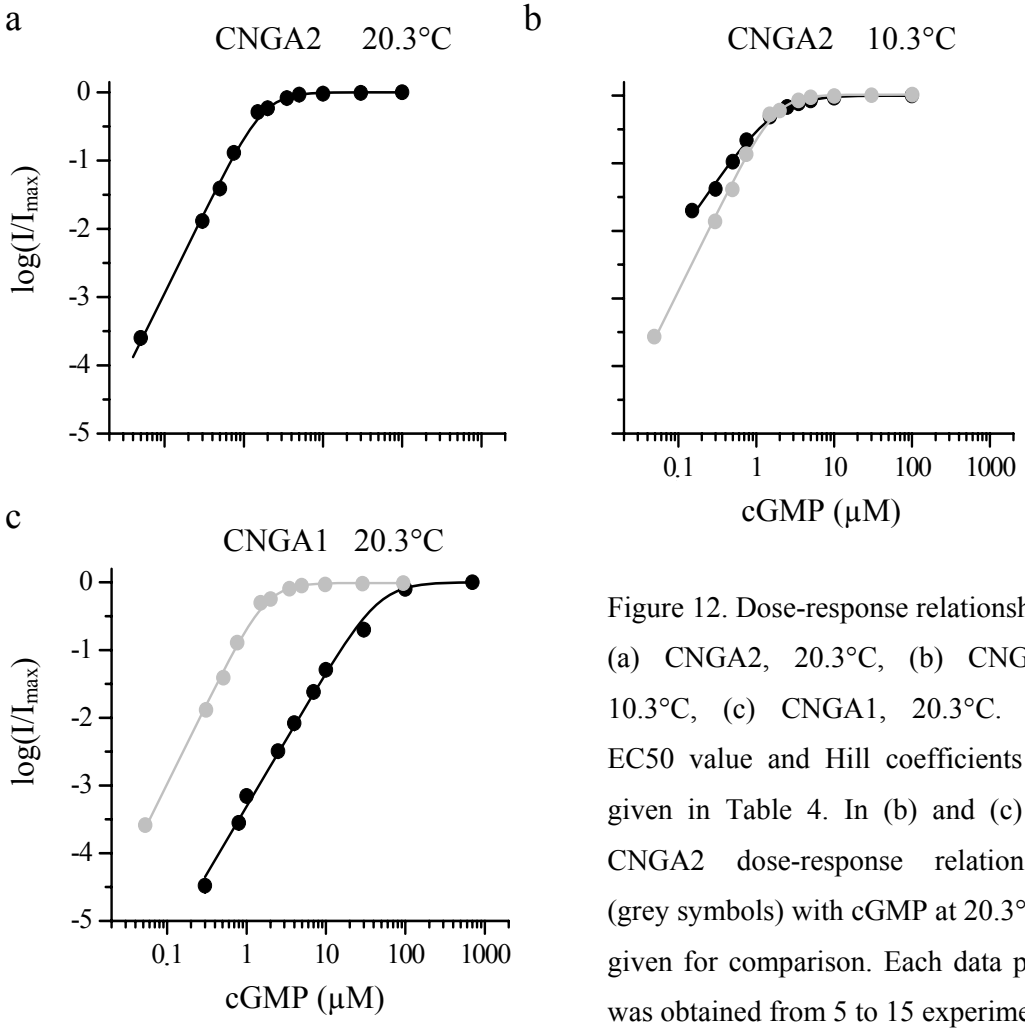

Figure 12. Dose-response relationships. (a) CNGA2, 20.3°C, (b) CNGA2, 10.3°C, (c) CNGA1, 20.3°C. The EC50 value and Hill coefficients are given in Table 4. In (b) and (c) the CNGA2 dose-response relationship (grey symbols) with cGMP at 20.3°C is given for comparison. Each data point was obtained from 5 to 15 experiments.

Dose-response relationships for activation of CNGA2 and CNGA2/A4/B1b channels by cAMP at 20.3°C are shown in Figure 13. The experimental data were fitted by equation (2) yielding the EC_{50} value of 46.05 μM for CNGA2 (Figure 13a) and 4.53 μM for CNGA2/A4/B1b channels (Figure 13b).

These results confirm that CNGA4 and CNGB1b subunits increase the cAMP sensitivity of olfactory channels (Bönigk et al., 1999). Mean values of EC_{50} and Hill coefficient (H) for CNGA2 and CNGA2/A4/B1b activated with cAMP are summarized in Table 5.

Table 5. EC_{50} values and Hill coefficient (H) for CNGA2 and CNGA2/A4/B1b channels activated with cAMP.

	EC_{50} (µM cAMP)	H
CNGA2	46.05	2.32
CNGA2/A4/B1b	4.53	1.95

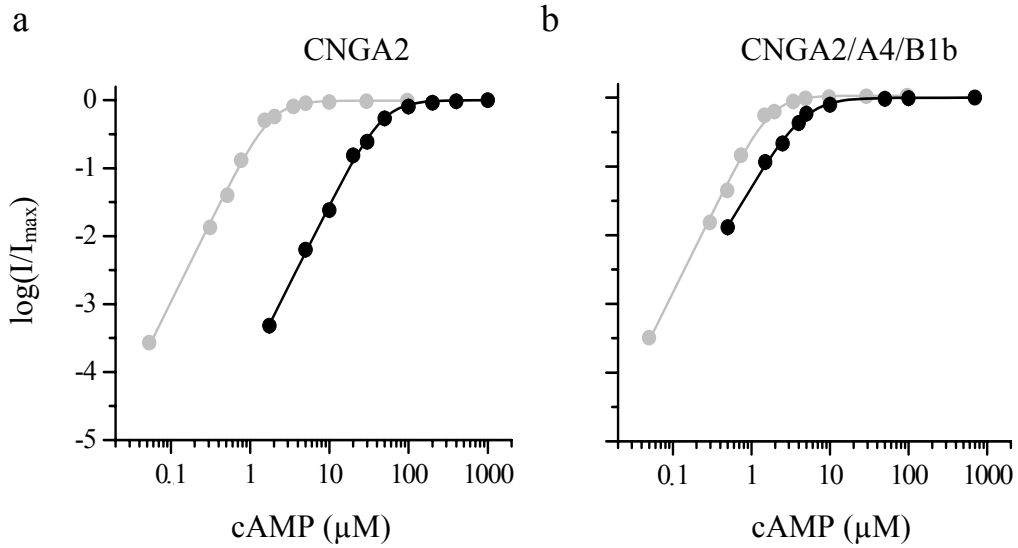

Figure 13. Dose-response relationships for CNGA2 (a) and CNGA2/A4/B1b (b) channels at 20.3°C for cAMP. The EC_{50} values and Hill coefficients are given in Table 5. The CNGA2 dose-response relationship (grey symbols) with cGMP at 20.3°C is given for comparison. Each data point was obtained from 5 to 12 experiments.

Figure 14 shows the dose-response relationships for the chimeric channels o1r and r1o (see above) at 20.3°C. It was shown previously (Möttig et al., 2001) that the EC_{50} value of N-terminal chimeras behaves as if the N-terminus region confers a portion of the typical EC_{50} value to the other channel. The chimera o1r, a CNGA1 channel with CNGA2 N-terminus, shifts the EC_{50} value to a lower cGMP concentration (Figure 14a) compared to CNGA1 channels (Table 4). The chimera r1o, a CNGA2 channel with CNGA1 N-terminus shifts

the EC_{50} value to higher cGMP concentration (Figure 14b) compared to CNGA2 channels (Table 4). The respective Hill coefficients are given in Table 6.

Table 6. EC_{50} values and Hill coefficient (H) for the chimeras o1r and r1o activated with cGMP.

	EC_{50} (µM cGMP)	H
o1r	9.41	1.49
r1o	7.28	1.80

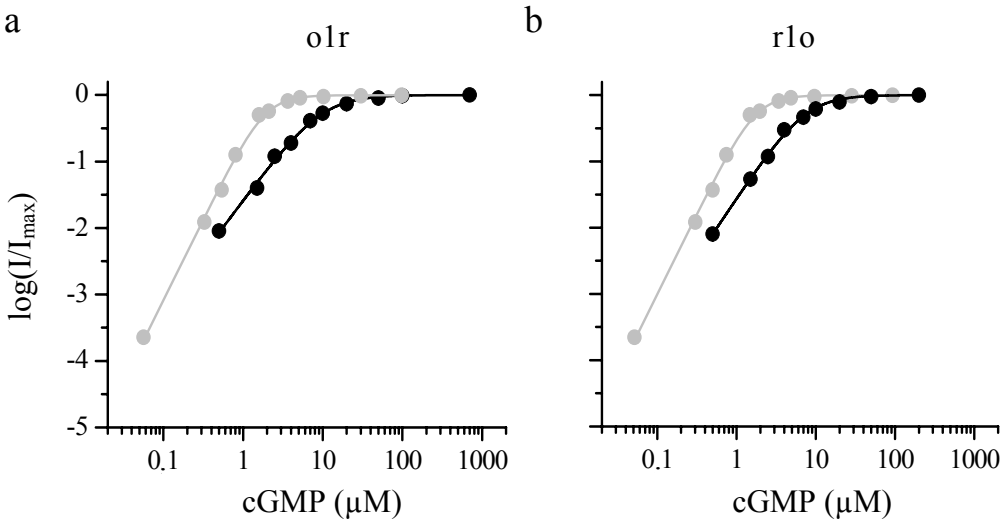

Figure 14. Dose-response relationships for o1r (a) and r1o (b) channels at 20.3°C activated by cGMP. The CNGA2 dose-response relationship (grey symbols) with cGMP is given for comparison. Each data point was obtained from 7 to 10 experiments.

The determined values of EC_{50} and H were inserted in equation (1) to determine the concentration of the free cyclic nucleotide liberated by flash photolysis from the caged cNMP.

3.1.2. Activation of CNGA1 channels by cGMP concentration jumps

In order to cover a wide range of ligand concentrations, three caged compounds with different properties were used: DEACMcGMP, BCMACMcGMP and BCMCMcGMP.

Upon irradiation of the patch expressing CNGA1 channels with flashes of UV light, large currents were recorded. The response consisted of a rapid rise in the current followed by a relative stable level for several seconds (see Material and Methods).

The amplitude of the light-induced current was dependent on voltage (Figure 15), on intensity of the light flashes (Figure 16), and on the concentration of the caged compound used (Figure 17a). Figure 15a shows the light-induced activation of CNGA1 channels at four different voltages: -100 mV, -50 mV, +50 mV, +100 mV. The curves were fitted by the sum of two exponentials equation (4). The activation components (A_{fast}, A_{slow}) and time constants (τ_{fast}, τ_{slow}) were inserted in equation (8) to determine the mean activation time constant τ_{mean}:

$$\tau_{mean} = (A_{fast}/(A_{fast}+A_{slow}))\ \tau_{fast} + (A_{slow}/(A_{fast}+A_{slow}))\ \tau_{slow} \qquad (8).$$

τ_{mean} were plotted as a function of voltage (Figure 15b). The plot indicates that the activation of CNGA1 channels at negative voltages is faster compared with the activation at positive voltages.

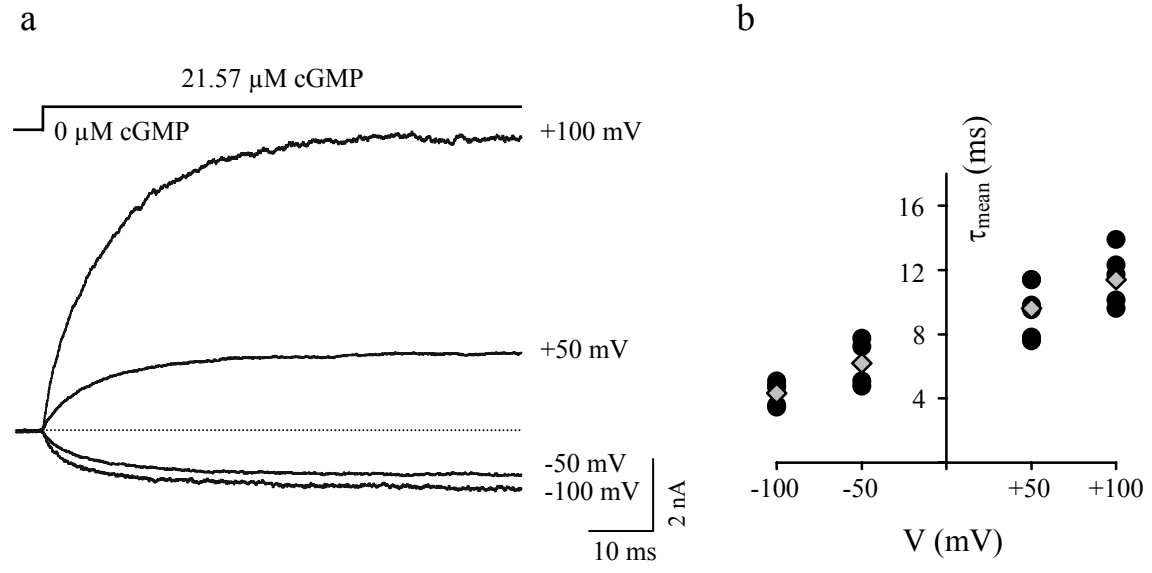

Figure 15. (a) Voltage dependence of CNGA1 current response induced by 21.57 µM cGMP.
(b) Plot of the mean activation time constant, τ_{mean}, at different voltages. The circles represent the result from individual patches; the grey symbols represent the mean of 5 to 8 individual measurements.

In the experiment shown in Figure 16, the light-induced CNGA1 currents recorded under conditions in which the light intensity was changed, were examined.

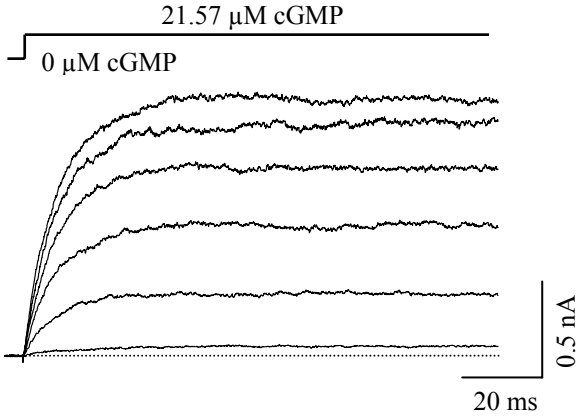

Figure 16. Intensity dependence of light-induced response. The curves represent consecutive current traces from a CNGA1 patch recorded at different light intensities. The activating DEACMcGMP concentration of 30 µM is kept constant during the experiment.

As expected, the amplitude of the CNGA1 current increases when increasing the light intensity.

Light-induced CNGA1 currents were elicited consistently over a wide range of caged cGMP concentrations (Figure 17a). The curves were fitted (red curve) with a sum of two exponentials (4), yielding the fast and slow time constant (τ_{fast}, and τ_{slow}) and their relative contributions, A_{fast} and A_{slow}. If cGMP binds to equivalent sites at the subunits and the binding rate limits the activation process, then the activation time course must be monotonically slowed in the direction to lower cGMP concentrations. Instead, both time constants are faster at both, lower and higher cGMP concentrations if compared to those at 21.57 µM cGMP. Figure 17b shows that increasing cGMP concentrations first increase both time constants until concentrations close to the EC_{50} value and then decrease again to the highest concentrations. The decrease of the time constants towards smaller cGMP concentrations than 21.57 µM shows that the activation process is not rate limited by the binding of cGMP but by conformational changes of the channel. Therefore, the determined time constants describe a conformational change associated with channel activation, which is slowest close to the EC_{50} value.

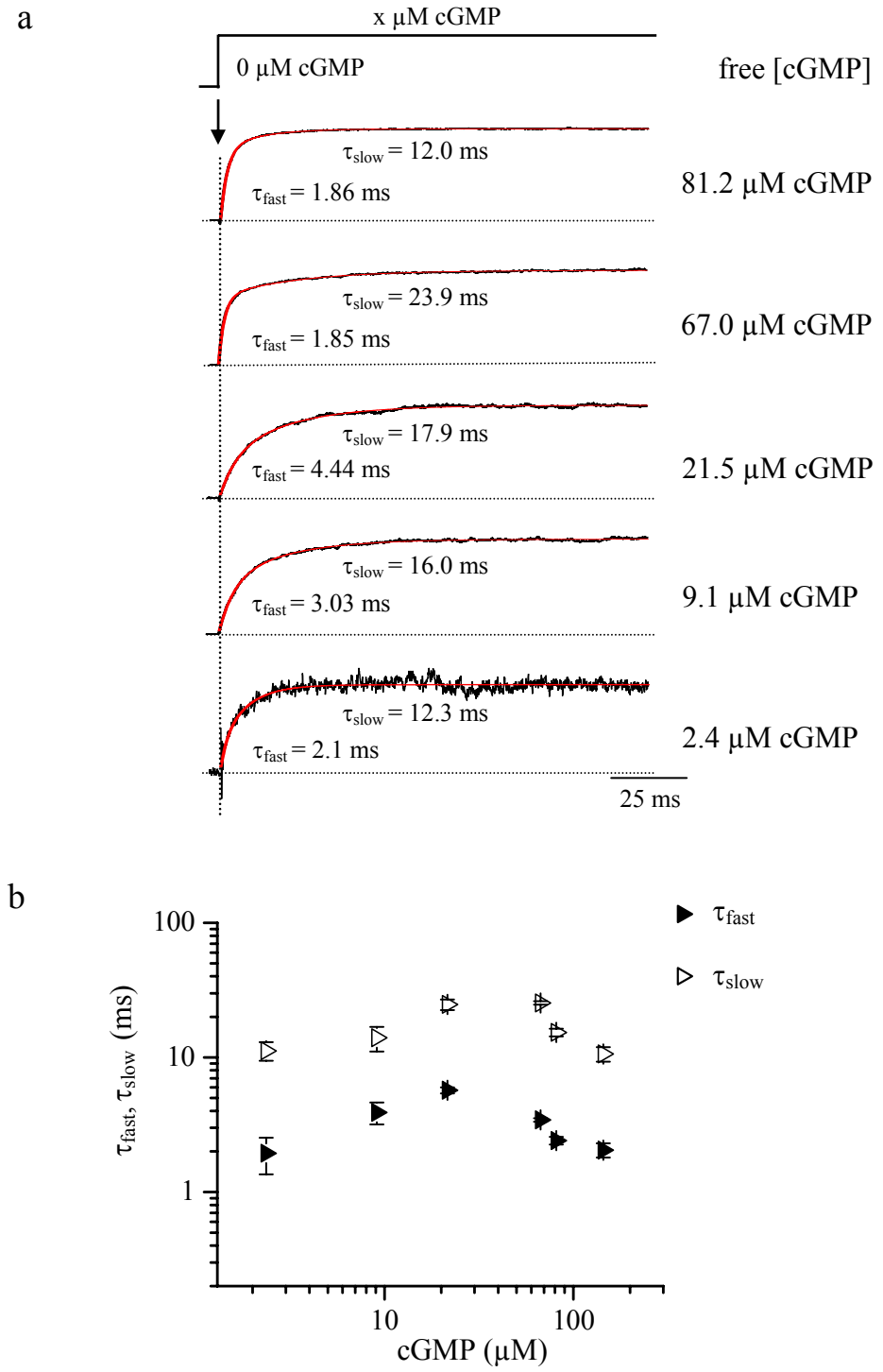

Figure 17. (a) Activation of CNGA1 currents by step-like changes of cGMP concentration. The black curves represent the normalized currents induced by flash photolysis of the caged cGMP. The gray lines represent the double exponential fit of the experimental data. The black arrow indicates the time point when the light flash was applied. (b) Plot of the mean activation CNGA1 time constants (τ_{fast}, τ_{slow}) as function of the cGMP concentration. The data points at 67.0 µM cGMP were determined using BCMCM cGMP and those at 81.3 µM cGMP using BCMACMcGMP. Each data point was obtained from 5 to 11 individual measurements.

3.1.3. Activation of CNGA2 channels by cGMP concentration jumps

Activation of homotetrameric CNGA2 channels was studied using DEACMcGMP. The activation appeared in the time range of tens to hundreds of milliseconds. Hence, CNGA2 channels activate more than 10 times slower than CNGA1 channels. The activation time course was studied over a wide range of cGMP concentrations and fitted with the sum of two exponentials equation (4), yielding the fast and slow time constant, τ_{fast}, and τ_{slow}, and their relative contribution, A_{fast}, and A_{slow}.

Both CNGA2 time constants depend on the cGMP concentration as follows (Figure 18b): Starting from the lowest cGMP concentration of 0.06 µM, they decrease to 0.15 µM, increase until 0.74 µM, and decrease again to the highest concentrations tested. This means that starting from the cGMP concentration of 0.15 µM and toward 0.74 µM there is an increase of the CNGA2 activation time constants.

A similar phenomenon was observed for CNGA1 channels (c.f. Figure 17b). Therefore, also the activation process of CNGA2 channels is limited by conformational changes of the channel protein and not by the binding of the ligand to the binding site at all concentration exceeding 0.15 µM cGMP.

At the lowest cGMP concentrations (from 0.06 µM to 0.15 µM), the decrease of the activation time constants with increasing cGMP suggests that the activation process could be limited by either the diffusion of the cGMP to the binding site or another conformational change of the channel preceding that at higher cGMP concentrations.

The contribution of the fast and slow time constant, A_{slow} and A_{slow}, also depends on the cGMP concentration: The contribution of the slow exponential, A_{slow}, dominates at intermediate cGMP concentrations (between 0.13 µM and 3.64 µM), whereas the contribution of the fast exponential, A_{fast}, dominates at both high and low concentrations (> 7.2 µM and < 0.1 µM cGMP; Figure 19).

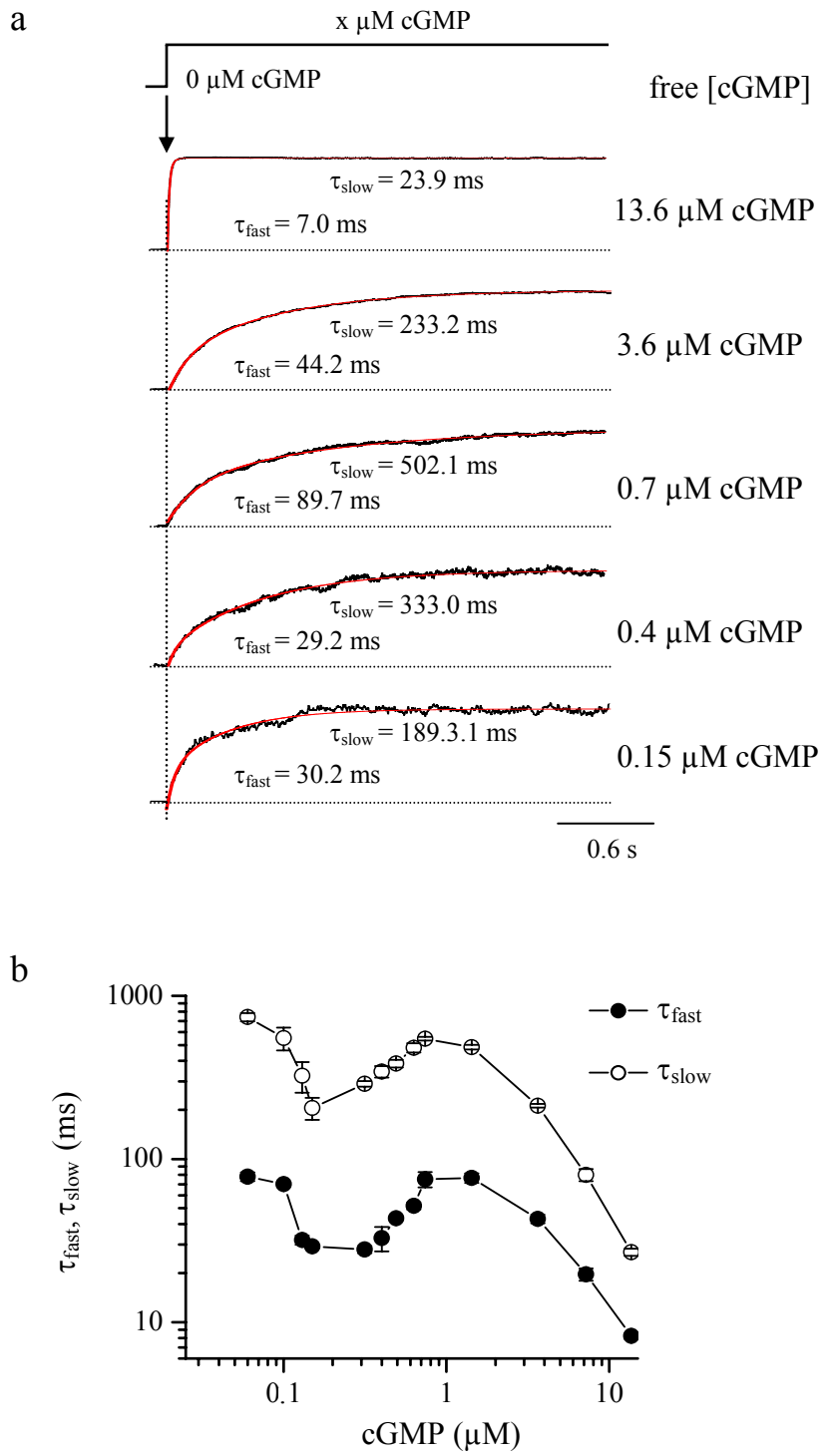

Figure 18. Activation time course of CNGA2 channels by step-like changes of the [cGMP]. (a) Normalized current traces (black curves) at five different cGMP concentration steps from zero to the indicated concentration by flash photolysis. The red lines represent the double exponential fit of the experimental data. As caged compound DEACMcGMP was used. The transmembrane voltage was +100 mV. (b) Plot of the activation time constants (τ_{fast}, τ_{slow}) as function of the cGMP concentration. Each data point was obtained from 5 to 15 individual measurements.

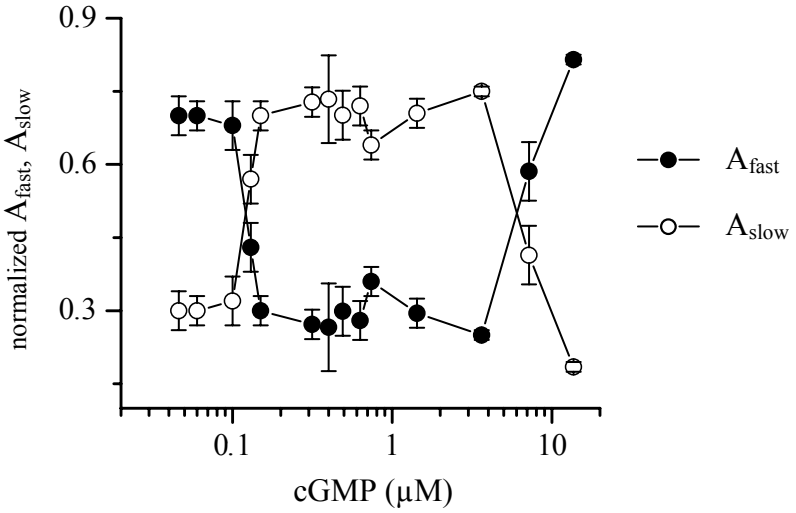

Figure 19. Relative contribution of the fast and slow exponential, A_{fast} and A_{slow}, to the activation time course of CNGA2 currents.

Figure 20a shows light-induced CNGA2 currents at 13.6 μM free cGMP at four different voltages: -100 mV, -50 mV, +50 mV, +100 mV. To see whether the flash-induced activation is voltage dependent, the four traces recorded at different voltages were superimposed (Figure 20b). In contrast to the experiment in Figure 15, this shows that CNGA1 activation is voltage dependent that of CNGA2 channels does not depend on voltage.

From the data so far, we can conclude the following: 1. The CNGA1 activation time constants were significantly faster than those for CNGA2 currents (Figure 17, 18); 2. In contrast to the voltage dependent CNGA1 activation that of CNGA2 channels does not depend on voltage (Figure 20); 3. Similar to CNGA1 activation time constants, the CNGA2 time constants developed a maximum close to the EC_{50} value (Figure 17, 18). These results lead to the hypothesis that at the concentrations around the EC_{50} value, activation of CNGA1 and CNGA2 channels is not rate limited by the binding of cGMP to equivalent sites but by conformational changes within the channel protein.

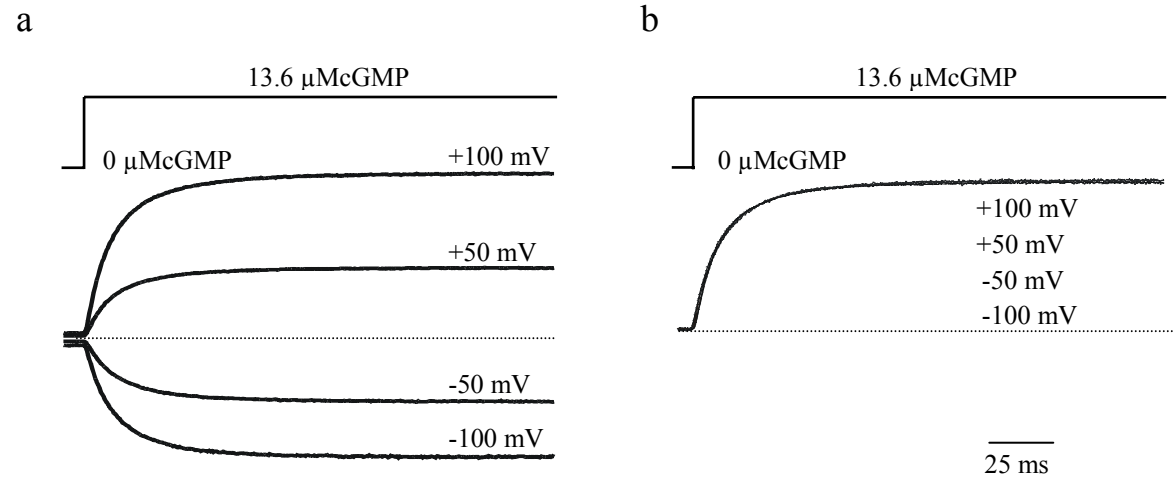

Figure 20. (a) Activation of CNGA2 currents by cGMP liberated by photolysis of 30 µM DEACMcGMP at four different voltages. (b) Superimposition of the normalized CNGA2 currents at -100 mV, -50 mV, +50 mV, and +100 mV.

3.1.4. Temperature coefficient Q_{10}

To gain further insight into the reactions underlying the activation of CNGA2 channels by cGMP steps, we studied the cGMP-step induced activation of CNGA2 channels at 10.3°C and determined the temperature coefficient Q_{10} for both time constants.

If the diffusional access of cGMP to the binding site is rate limiting, the Q_{10} value would be only 1.4. If a conformational change of the channel were rate limiting, the Q_{10} value could be 2 or larger. Lowering the temperature from 20.3°C to 10.3°C increased both time constants over the whole range of cGMP concentrations (Figure 21a). To obtain values at both temperatures at the same concentration, the values of τ_{fast} and τ_{slow} for 20°C were determined by linear interpolation. The resulting Q_{10} values ranged from 1.4 to 3.5, in the low cGMP range < 0.15 µM from 1.8 to 3.3 (Figure 21b). Because the values in the low cGMP range significantly exceed the theoretical Q_{10} value for diffusion, also at the lowest cGMP steps used herein, rate limitation must be inferred by a conformational change of the channel and not by diffusion of cGMP to its binding sites.

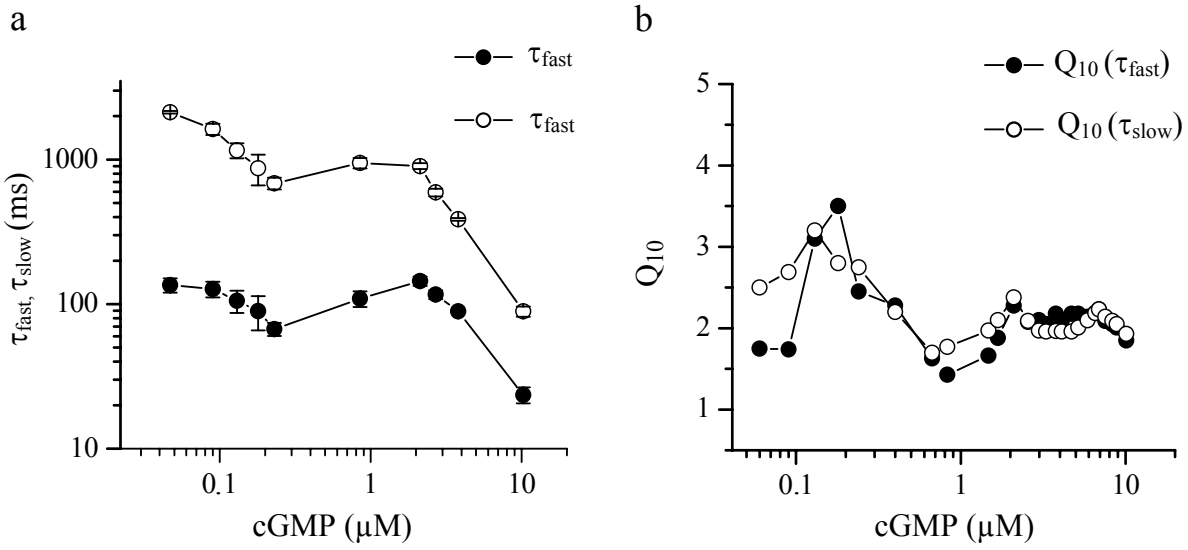

Figure 21. (a) CNGA2 activation time constants, τ_{fast} and τ_{slow}, at 10.3°C as function of the cGMP concentration. Each data point was obtained from 5 to 10 experiments. (b) Temperature coefficient Q_{10} for τ_{fast} and τ_{slow} as function of the cGMP concentration. The different Q_{10} values of ~2 at cGMP concentrations larger than the EC_{50} value and ~3 at cGMP concentrations between 0.1 - 0.3 μM suggest different rate limiting reactions in these cGMP concentration ranges.

The Q_{10} values produce a characteristic profile over the whole cGMP range and this profile is roughly similar for both time constants: The Q_{10} value is ~2 at concentrations larger than the EC_{50} value and ~3 at the low cGMP concentrations of 0.1 - 0.3 μM (Figure 21b). The Q_{10} value decreases towards the lowest cGMP concentrations used (< 0.1 μM). This result confirms that different conformational changes rate limit activation in different concentration ranges. The roughly similar profiles of the Q_{10} values for both time constants indicate that the molecular reactions generating both time constants are closely related.

3.1.5. Activation of CNGA1 and CNGA2 channels by voltage jumps

We studied voltage-dependent activation in CNGA1 and CNGA2 channels and compared the time courses with those of the cGMP-step induced activation to investigate whether both types of activation are related.

The kinetics of activation were examined by observing the relaxation in the current when the voltage was switched from -100 to +100 mV. Upon stepping the holding voltage of -

100 mV to +100 mV, an instantaneous outwardly directed current was followed by a time-dependent current that increased to a new steady-state level. This activation to the steady-state level appears in the millisecond time scale and it was attributed to the allosteric reaction of the channels (Benndorf et al., 1999).

Stepping from -100 to +100 mV generated currents with pronounced activation (Figure 22).

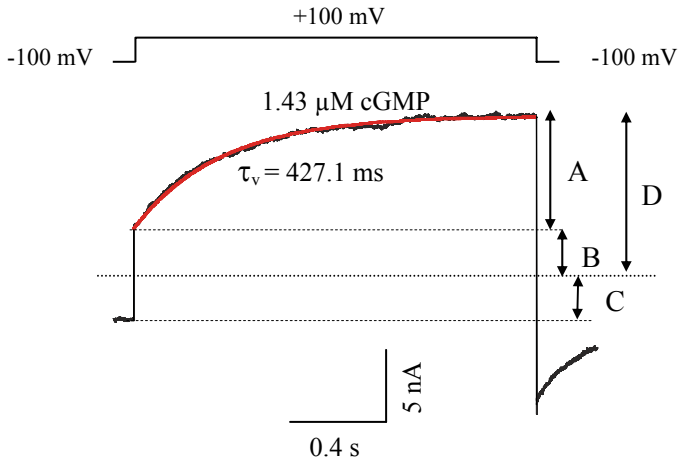

Figure 22. Activation time course (black curve) of a CNGA2 channel by 1.43 µM cGMP when stepping the voltage from -100 to +100 mV. The time course was fitted (red curve) with a single exponential equation (3) yielding the time constant τ_v. A: activation component, B: instantaneous outwardly directed current at +100 mV following depolarization, C: steady-state current at -100 mV, D: steady-state current at +100 mV.

The CNGA1-activation time course induced by voltage steps could be described with a sum of two exponentials (Figure 23). The resulting time constants, $\tau_{v,fast}$ and $\tau_{v,slow}$, approximate the values induced by cGMP steps only at the higher range of the cyclic nucleotide concentrations used, between 20.5 µM and 82 µM cGMP. At concentrations lower than 20.5 µM cGMP, $\tau_{v,fast}$ is smaller compared to τ_{fast}, the cGMP jump-induced activation time constant. $\tau_{v,slow}$ is related similarly to τ_{slow} . At the slowest concentration of cGMP used, $\tau_{v,slow}$ approximates τ_{fast} obtained from concentration steps. In conclusion, the CNGA1 activation time constants induced by voltage steps are in the same range with the activation time course induced by cGMP steps only at high and intermediate concentrations while at small concentrations the voltage dependent activation is more rapid. This finding suggests that at high concentrations both, the voltage- and the cGMP

jumps-induced activation are limited by the same conformational changes of the channel, whereas at low concentrations they are limited by different reactions.

Figure 23 shows a double logarithmic plot of the CNGA1 $\tau_{v,slow}$ and $\tau_{v,slow}$, in comparison to the activation time constants of cGMP step-induced activation.

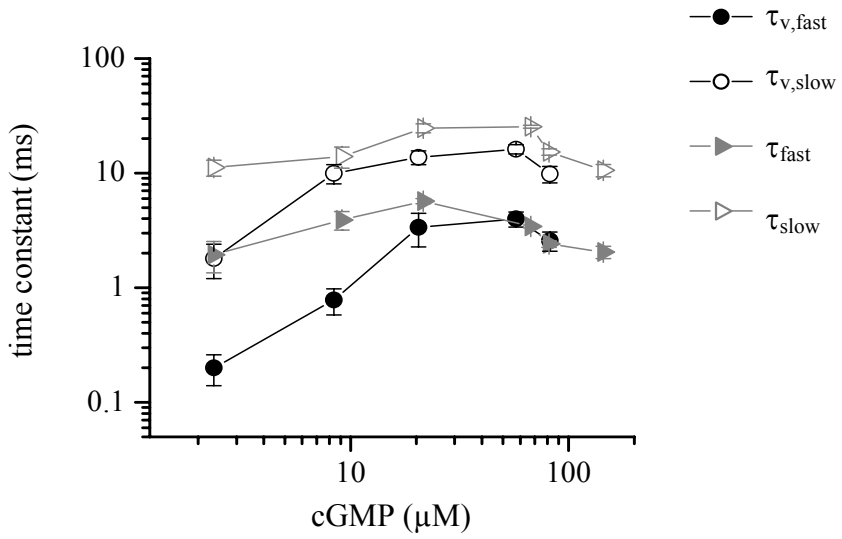

Figure 23. Activation time constants of CNGA1 channels ($\tau_{v,fast}$, $\tau_{v,slow}$) as function of cGMP concentration with voltage pulses from -100 to +100 mV at constant cGMP. For comparision, τ_{fast} and τ_{slow} obtained from cGMP jumps (grey symbols) at +100 mV are also included. Each data point was obtained from 5 to 15 experiments.

In contrast to the results obtained from the concentration steps experiments, the voltage induced-activating component of CNGA2 channels could be described with a single exponential equation.

The resulting time constant, τ_v, depends on the cGMP concentration in a bell-shaped fashion (Figure 24). At intermediate cGMP concentrations, between 0.15 μM and 5.8 μM cGMP, τ_v has values close to τ_{slow} whereas at both low and high cGMP, < 0.1 μM and > 7.1 μM, τ_v is similar to τ_{fast}. In conclusion, τ_v is always similar to the dominating time constant of the cGMP-step induced activation.

These results suggest that similar molecular reactions contribute to the voltage- and cGMP-step induced activation over the all range of CN concentrations and that part of these reactions takes place in the transmembrane field.

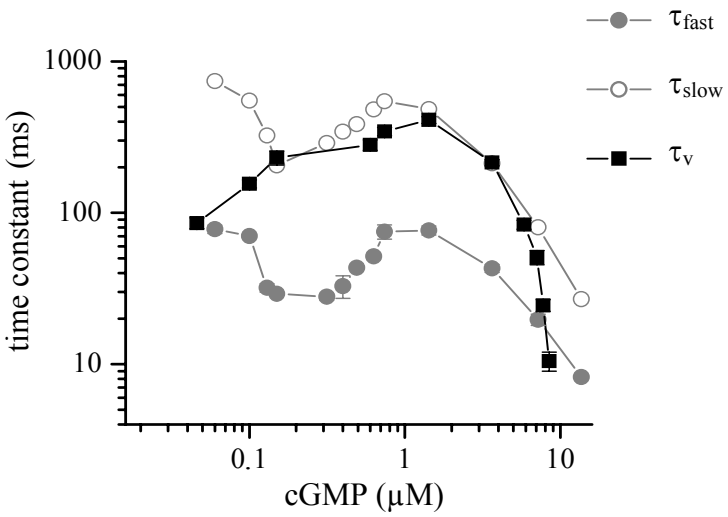

Figure 24. Activation time constant of CNGA2 channels (τ_v) as function of cGMP concentration with voltage pulses from -100 to +100 mV at constant cGMP. For comparison, τ_{fast} and τ_{slow} obtained from cGMP jumps (grey symbols) at +100 mV are also included.

3.1.6. Activation of r1o and o1r chimeric channels by cGMP concentration jumps

We next considered whether the transmembrane region determines the activation time course alone or in combination with intracellular channel parts. As an example of an intracellular domain, we considered the N-terminus.

We used chimeric constructs between CNGA1 and CNGA2 channels: a CNGA1 channel with CNGA2 N-terminus (chimera o1r) and a CNGA2 channel with CNGA1 N-terminus (chimera r1o) (Figure 25). For terminology of the chimeras see Möttig et al., 2001.

Möttig et al. (2001) showed that the N-terminus contributes to the difference in the EC_{50} values of CNGA1 and CNGA2 channels. For a CNGA1 channel with CNGA2 N-terminus (chimera o1r), the EC_{50} value is shifted to a lower cGMP concentration whereas for a CNGA2 channel with CNGA1 N-terminus (chimera r1o) the EC_{50} value is shifted to a higher cGMP concentration.

If the inserted N-terminus co-determines the speed of activation, one would expect a combined change of the EC_{50} value and the activation speed and if not, the inserted N-terminus should only change the EC_{50} value.

As a result, the inserted N-terminus from CNGA2 in a CNGA1 background (o1r) decreased EC_{50} to a value of 9.41 µM (Figure 14a) and increased both time constants (Figure 26).

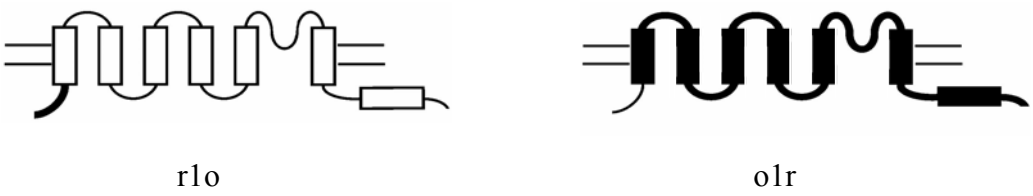

Figure 25. Structure of the chimeras between CNGA1 and CNGA2 channels. Black boxes and fat lines indicate CNGA1 sequences, white boxes and thin lines CNGA2 sequences.

The o1r activation time constants induced by cGMP jumps to a concentration near the EC_{50} value were 2.4 times (τ_{slow}) and 3.5 times (τ_{fast}) larger than the corresponding CNGA1 time constants. Conversely, the inserted N-terminus from CNGA1 in a CNGA2 background (r1o) increased the EC_{50} to 7.28 µM (Figure 14b) and decreased both time constants (Figure 26). The time constants of r1o activation induced by a concentration equivalent with the EC_{50} value were 1.7 times (τ_{slow}) and 1.13 times (τ_{fast}) faster than the corresponding CNGA2 activation time constants.

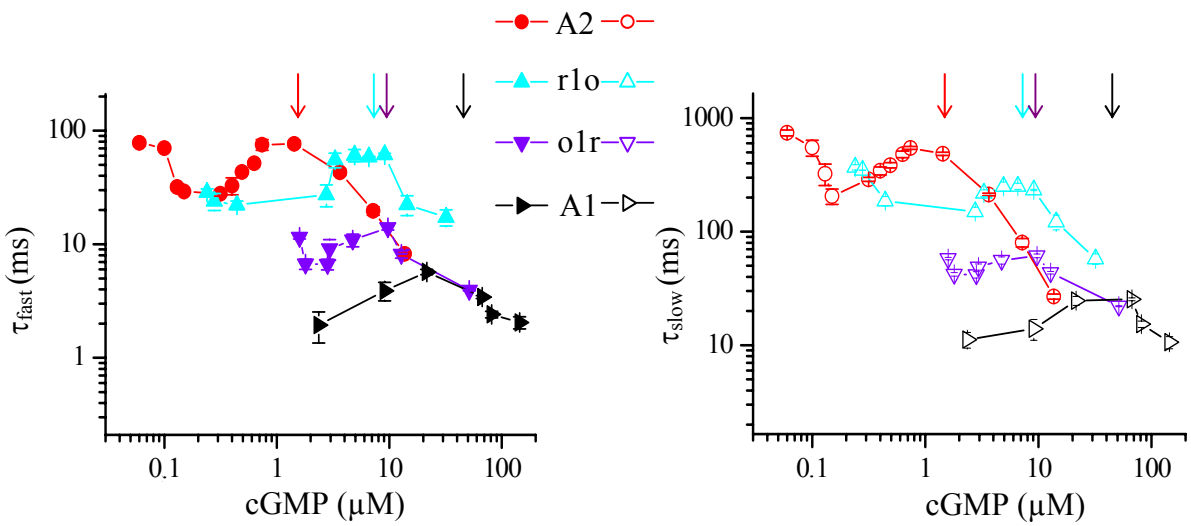

Figure 26. Plot of the τ_{slow} (open symbols) and τ_{fast} (filled symbols) as function of the cGMP concentration for CNGA1 channels (black symbols), chimera o1r (violet symbols), chimera r1o (blue symbols) and for CNGA2 channels (red symbols). The arrows

indicate the respective EC_{50} values determined by concentration-response relationships. The activation time course of CNGA1 and CNGA2 are given for comparison.

In general, the o1r and r1o activation time constants are similar with those of CNGA1 and CNGA2 channels. The time constants are at their highest point at the concentration around the EC_{50} value, develop a minimum at lower concentrations and increase again at the lowest concentrations. This result suggests that the activation of CNG channels also involves intracellular domains.

3.1.7. Activation of CNGA2 channels by cAMP concentration jumps

If in the whole range of tested cGMP concentrations, conformational changes of the channel rate limit the activation time course by cGMP steps, then a cyclic nucleotide with significantly higher EC_{50} value, as cAMP, should generate similar activation time courses at respectively higher concentrations. For CNGA2 channels, this would mean that the profile of the time constants τ_{fast} and τ_{slow} in Figure 18b would be simply shifted to higher concentrations. Any other changes would indicate that the cyclic nucleotide modulates the kinetics of the conformational changes. In addition, using a ligand with significantly higher EC_{50} value (cAMP), allows to elegantly confirming that the diffusion of the ligand to its binding site does not rate limit the CNGA2 activation time course.

We studied activation of CNGA2 channels with steps of the cAMP concentration. CNGA2 channels have a 26 times higher EC_{50} value with cAMP than with cGMP (Figure 13a).

cAMP steps to a concentration near the EC_{50} value activated CNGA2 currents with similar kinetics as did the cGMP steps (Figure 27).

The values for the CNGA2 activating time constants with cAMP steps, τ_{fast} and τ_{slow}, were roughly similar to those for cGMP steps, but shifted to higher concentrations (Figure 28a). Similar with CNGA1 and CNGA2 activation time constants as function of cGMP concentration, with cAMP, the curves also developed a maximum close to the EC_{50} value. Consequently, normalization of the cyclic nucleotide concentrations with respect to the EC_{50} values yields approximately similar relationships (Figure 28b).

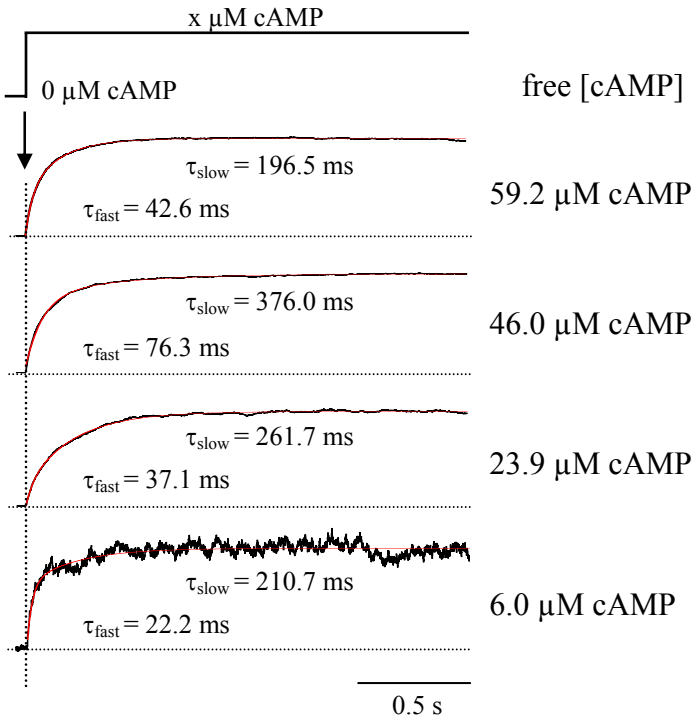

Figure 27. Activation of homotetrameric CNGA2 currents by step-like changes of the cAMP concentration. Examples of normalized current traces (black curves) at cAMP concentration steps from zero to concentrations in the range of the EC_{50} value. The transmembrane voltage was +100 mV. The traces were fitted (red curves) with the sum of two exponentials, yielding the activating time constants τ_{fast} and τ_{slow}. The black arrow indicates the time point when the light flash was applied.

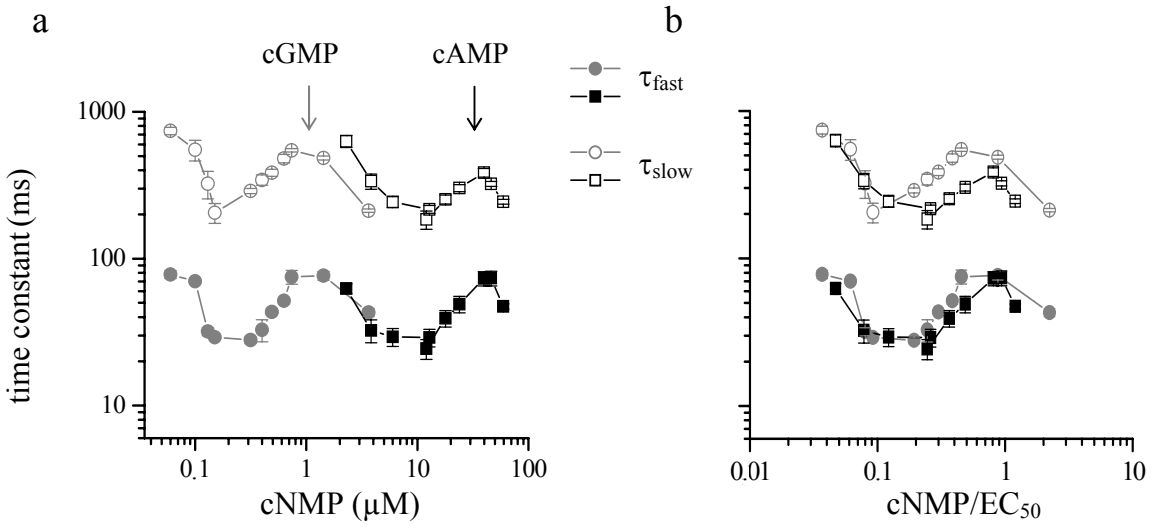

Figure 28. Activation time constants of CNGA2 channels for cAMP and cGMP steps. (a) Plot of τ_{fast} (filled symbols) and τ_{slow} (open symbols) as function of cAMP (black symbols) and

cGMP (grey symbols) concentration; (b) Plot of τ_{fast} and τ_{slow} as function of the cyclic nucleotide concentration normalized with respect to the EC_{50} value. Same symbols as in (a). The profiles are roughly similar, except that with cAMP the time constants are some smaller at the higher relative concentrations. The data for CNGA2 channels activated by cGMP steps are indicated for comparison. Each data point was obtained from 5 to 10 experiments.

In line with the above hypothesis, this result suggests that with both cyclic nucleotides the activation time course is rate limited by similar conformational changes of the channel. Again, we can conclude that the diffusion plays no role in channel activation. The main difference between both cyclic nucleotides for the gating arises from different affinities.

Besides the overall similar activation time courses with cAMP and cGMP, at $cNMP/EC_{50} > 0.3$ both time constants are smaller with cAMP than with cGMP (Figure 28b). This result suggests that the specific structure of cyclic nucleotides also modulate the conformational changes following the binding reactions.

The contribution of the fast and slow time constants, A_{fast} and A_{slow}, also depends on the cAMP concentration: Similar with the results obtained with cGMP steps (Figure 19), the contribution of the slow exponential, A_{slow}, dominates at intermediate cAMP concentrations (between 6.0 µM and 59.2 µM cAMP), whereas the contribution of A_{fast} dominates at low concentrations (< 3.83 µM cAMP) (Figure 29). Unfortunately, recordings at cAMP concentrations higher then 59.2 µM were not possible.

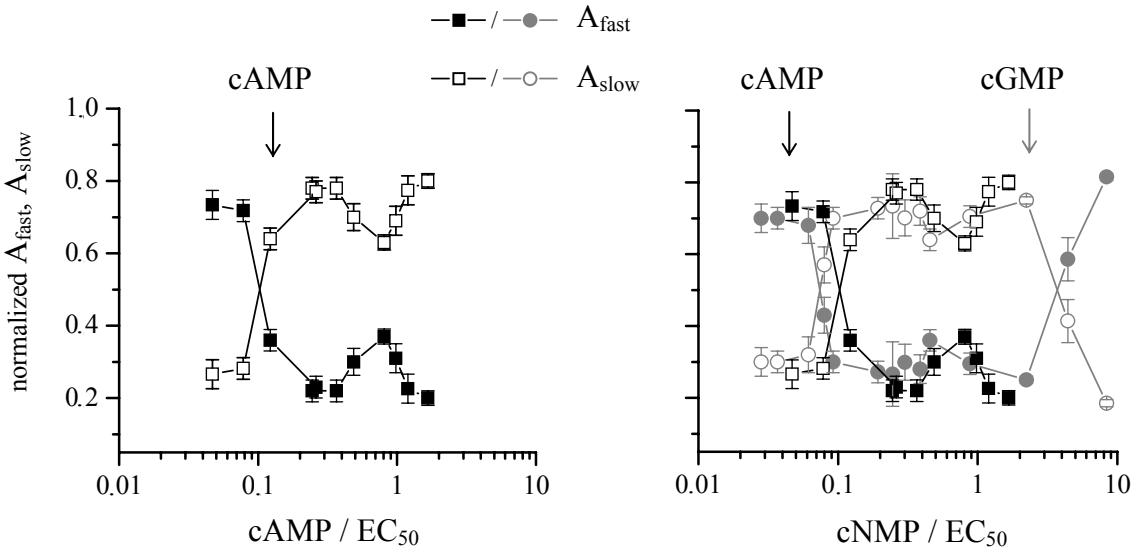

Figure 29. Relative contribution of the fast and slow exponential, A_{fast} and A_{slow}, to the CNGA2 activation time course. (a) Plot of A_{fast} (filled symbols) and A_{slow} (open symbols) as

function of cAMP (black symbols) normalized with respect to the EC_{50} value; (b) Plot of A_{fast} and A_{slow} as function of the cAMP (black symbols) and cGMP (grey symbols) normalized with respect to the EC_{50} value. Same symbols as in (a). In (b) the data for CNGA2 channels activated by cGMP concentration steps are indicated for comparison.

3.1.8. Activation of CNGA2/A4/B1b channels by cAMP concentration jumps

We further tested whether the results so far also reflect properties of native olfactory channels. The CNG channels from the olfactory sensory neurons are heterotetramers with a subunit composition CNGA2:CNGA4:CNGB1b of 2:1:1 (Zheng and Zagotta, 2004). The CNGA2/A4/B1b channel resembles the native olfactory channel with respect of its sensitivity to cAMP, discrimination between Na^+ and K^+, single-channel conductance, kinetics of open-closed transition, whereas other subunit combinations (CNGA2/A4 or CNGA2/B1b) display pronounced differences with respect to the native channel (Bönigk et al., 1999).

The resulting dose-response relationship for CNGA2/A4/B1b channels with free cAMP provided an EC_{50} value of 4.53 μM (Figure 13b), which is similar to that for recombinant heterotetrameric (Sautter et al., 1998; Bönigk et al., 1999; Bradley et al., 2001) and native olfactory channels (Frings et al., 1992; Bönigk et al., 1999; Bradley et al., 2001).

The CNGA2/A4/B1b activation time course was studied over a wide range of cAMP concentrations using as caged compound DEACMcAMP. The activation time course was fitted with the sum of two exponentials equation (4), yielding the fast and slow time constant and their relative contribution, τ_{fast}, τ_{slow}, A_{fast}, and A_{slow}, respectively (Figure 30). Both time constants depend on the cAMP concentration as follows: Starting from the lowest cAMP concentration, they decrease from the concentration of 0.44 μM to 1.3 μM, increase until 3.06 μM, and decrease again to the highest concentrations. When normalizing the cAMP concentration with respect to the EC_{50} value (Figure 31), the time constants for cAMP steps (Figure 30) equalled those obtained with homotetrameric CNGA2 channels (Figure 18b). These results suggest that in hetero- and homotetrameric channels, mainly the cAMP binding, and not the allosteric reaction is different.

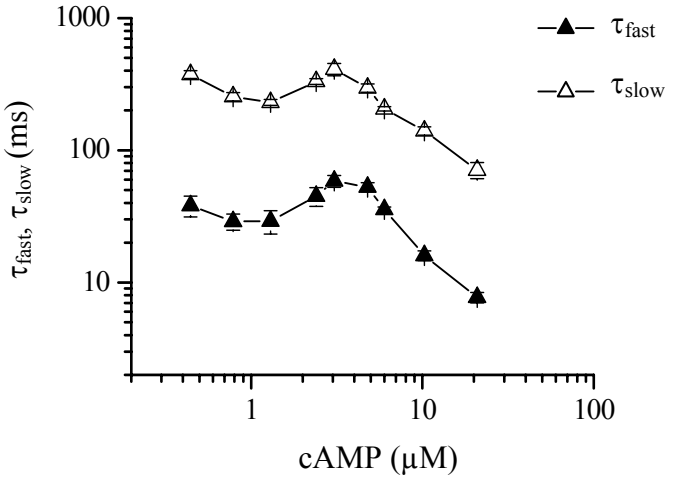

Figure 30. Activation of CNGA2/A4/B1b channels by step-like changes of the cAMP concentration. Plot of the CNGA2/A4/B1b channel activation time constants (τ_{fast}, τ_{slow}) as function of the cAMP concentration. Each data point was obtained from 5 to 10 experiments.

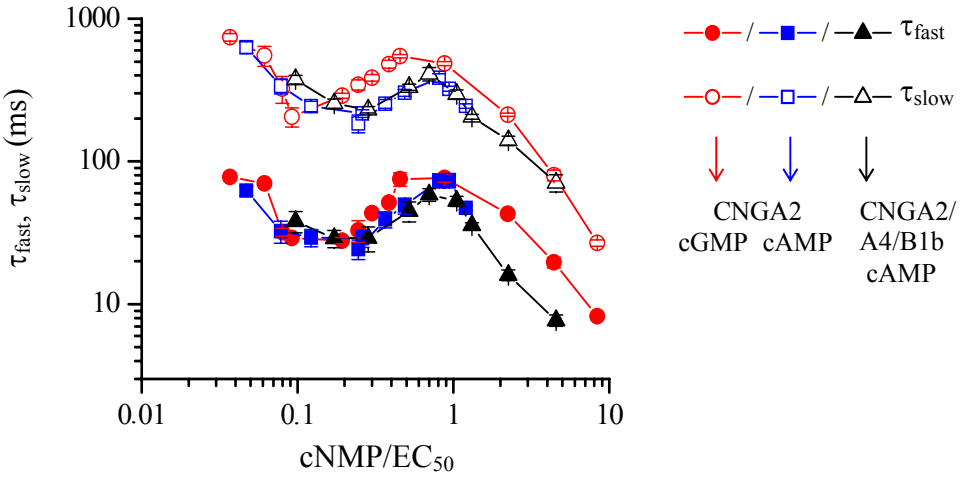

Figure 31. Plot of τ_{fast} (filled symbols) and τ_{slow} (open symbols) of CNGA2 (blue symbols) and CNGA2/A4/B1b (black symbols) channels as function of the cAMP concentration normalized with respect to the EC_{50} value. The profiles are roughly similar. The data for CNGA2 channels (red symbols) activated by cGMP steps are indicated for comparison.

The contribution of the CNGA2/A4/B1b fast and slow time constants, A_{fast} and A_{slow}, also depend on the cAMP concentration.

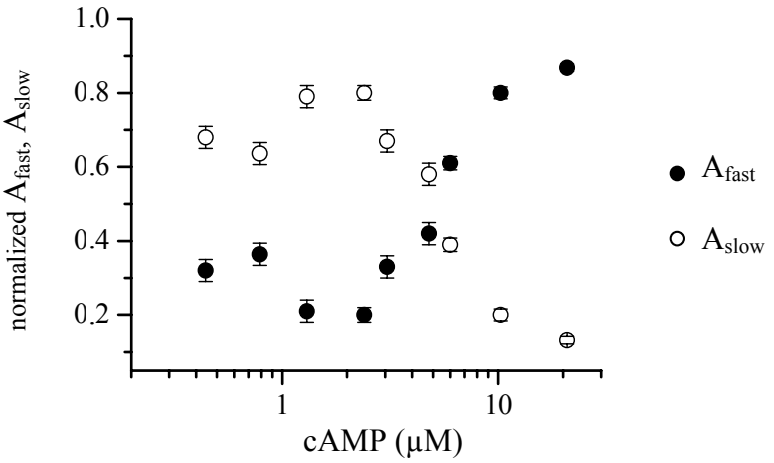

Figure 32. Relative contribution of the fast and slow exponential, A_{fast} and A_{slow}, to the CNGA2/A4/B1b activation time course. Plot of A_{fast} (filled symbols) and τ_{slow} (open symbols) as function of the cAMP concentration.

The results were similar to those with CNGA2 channels activated by cGMP and cAMP steps (Figure 19 and Figure 29a). In the range of cAMP concentrations tested, the slow exponential dominates at cAMP concentrations lower than 4.79 μM and the fast exponential dominates at high concentrations (higher than 6.0 μM cAMP) (Figure 32).

3.2. Single-channel currents

We addressed the question how many subunits contribute to the activation of the channels and we also tried to explain the data with respect to the mechanism of ligand binding. To approach this goal we recorded and analyzed the gating of single CNGA2 channels because single channel activity provides additional information.

We examined the kinetics of the CNGA2 single channels under steady-state conditions. Figure 33, left panels, presents current traces showing openings of a CNGA2 channel at +100 mV, and 100 μM cGMP (a) or 2 mM cAMP (b). At saturating concentration of both cGMP and cAMP the channel is predominantly in the open state which is interrupted only rarely by very short closings. There was no bursting behavior. Because of the long periods spend in the open configuration the open probability was almost 1 for both CN.

Previous work on multichannel patches suggested that CNG channels could open spontaneously with very low probability in the absence of the cyclic nucleotide (Li and Lester, 1998, Tibbs et al., 1997; Picones and Korenbrot, 1995). Figure 33c shows current traces with openings of a CNGA2 channel recorded at +100 mV in the absence of the ligand.

The lack of flicker and the lack of subconductance states are in contrast to the native rat olfactory CNG channels (Frings et al., 1992), the expressed homotetrameric bovine photoreceptor CNG channels (Ruiz and Karpen, 1997), expressed heterotetrameric olfactory channels (Bradley et al., 1994) and homotetrameric CNGA1 channels (Kusch et al. 2004). In the absence of the ligand, the spontaneous openings were very brief.

Figure 33a,b (right panels) show open-time histograms for a CNGA2 channel recorded at saturating concentrations of cGMP and cAMP. The open-time histograms could be described with a monoexponential equation in case of activation with saturating concentrations by both ligands, with time constants of 96.1 ms for cGMP and 88.8 ms for cAMP.

Figure 33c (right panel) shows the open-time histogram for a CNGA2 channel in the absence of any ligand. The best fit was provided by a sum of two exponentials equation. The resulting mean open times calculated using equation (7) and open probabilities are shown in Table 7.

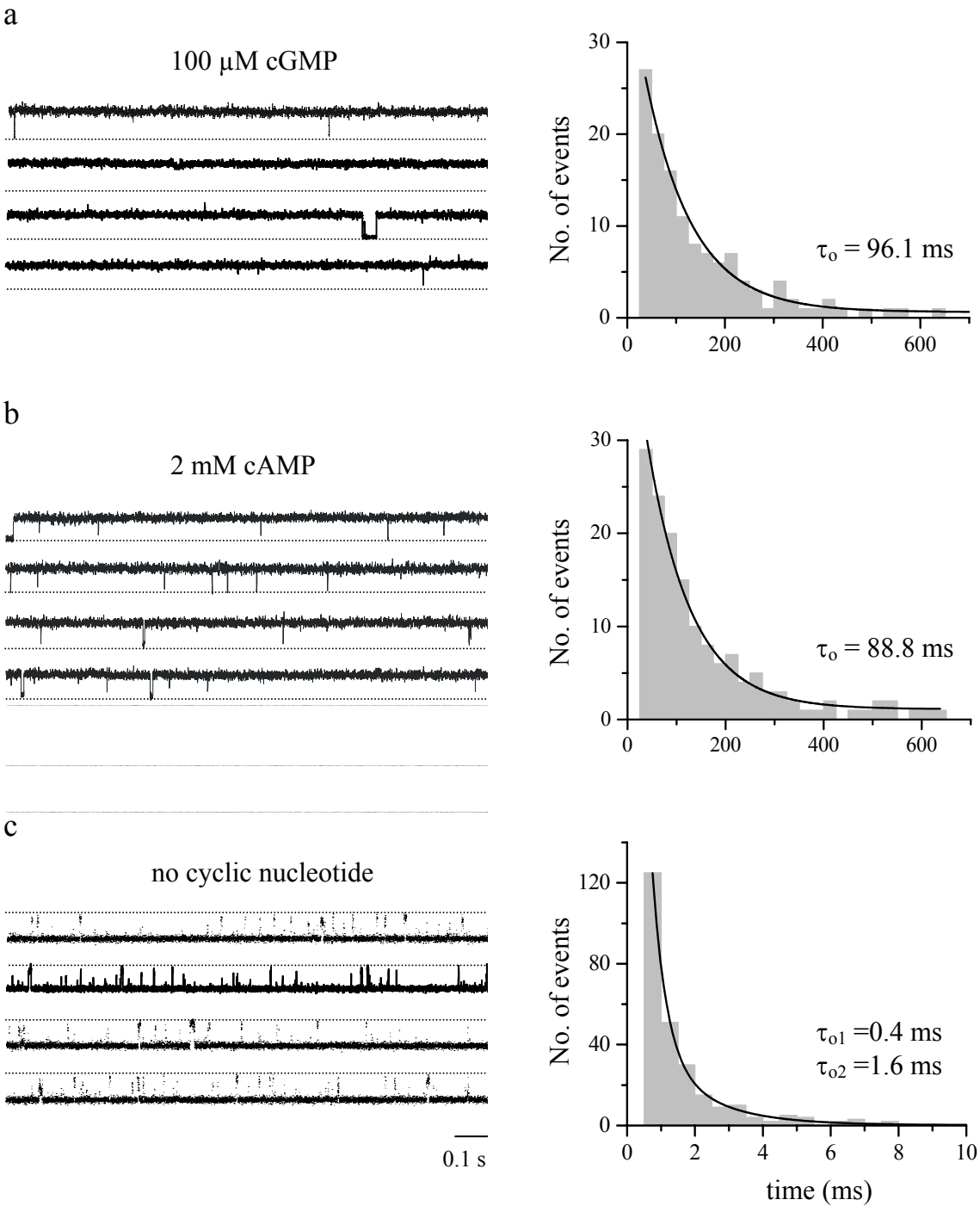

Figure 33. Open time of CNGA2 channels at saturating and zero cyclic nucleotide. (a) 100 μM cGMP, single-channel patch. (b) 2 mM cAMP, single-channel patch. Both open-times distributed monoexponentially. (c) No cNMP, multichannel patch (~175 channels). The open-time histogram yielded two time constants, τ_{o1} and τ_{o2}.

Table 7. Single-channel parameters in the absence of any cyclic nucleotide and at saturating concentrations of cGMP and cAMP.

	τ_o (ms)	P_o	k_{CO} (s^{-1})	k_{OC} (s^{-1})	No. of patches
no cyclic nucleotide	1.10 ± 0.08	$1.2\times10^{-4} \pm 1.4\times10^{-5}$	0.1	909	7
100 µM cGMP	93.2 ± 10.6	0.99 ± 0.001	1062	10.7	5
2 mM cAMP	75.2 ± 5.4	0.99 ± 0.002	1317	13.3	4

The mean open time τ_o, at 0 µM cGMP, was calculated according to equation (7). P_o is the open probability. The rate constants, k_{CO} and k_{OC} were determined from the means according to equations (9 a and b).

If conformational changes associated with the pore opening are rate limiting for the activation process, then the binding of cGMP, and the associated reactions, must be much faster than the allosteric reaction of the CNG channel opening. Ruiz and Karpen (1997, 1999) reported that partially liganded CNGA1 channels open frequently to sublevels and sometimes as reported by Kusch et al. (2004) to superlevels. If the cGMP binding reaction plus the associated reactions are much faster than the allosteric opening reaction, then cGMP jumps from 0 to concentrations close to the saturating values should generate single channel currents opened to the stable level observed under steady-state conditions. On the other hand, if the cGMP binding reactions plus the associated reactions are slower than the allosteric opening reaction then the single channel should reach the steady-state level by first passing sublevels and superlevels.

Using the flash-photolysis technique, we could test this hypothesis by studying the activation of CNGA1 and CNGA2 single-channel currents. The channels were activated by cGMP steps from zero to a concentration close to the saturating values. The CNGA1 and CNGA2 channels activated by stepping directly to the level observed at saturating concentration (Figure 34 a,b). No intermediate levels or superlevels were passed when the CNG channel switched from the closed to the open state. In particular for CNGA1 channels this result supports the notion that the binding of cGMP is much faster than the allosteric reaction.

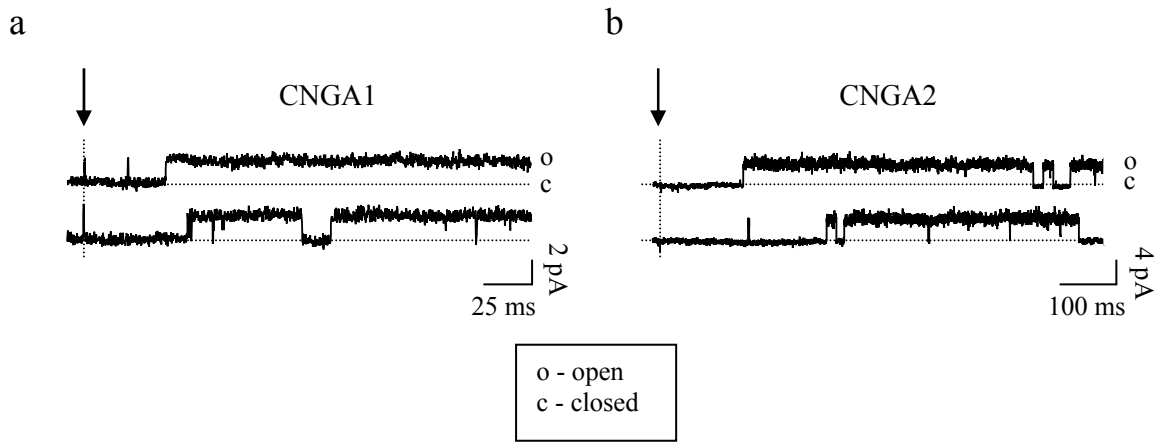

Figure 34. Flash-photolysis induced activation of single CNGA1 and CNGA2 channels. Consecutive traces of CNGA1 (a) and CNGA2 (b) single channels activated by 81.26 µM cGMP and 7.2 µM cGMP, respectively. The cGMP concentrations were estimated from macroscopic current activated with the same concentration of the caged cGMP (DEACMcGMP for activation of CNGA2 channels and BCMACMcGMP for activation of CNGA1 channels). The black arrow represents the time point when the light flash was applied and the free cGMP was released from the caged compound.

3.3. Kinetic models

Based on the time constants that characterize the kinetics of cNMP-steps induced CNGA2 currents and the kinetic parameters of non-liganded and fully liganded single channels, kinetic models were fitted to the data. For the fits, to reduce the number of free parameters, we used the open probability P_o and the mean open time τ_o determined at both zero and saturating cNMP concentration. Assuming that at both conditions each model reduces to a two-state model according to

$$C \underset{k_{OC}}{\overset{k_{CO}}{\rightleftharpoons}} O \qquad \text{(Scheme 3)}$$

the rate constants k_{CO} and k_{OC} could be calculated directly from the means in Table 7 according to

$$k_{CO} = P_o/[\tau_o(1-P_o)] \qquad (9a)$$

$$k_{OC}=1/\tau_o \qquad (9b)$$

The models were globally fitted to seven traces covering a wide range of cGMP concentrations (Figure 35). The traces were selected such that the time constants obtained by the fit with a biexponential function maximally matched the means provided by Figure 31. The current amplitudes were normalized with respect to the determined open probability at each concentration. The rate constants for the transition $C_2 \leftrightarrow O_2$ were equated to those of the transition $C_1 \leftrightarrow O_1$ because the fitting routine reduced the open probability of the single liganded channel consistently to lower values than that of the non-liganded channel, which is counterintuitive.

In the first phase of our modeling strategy, the Monod-Wyman-Changeux (MWC) model, the Coupled-Dimer (CD) model and also variations of these models with different numbers of open states and binding reactions were tested.

With a Monod-Wyman-Changeux model (Scheme 2) with four binding reactions (c.f. Goulding et al., 1994) the rate constants k_3 and k_4 were determined with:

$$P_o(0)=k_3/(k_3+e^4k_4) \tag{10a}$$

$$\tau_o(0)=1/e^4k_4 \tag{10b}$$

$$P_o(\text{sat})=f^4k_3/(f^4k_3+k_4) \tag{11a}$$

$$\tau_o(\text{sat})=1/k_4. \tag{11b}$$

To solve these equations, two different allosteric parameters, e and f, had to be used (Scheme 4). Using the values from Table 7, the results were $k_3 = 1.09\text{x}10^{-1}\ s^{-1}$, $k_4=10.73\ s^{-1}$, $f=9.94$, $e=3.03$. The fit yielded $k_1=3.03\text{x}10^6\ M^{-1}s^{-1}$ and $k_2=3.24\ s^{-1}$.

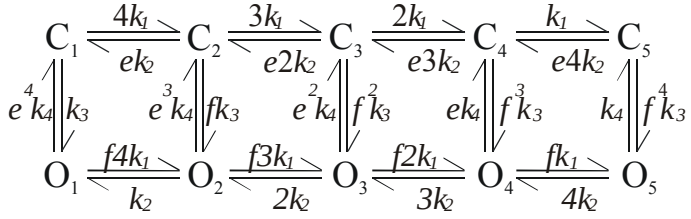

(Scheme 4)

The fit with the MWC model with the binding of four ligands to equivalent sites shows that this type of model does not adequately describe the activation time course and the steady-state current at the same time (Figure 35a). Particularly inconsistent is that the model predicts pronounced sigmoidal activation whereas the experimental data are exponential.

The Coupled-Dimer (CD) model (Liu et al., 1998) predicts that each dimer can bind two ligands and the channel is assumed to be open only if both dimers are in an open state. In the case of the fit with the Coupled-Dimer model (Scheme 5): the rate constants k_3 and k_4 were determined from the relations:

$$P_o(0)=[k_3/(k_3+e^2k_4)]^2 \quad (12a)$$

$$\tau_o(0)=1/2e^4k_4 \quad (12b)$$

$$P_o(sat)=[f^2k_3/(f^2k_3+k_4)]^2 \quad (13a)$$

$$\tau_o(sat)=1/2k_4. \quad (13b)$$

Again, two different allosteric parameters, e and f, were used. The results were k_3=5.03 s^{-1}, k_4=5.36 s^{-1}, f=14.52, e=9.19. The fit yielded k_1=2.8x10^6 $M^{-1}s^{-1}$ and k_2=4.6 s^{-1}.

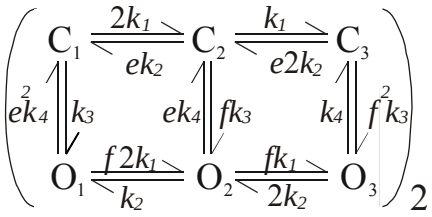

(Scheme 5)

When fitting the data with the CD model we obtain also a negative result, the sigmoidicity was too large (Figure 35b). It should be stressed, however, both models can fully describe the steady-state currents alone, reflecting the dose-response relationship (not shown).

Further were tested 11 variants of the MWC model and 7 variants of the CD model, differing in the number of open states (3 to 5) and the number of ligands (2 to 4). Similar with the results obtained when fitting the data with the MWC model, all these variants produced activation time courses with too much sigmoidicity.

Therefore, cooperative models with unequal binding sites were considered. There were fitted 78 different models (1) with two, three, or four binding reactions, (2) with ligand binding in the closed and open states, only in the closed states, and all intermediate cases, and (3) with all combinations of transitions between partially liganded closed and open states.

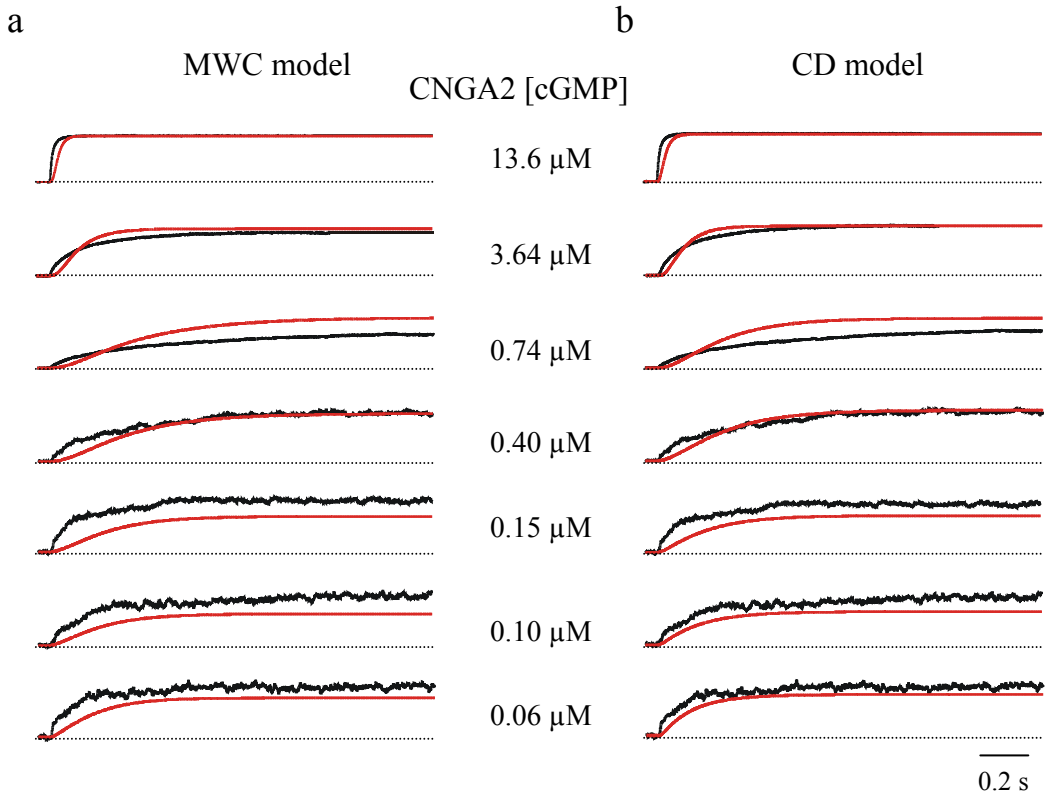

Figure 35. Kinetic schemes with independent ligand binding are inadequate to describe the time courses of cGMP-step induced activation of CNGA2 channels. Seven normalized current traces (black curves) covering a wide range of concentrations were globally fitted (red curves). (a) Monod-Wyman-Changeux (MWC) model with four binding reactions. (b) Coupled-Dimer (CD) model.

Best fits were obtained with models where all rate constants of binding and unbinding were free parameters. Models with three binding reactions were significantly superior over those with only two binding reactions. The models with four binding reactions were "reduced" by the fit to models with three binding reactions by setting P_o of the fully liganded state to paradoxically low values at high cGMP. Moreover, among models with three binding steps, those with ligand binding in the closed states only were superior over those with ligand binding in both closed and open states.

The model with the best fit includes pronounced negative and positive cooperativity for the second and third binding reaction, respectively (Figure 36a): The first binding event is fast and does not lead to noticeable opening. The second binding event is by three orders of magnitude slower but switches to a state from which opening is extremely promoted. The third binding event is fast again and channel opening is similarly stabilized as for the double-liganded channel.

In conclusion: the sequence of the ligand affinity for the three binding reactions is high, low, high and only the second binding reaction switches the open probability from extremely low to extremely high values.

Fitting this model to respective traces activated with cAMP steps produces a similar pattern of rate constants as with cGMP steps (Figure 36b). The main difference between both cyclic nucleotides is that with cAMP the rate constants for the three binding reactions are slowed by similar factors, ranging from 27 to 65, whereas the unbinding reactions differ by less than fourfold. At the respective EC_{50} values, the first two binding events are similarly fast whereas the third binding event is more than two times slower with cAMP than with cGMP. The faster activation time course with cAMP than with cGMP, if compared with respect to the EC_{50} values (c.f. Figure 31), results from the faster transition $C_3 \leftrightarrow O_3$, indicative that the cyclic nucleotide does not only determine the binding reaction but also modulates the opening reaction.

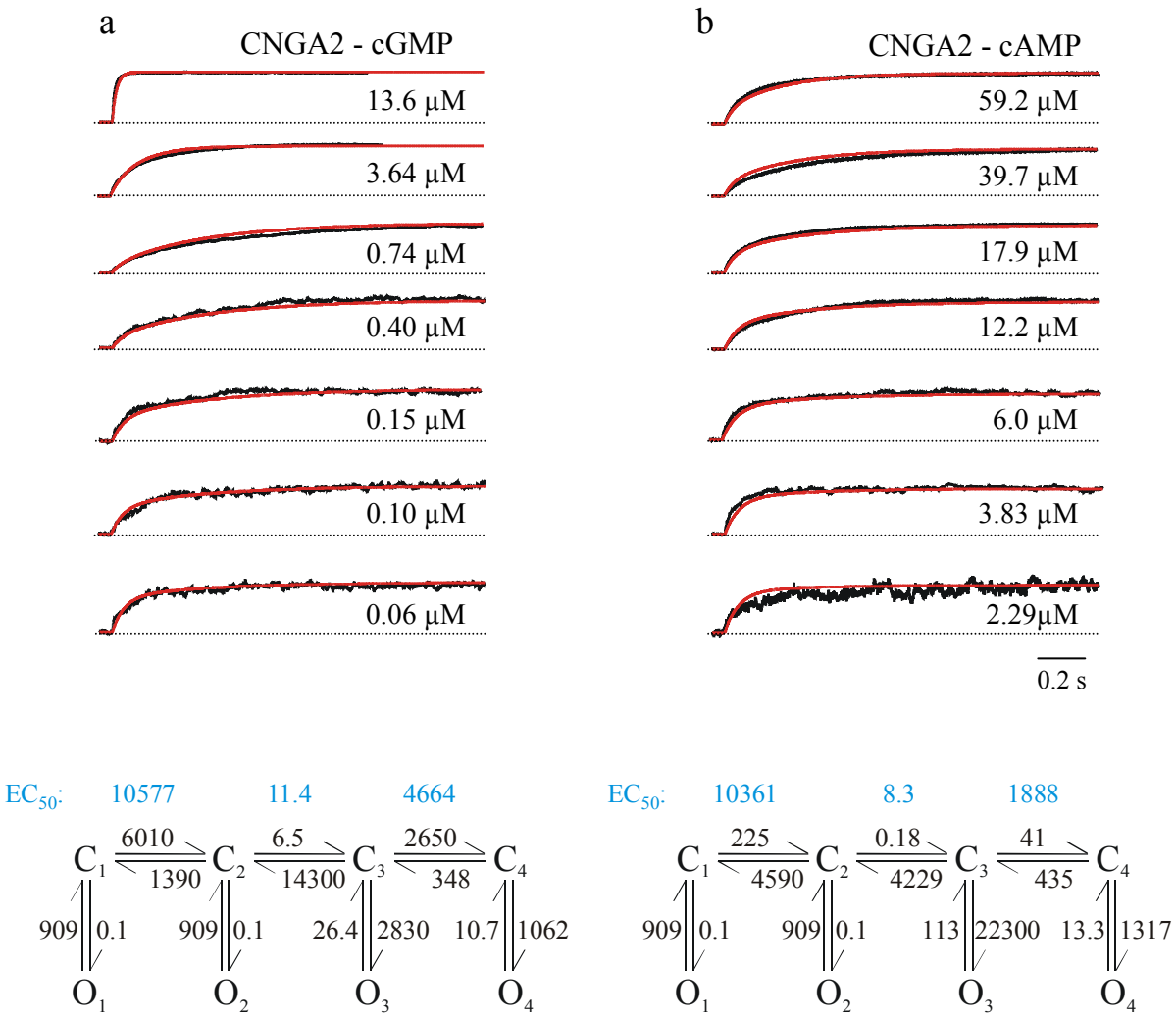

Figure 36. Kinetic scheme describing activation time courses of CNGA2 channels induced by concentration steps of the cyclic nucleotide. Seven normalized current traces (black curves) covering a wide range of concentrations were globally fitted (red curves). The black numbers in the kinetic schemes indicate rate constants with the units $M^{-1}s^{-1}$ for the binding reactions and s^{-1} for all other reactions. The blue numbers indicate rate constants at the EC_{50} value with the unit s^{-1}. (a) cGMP steps. The model with three highly cooperative binding events describes both the activation time courses and the steady-state currents (dose-reponse relationship) adequately. (b) cAMP steps. The rate constants at saturating cAMP were determined from single-channel recordings at 2 mM cAMP (Tabel 7, Figure 34b). The three binding reactions are slowed 36 to 54 fold with respect to cGMP.

4. Discussion

In this study, CNG channel activation by flash-photolysis induced jumps of cGMP or cAMP has been investigated. We focused on studying the current under non-steady state conditions to gain insights in the sequence of conformational changes that are not accessible with measurements under steady-state conditions. In addition, the flash photolysis-induced activation time course of CNG channels was compared to that induced by voltage jumps.

4.1. Dose-response relationships

The standard approach to study the activation of CNG channels is to measure the dose-response relationship for cNMPs under steady-state conditions. To characterize a dose-response-relationship, generally the Hill equation (2) is used. This equation characterizes a concentration leading to 50% activation (EC_{50}) and an exponent (H, Hill coefficient) that defines the steepness of the relationship and thus represents an estimate for the numbers of ligand binding to the channel when assuming infinite cooperativity (Hill, 1910). When this model is applied to channel activation, the unliganded channel is assumed to be closed and the fully liganded channel is assumed to be open.

In both channels, CNGA1 and CNGA2, the relation between the CN concentrations and channel opening is steep, with a Hill coefficient between 1.95 and 2.35 on double-logarithmic coordinates (Table 4 and 5). This implies that at least two molecules of cGMP or cAMP are necessary for activation of the channels. When working on rod single channels locked in different liganded states, Ruiz and Karpen (1997) showed that the binding of three cGMPs is needed for a significant opening of the channels. However, the Hill coefficients reported so far for the CNG channels are quite variable, ranging from 1.5 to 3.4. Ruiz et al. (1999) offered one possible explanation for the variability of the slope of the dose-response relationships. They suggested that shallow dose response-relationships arise in macropatches from mixtures of channels with high Hill coefficients and variable sensitivity to cyclic nucleotides.

Because of the steepness of the dose-response relationships in the physiological range of concentration (less than 5 μM cGMP in retinal rods), a small variation in the CN concentration in the cytoplasm causes a large change in the open probability. This is of

great importance for the phototransduction cascade because it contributes to a high amplification at low light intensities.

For the CNGA1 channel from rod photoreceptors, cGMP is a much more efficient agonist than cAMP, i.e. saturating cGMP concentrations cause much higher open probability than saturating cAMP concentrations. This difference between the cyclic nucleotides is consistent with the central role of this second messenger in visual signal transduction (Stryer, 1986).

The CNG channels from the olfactory sensory neurons are opened equally well by cAMP and cGMP (Figure 12a, 13a). In addition, it is shown herein that CNGA2 channels are 26.2 times less sensitive to cAMP than to cGMP (Figure 13a, Table 5). Similar results were obtained by Bradley et al. (1994); they reported that the EC_{50} of cGMP is about 30 times smaller than that of cAMP and a major portion of this difference is explained by differences in the binding reaction and not in the gating process.

Moreover, it is shown that the temperature doesn't have an influence on the EC_{50} value for CNGA2 channels. When decreasing the temperature from 20.3° C to 10.3° C, the EC_{50} value for cGMP remained nearly unchanged (1.7 µM cGMP) (Figure 12a, b).

The present data are in line with the previous results showing that homotetrameric CNGA2 channels from olfactory sensory neurons (OSNs) have a much higher sensitivity for cGMP than homotetrameric CNGA1 channels (Figure 12a, c). At 20.3° C, the EC_{50} value for CNGA2 channels for cGMP is 26 times smaller than that for CNGA1 channels (Table 4).

The EC_{50} values obtained in this study, 1.76 µM for CNGA2 channels and 46.5 µM for CNGA1 channels**,** fit with the ones reviewed by Trudeau and Zagotta in 2003 (2 µM cGMP for CNGA2 channels, 40-60 µM cGMP for CNGA1 channels).

The present data also confirm the EC_{50} value of CNGA2/A4/B1b channels, suggesting that our channels were also composed of 2 CNGA2 subunits, one CNGA4 subunit, and one CNGB1b subunit (Zheng and Zagotta, 2004). Coexpression of CNGA2 with CNGA4 and CNGB1b subunits results in similar efficiency of cGMP and cAMP. In addition, the EC_{50} value for CNGA2/A4/B1b channels with cAMP, determined herein (4.53 µM; Figure 13b, Table 5) is very close to that of native olfactory channels of 4 µM cAMP (Bönigk et al., 1999; Trudeau and Zagotta, 2003). This result shows that CNGA4 and CNGB1b subunits increase the sensitivity of the CNGA2 channel to cAMP by a factor of 10 (Figure 13a, Table 5).

Numerous studies focused on the molecular basis of ligand sensitivity and selectivity. The search for key residues involved in binding and gating was guided by previous work on

ligand binding and activation in PKA, PKG, and the CAP protein. It was revealed that several regions determine the apparent affinity of CNG channels, including the cNMP-binding domain, the C-linker region, the N-terminal domain, and the pore region (Möttig et al., 2001).

Using chimeras constructed between the CNG channel from vertebrate photoreceptors and from the OSNs, it could be confirmed that the N-terminus is one of the determinants of the characteristic EC_{50} of CNG channels. The olfactory N-terminus decreased the EC_{50} value compared to the rod N-terminus (Figure 14a,b). Chimera o1r, CNGA1 channel with CNGA2 N-terminus, has a lower EC_{50} value compared to that of the CNG channel from photoreceptors (9.41 µM cGMP compared to 46.5 µM) and chimera r1o, CNGA2 channel with CNGA1 N-terminus, have a higher EC_{50} value compared to that of the CNG channel from OSNs (7.28 µM cGMP compared with 1.76 µM cGMP) (Table 6). Moreover, the inserted N-terminus determined not only a change of the EC_{50} value but also influenced the speed of the activation process. These results show that the N-terminus is one of the rate limiting factors for the CNG channels activation.

Gordon et al. (1997) reported that CNGA1 channels form a disulfide bond between the cysteine residues at position 35 in the amino-terminal region and 481 in the C-linker of the carboxyl-terminal region. They conclude that this interaction between the N-terminus and the C-linker stabilizes the open state by a decrease of both the EC_{50} value and the number of ligands required for opening. Due to the fact that the olfactory N-terminus does not contain the respective CNGA1 cysteine residues, the N-terminus must stabilize the open state by a mechanism, which does not involve the disulfide bound discussed above (Möttig et al., 2001).

4.2. Activation kinetics of CNG channels

4.2.1. Activation kinetics by CN concentration jumps

Flash-photolysis of caged CN was used to examine the conformational changes associated with the gating of CNG channels. The response of the channels to the liberated CN caused a rapid increase of the current to a stable level. After a few seconds the current decreased slowly due to the replacement of the CN by ligand-free solution (Figure 7). Similar time courses of the photolysis-induced current were observed when testing two caged

compounds, caged 8-Br-cAMP and caged 8-Br-cGMP, on CNG channels of bovine olfactory sensory neurons (Hagen et al., 1996). Karpen and coworkers (1988) studied the flash-induced activation of CNG channels from the rod outer segments of the larvar tiger salamander, *Ambystoma tigrinum*, and they observed fast activation. The current reached a maximum in less than 200 ms. The following decline was slow. Karpen and coworkers (1988) attributed the slow decline to a drop in cGMP concentration near the membrane due to the formation of a small slab of adhering disc rims at the cytosolic face of the patch.

In our experiments, the activation of homotetrameric CNGA2 channels by cGMP and cAMP jumps displayed a characteristic profile: starting form the lowest ligand concentration tested, the activation time constants decreased until a minimum, then increased with a maximum close to the EC_{50} value and further decreased (Figure 28a). Furthermore, activation of heterotetrameric CNGA2/A4/B1b with cAMP showed similar time constants to those of the homotetrameric CNGA2 channels when related to the EC_{50} value (Figure 31).

These results show that at all cyclic nucleotide concentrations larger than the minimum the activation cannot be rate limited by the binding of the ligand but by conformational changes within the channel protein. At concentrations below the minimum, the decrease of the activation time constants with increasing ligand concentrations suggests that another process is rate limiting for the activation process than at concentrations larger than the minimum. This process could be either the binding of the ligands to their binding sites or specific conformational changes of the channel preceding those limiting the activation speed at higher CN concentrations. The similarity of the activation time courses at the lowest cAMP and cGMP concentrations strongly suggests that the binding alone cannot be the rate-limiting process at the lowest CN concentrations. If the profile of the time constants at low CN concentrations describes conformational changes of the channel associated with the binding of the ligand then these time constants would characterize conformational changes following the binding. The ligand binding itself must be faster than these conformational changes.

CNGA1 channels also produce maximally slow time constants close to the EC_{50} value. However, at the lowest concentrations where reasonably larger currents could be elicited, the time constants did not decrease to higher concentrations (Figure 17b). One may speculate that this difference to olfactory channels is caused by the fact that for CNGA1 channels measurements at sufficiently low concentrations are simply impossible because of the low sensitivity of these channels to cyclic nucleotides.

Comparing the over-all activation time course of CNGA1 and CNGA2 channels, activation of CNGA2 channels is about 20 times slower than the activation of CNGA1 channels. When studying native CNG channels from salamander olfactory-receptor neurons and recombinant rat olfactory CNG channel exposed to short pulses of known concentrations of cGMP or cAMP, Zufall et al. (1993) observed that both the activation and deactivation kinetics of the olfactory CNG channels were much slower than the rapid changes in CN concentration. However, methodical limitations associated with the used solution switcher should be taken into account when interpreting these data. Kinetic data obtained from phototransduction studies showed that the rate constant for retinal CNG channel activation is at the diffusion-control limit, and the channel responds to the instantaneous cGMP change (Yau and Baylor, 1989). A slower activation of olfactory CNG channels compared to that of retinal channels (Karpen et al., 1988) was also reported by Hagen et al. (1996). In this study on CNG channels from bovine olfactory sensory neurons, these authors used flash photolysis of caged 8-Br-cAMP and caged 8-Br-cGMP. The difference in the activation time course between the two CNG channels might closely mirror the different requirements of the two sensory cascades: The olfactory receptor cell has to discriminate between a large number of different odor molecules. To achieve this without loss of sensitivity it appears to use an intracellular amplification system that gains increased sensitivity at the expense of extended time. In contrast, photoreceptors have only to sense light and often quick changes of the light intensity have to be processed.

The finding that the activation time course of the heterotetrameric CNGA2/A4/B1b channels (Figures 31) matches the one of homotetrameric CNGA2 channels indicates that both types of channels work similar. The difference between the homo- and heterotetrameric channels lies in the ligand binding whereas the allosteric reaction of channel must be similar. This conclusion is noticeable because two of the four subunits are different. Possible explanations are that the CNGA4 and CNGB1b subunit contribute similarly to the allosteric reaction like their CNGA2 counterparts in homotetrameric channels. Alternatively, the CNGA4 and/or the CNGB1b subunit could not be involved in the allosteric reaction. Because of the similarity of the activation time course in homo- and heterotetrameric channels, this would mean in turn that also in homotetrameric channels activation is rate limited by either two or three subunits only.

When studying the activation of CNGA2 channels as function of both ligands, cGMP and cAMP, and also of CNGA2/A4/B1b as function of cAMP, we observed that the contributions of the fast and slow component, A_{fast} and A_{slow}, were roughly similar (Figures

19, 29 and 32). For both homotetrameric and heterotetrameric channels the slow exponential dominates at intermediate concentrations of the ligand and the fast exponential dominates at both low and high concentrations.

In addition, using N-teminal chimeras between the CNG channels from vertebrate photoreceptors and OSNs, it was observed that the activation time course followed a similar pattern as for homotetrameric CNGA1 and CNGA2 channels. The o1r and r1o activation time constants showed a maximum around the EC_{50} value. Moreover, the inserted N-terminus determined not only a change of the EC_{50} value but also the activation speed of the chimera. These results show that the activation of the channels is a complex allosteric process which is rate limited not only by transmembrane parts but also by intracellular domains, as the N-terminus.

When studying the voltage dependence of the gating kinetics of olfactory channel with short pulses of CN concentrations, Zufall et al. (1993) observed that the activation of the current, in contrast to deactivation, was voltage independent and they suggested that the entire voltage sensitivity for channel activation is determined by the rate constant of channel closing. Herein, we confirmed that the activation time course of CNGA2 is voltage independent (Figure 20). On the other hand, CNGA1 channels showed pronounced voltage dependence of activation (Figure 15). The cause of this difference between the channels remains unknown.

4.2.2. Activation kinetics by voltage jumps

Voltage-dependent activation of CNGA1 and CNGA2 channels was studied by depolarizing the membrane and studying macroscopic currents at a constant concentration of CN. At subsaturating concentrations of cGMP and cAMP, the current underwent a time-dependent increase to a steady-state level.

Working on CNGA1 channels, Benndorf et al. (1999) showed that when changing the voltage from negative to positive values, the mean open time increases dramatically and concomitantly the frequency of openings decreased. The increase of the open time is explained by unresolved closures due to immediately reopening of the fully liganded channel. When depolarizing multichannel CNGA1 patches from -100 to +100 mV, herein it was observed the activation time course could be described with a sum of two exponentials (Figure 23), similar to the activation time course following CN jumps. In case

of CNGA2 activation by the same voltage steps, the activating component could be described with a single exponential (Figure 24) though activation by CN jumps was biexponential. It is therefore presumed that CNGA2 channels activation induced by cyclic nucleotide concentration jumps is a complex process which includes reactions absent in the voltage-step induced activation. In contrast, in CNGA1 channels, activation by voltage steps and CN jumps is rate limited by similar reactions.

In CNGA2 channels and low CN concentrations, voltage dependent activation significantly differs from activation induced by CN jumps. This finding can be interpreted in the way that at low cGMP both types of activation are rate limited by different reactions, possibly by conformational changes associated with the ligand binding.

Voltage-dependent activation in the CNG current from salamander rod outer segments was also observed by Karpen et al. (1988) when switching the voltage from -50 to +50 mV. They reported that activation became faster as the cGMP concentration increased and reached a limiting rate above 50 μM. This shows that an intramolecular conformational change becomes rate limiting at high concentrations. The differences to our results could be explained by the fact that Karpen's study was performed on native channels. Several studies showed previously that all aspects of channel activation are influenced by the subunit composition of CNG channels and by the system they are expressed in (Bradley et al., 2001; Bönigk, et al., 1999; Dzeja, et al., 1999). However, there are a number of points to be taken into consideration. First, in a series of experiments with rat heterotetrameric CNGA2/A4/B1b channels, expressed in *Xenopus* oocytes, voltage-dependent activation time course underwent a similar pattern as for homotetrameric CNGA1 and CNGA2 channels (data not shown). The only difference consists in the fact that the activation kinetic of heterotetrameric channels were described by a sum of two exponentials. Second, in the study of Karpen et al. (1988) the experiments were performed in Na^+-containing solution whereas in this study a K^+-containing solution was used. Significant influence of the permeating ions on the gating of CNG channels has been shown by Bucossi et al. (1997) and Kusch et al. (2004). Hence, effects of the permeating ions on the gating could account for the differences between the results.

4.2.3. Temperature dependence of CNGA2 activation

Reaction rates depend on the temperature in a characteristic manner. The Q_{10} value describes this dependence. Q_{10} values of ~1.4 suggest that diffusional processes rate-limit the reaction whereas larger Q_{10} values suggest that conformational changes are rate limiting. The temperature dependence of the gating of ion channels has been studied extensively (Hodgkin and Huxley, 1952; Bezanilla and Taylor, 1978; Benndorf and Koopmann, 1993; Correa et al., 1992). Enthalpic and entropic components have been considered.

Studying the gating kinetics of Batrachotoxin-modified Na^+ channels, Correa et al. (1992) reported that the main effect of an increase in temperature on channel kinetics consists of an increase in the transition rates and a shift of the open probability to more positive potentials. They also showed that an increase in temperature seems to favor the closed states over the open configuration.

A modest temperature dependency with a Q_{10} between 1.5 and 2.5 has been reported for rapidly activating, voltage-gated Na^+- and K^+-currents in neuronal and in muscular tissues (Beam and Donaldson, 1983; Frankenhaeuser and Moore, 1963). On the other hand, for the very slowly activating, voltage-gated potassium conductance, I_{Ks}, recorded in guinea pig cardiac myocytes, an increase in temperature resulted in an acceleration of activation with a Q_{10} of 4-6 (Bachmann et al., 2001).

In this study, the effect of the temperature on the CNGA2 channel activation was investigated to distinguish between diffusion or conformational changes rate limiting the activation process.

When lowering the temperature from 20.3°C to 10.3°C, both time constants, τ_{fast} and τ_{slow}, increased. At 10.3°C, the activation kinetics of CNGA2 channels were basically similar to the one at 20.3°C but only much slower (Figure 21a). If a simple diffusion-limited mechanism would have been responsible for the CNG gating, a Q_{10} of ~1.4 (Pusch et al., 1997) would have been expected. The resulting Q_{10} values were between 1.4 and 3.5 (Figure 21b). Because at low cGMP the Q_{10} values clearly exceeded the theoretical value for diffusion, it is concluded that also at the lowest ligand concentration used, conformational changes within the channel protein are rate limiting for the activation process and not diffusion of the ligand to the binding sites.

Based on the characteristic dependence of Q_{10} values on the cGMP concentration, it is assumed that activation is rate limited by more then one conformational change. These

different conformational changes seem to influence the activation time course in different concentration ranges. The result that diffusion is not rate limiting for the CNG activation process could be confirmed with cAMP concentration steps at the lowest concentrations (see 4.2.1.) (Figure 28).

Nevertheless, with a Q_{10} value between 1.4 and 3.5, it can be concluded that temperature has only mild effects on the CNG gating, which is compatible with the idea of structurally simple conformational changes compared to e.g. ClC-0 chloride channels showing a Q_{10} value of as much as 40 (Pusch et al., 1997).

Fitting of the data at 10.3°C to the model used to describe activation (Figure 36) should give more insight into the conformational changes of the channel during activation. Moreover, one can expect further insight into the temperature dependence of the individual rate constants.

Apart from being a biophysical tool, the temperature dependence of the activation may also be of physiological importance, e.g., when evaluating the smelling at low temperatures.

4.2.4. Single-channel properties

We observed that at saturating cGMP and cAMP and at +100 mV, CNGA2 channels open to a single level (Figure 33a,b). Furthermore, the channels activate by switching directly to this level without any sublevels preceding the main open level. A direct switching to the open level was also observed when studying CNGA1 and CNGA2 single-channel currents by jumps of the cGMP concentration to a value close to the saturating concentration (Figure 34).

Ruiz and Karpen (1997, 1999) reported that CNGA1 channels locked in partially liganded states by the use of a photoaffinity analogue of cGMP, 8-*p*-azidophenacylthio-cGMP (APT-cGMP) produce distinct sublevels, which they also identified with freely diffusible cGMP. In a previous study on CNGA1 channels (Kusch et al., 2004), it was shown that a saturating concentration of cGMP generates long openings at a single open level whereas low cGMP concentrations generate short openings with a great variability of levels, including sublevels and superlevels. The differences between the results of Ruiz and Karpen (1997,1999) and the amplitude heterogeneity found by Kusch and coworkers (2004) possibly arise from the slower time course of the allosteric reaction compared to the binding/unbinding reaction of the free cGMP. Permanent binding of the APT-cGMP could

alter the channel gating and thereby cause different results regarding single-channel conductance.

Another finding in this study is the similarity of the gating paramenters at saturating cGMP and cAMP (Table 7). This similarity confirms that both CNs can maximally activate the olfactory channel (Figure 33a,b) and that also the open-close gating is equal. The open probability of the channel is 0.99 with both ligands. Li and Lester (1999) reported similar results at -60 mV; they observed that cGMP and cAMP produce comparable probability for the conformational transition to open rat CNGA2 channels. On the other hand, macroscopic currents were interpreted such that cGMP favors to open the channel significantly compared to cAMP (Varnum et al., 1995).

Previous work on multichannel patches suggested that CNG channels are able to open spontaneously with very low open probability in the absence of ligand. These spontaneous openings are part of the normal gating reaction of the CNG channel (Tibbs et al., 1997). The open probability has been estimated to be 1.25×10^{-4} for chimeras between CNGA1 and CNGA2 channels (Riuz and Karpen, 1997) and 2.25×10^{-3} for rat CNGA2 channels. In the absence of the cyclic nucleotide, we observed very brief openings of the CNGA2 channels with an open probability of $1.2\times10^{-4} \pm 1.4\times10^{-5}$. This value is lower than the one of CNGA2 channels reported previously. Since there is a much higher risk to overestimate than to underestimate the open probability, our lower value might be closer to the truth.

The analysis of single-channel currents allowed us to specify the rate constants at zero and saturating CN, which helped to reduce the number of free parameters in the fitting strategies with the kinetic models.

4.3. Kinetic models

The contradictory results of the previous studies upon the activation mechanism of CNG channels show that our knowledge of the molecular events underlying the gating is only poor. So far it is not known whether activation depends on independent gating reactions within the individual subunits of the channel as first suggested by Hodgkin and Huxley (1952) for Na^+ and K^+ channels, or on a concerted, cooperative interaction of the subunits, as suggested by Monod et al. (1965). Studies of the gating properties of heterotetrameric channels composed of both mutant and wild type subunits have provided evidence for a cooperative interaction among subunits of both K^+ channels (McCormack et al., 1994) and

CNG channels (Varnum and Zagotta, 1996). However, these studies could not measure the contribution of each subunit to channel gating.

To address some of these questions, kinetic models were fitted to the CNGA2 activation time courses induced by cGMP and cAMP steps.

Our results proved to be inconsistent with the predictions of the MWC model, in which the channels open in proportion to the number of ligands bound by an allosteric factor and also with the CD model, a variant of the MWC model, where the channel opens when both dimers enter the active state. These models predict pronounced sigmoidal activation whereas the experimental data are largely exponential (Figure 35). The same conclusion was drawn when fitting the data to numerous variants of the MWC and the CD models, differing in number of open states and ligands.

Instead, the data suggest that, despite the tetrameric and presumably symmetric structure of homomeric CNG channels, activation involves only three rate-limiting binding steps, in which the ligand affinity is high-low-high (Figure 36). When fitting this model to the activation time course induced by cAMP, we observed a similar pattern of rate constants, in which the CN binding was essentially slowed. The conclusion that only three subunits determine the activation time course of CNGA2 channels is remarkable because it implies functional asymmetry of a homotetrameric channel for which a symmetric structure would be plausible.

How then is it possible that three of the four subunits are selected for the gating? The simplest explanation is that the binding of the first ligand itself generates the asymmetry by decelerating the binding reaction in the other subunits in the sense of negative cooperativity. Once the second ligand binds, the affinity for the third ligand would be strongly increased while the binding site of the fourth subunit would become inaccessible. Taking into account that native CNG channels contain one B subunit, the assumption of only three gating subunits is not so surprising because one may speculate that evolution specialized the fourth subunit to a B subunit to modulate the channel function, as e.g. recently shown for the CNGB1b subunit by calmodulin complexed with Ca^{2+} (Bradley et al., 2004). For native olfactory channels, this consideration assumes that the CNGA4 subunit also contributes to the gating.

What is the physical nature of the reactions in the favoured gating scheme? The Q_{10} values for the activation gating (Figure 21b) showed that diffusion of the ligands to the binding sites of the channel is not rate limiting. However, when varying the rate of each binding event in scheme 3 at constant affinity, it turned out that the second and third binding

reaction critically determine the activation rate. Hence, within our model these two binding reactions cannot be considered anymore as simple binding reactions but must contain also conformational changes of the channel.
Whether or not the first binding event is diffusion controlled cannot be decided from these data because this binding event does not lead to channel activation. These conclusions mean that the systematic change of the Q_{10} value with channel activation (Figure 21b) attributes to the four reactions right to C_2.
For relating these reactions to intracellular or transmembrane channel parts, it seems to be an attractive idea to systematically modify these channel parts, e.g. by mutagenesis, and study the activation time course as described herein.

In conclusion, the data show that the activation kinetics of olfactory homotetrameric CNG channels induced by CN jumps are modulated by conformational changes of the channels and not by the ligand binding over the whole concentration range tested. Moreover, the same pattern of the activation kinetic was observed also for the heteroterameric CNGA2/A4/B1b channels. Activation of homotetrameric CNGA2 channels involves rate-limiting reactions of three subunits only and the ligand binding to these subunits is highly cooperative. Only the second binding step switches the channel from a very low to a very high open probability. Moreover, even in heterotetrameric CNGA2/A4/B1b channels these conformational changes are similar. The largely different apparent affinity of the two cyclic nucleotides cGMP and cAMP is mainly caused by a faster binding reaction of cGMP whereas the allosteric opening reactions are similar.
These results represent progress toward an understanding of the molecular processes in the activation of CNG channels and might also be suggestive for structurally related voltage-gated K^+ channels (Yellen, 2002), which also form obligatory heterotetramers in nature (Ottschytsch et al., 2002).

5. References

1. Ahmad, I., Korbmacher, C., Segal, A.S., Cheung, P., Boulpaep, E.L., Barnstable, C., Mouse cortical collecting duct cells shows nonselective cation channel activity and express a gene related to the cGMP-gated rod photoreceptor channel. *PNAS*, 1992. **89**(21): 10262-10266.
2. Altenhofen, W., Ludwig, J., Eismann, E., Kraus, W., Bönigk, W., Kaupp, U.B., Control of ligand specificity in cyclic nucleotide-gated channels from rod photoreceptors and olfactory epithelium. *Proc. Natl. Acad. Sci.* USA, 1991. **88**(21): 9868-9872.
3. Bacigalupo, J., Johnson, E.C., Vergara, C., Lisman, J.E., Light-dependent channels from excised patches of Limulus ventral photoreceptors are opened by cGMP. *PNAS*, 1991. **88**(18): 7938-7942.
4. Baumann, A., Frings, S., Godde, M., Seifert, R., Kaupp, U.B., Primary structure and functional expression of a Drosophila cyclic nucleotide-gated channel present in eyes and antennae. *EMBO J.*, 1994. **13**(21): 5040-5050.
5. Becchetti, A., Gamel, K., Torre, V., Cyclic nucleotide-gated channel: Pore topology studied through the accessibility of reporter cysteines. *J.Gen.Physiol.*, 1999. **114**(3): 377-392.
6. Becchetti, A., Gamel, K., The properties of cysteine mutants in the pore region of cyclic nucleotide-gated channel. *Pflungers Arch.*, 1999. **438**(5): 587-96.
7. Benndorf, K., Low-noise recording. In: Single-channel recording. E. Neher and B. Sakmann, Hrsg., *Plenum Press*, New York, London, 1993: 129-145.
8. Benndorf, K., Koopmann, R., Eismann, E., Kaupp, U.B., Gating by cyclic GMP and voltage in the α subunit of the cyclic GMP-gated channles from rod photoreceptors. *J. Gen. Physiol.*, 1999. **114**(4): 477-490.
9. Bennett, N., Ildefonse, M., Crouzy, S., Chapron, Y., Clerc, A., Direct activation of cGMP-dependent channels of retinal rods by the cGMP phosphodiesterase. *Proc. Natl. Acad. Sci.* USA, 1989. **86**(10): 3634-3638.
10. Biel, M., Altenhofen, W., Hullin,R., Ludwig, J., Freichel, M., Flockerzi, V., Dascal, N., Kaupp, U.B., Hofmann, F., Primary stucture and functional expression of a cyclic nucleotide-gated channel from rabit aorta. *FEBS Letters*, 1993. **329**(1-2): 134-138.

11. Biel, M., Zong, X., Distler, M., Bosse, E., Klugbauer, N., Murakami, M., Flockerzi,V., Hofmann, F., Another member of the cyclic nucleotide-gated channel family, expressed in testis, kidney and heart. *PNAS*, 1994. **91**(9): 3505-3509.
12. Bönigk, W., Bradley, J., Müller, F., Sesti, F., Boekhoff, I., Ronnett, G., Kaupp, U.B., Frings, S., The native rat olfactory cyclic nucleotide-gated channel is composed of three distinct subunits. *J. Neurosci.*, 1999. **19**(13): 5332-5347.
13. Bradley, J., Bönigk, W., Yau, K.-W., Frings, S., Calmodulin permanently associates with rat olfactory CNG channels under native conditions. *Nat. Neurosci.*, 2004. **7**(7): 705-710.
14. Bradley, J., Frings, S., Yau, K.W., Reed, R., Nomenclature for ion channel subunits. *Science*, 2001. **294**(5549): 2095-2096.
15. Bradley, J., Li, J., Davidson, N., Lester, H.A., Zinn, K., Heteromeric olfactory cyclic nucleotide-gated channels: a subunit that confers increased sensitivity to cAMP. *Proc. Natl. Acad. Sci.* USA, 1994. **91**(19): 8890-8894.
16. Bradley, J., Zhang, Y., Bakin, R., Lester, H.A., Ronnett, G., Zinn, K., Functional expression of the heteromeric olfactory cyclic nucleotide-gated channel in the hippocampus: A potential effector of synaptic plasticity in brain neurons. *J. Neurosci.*, 1997. **17**(6): 1993-2005.
17. Bucossi, G., Eismann, E., Sesti, F., Nizzari, M., Seri, M., Kaupp, U.B., Torre, V., Time-dependent current decline in cyclic GMP-gated bovine channels caused by point mutations in the pore region expressed in *Xenopus* oocytes. *J. Physiol.*, 1996. **493** (Pt 2): 409-418.
18. Careaga, C.L., Falke, J.J., Structure and dynamics of *Escherichia coli* chemosensory receptors.Engineered sulfhydryl studies. *Biophys. J.*, 1992. **62**(1): 209-216.
19. Chen, T.Y., Peng, Y.W., Dhallan, R.S., Ahamed, B., Reed, R.R., Yau, K.W., A new subunit of the cyclic nucleotide-gated cation channels in retinal rods. *Nature*, 1993. **362**(6422): 764-767.
20. Cobbs, W.H., Barkdoll, A.E. 3rd, Pugh, E.N. Jr., Cyclic GMP increases photocurrent and light sensitivity of retinal cones. *Nature*, 1985. **317**(6032): 64-66.
21. Coburn, C.M., Bargmann, C.I. A putative cyclic nucleotide-gated channel is required for sensory development and function in *C. elegans*. *Neuron*, 1996. **17**: 695-706.
22. Cook, N.J., Zeilinger, C., Koch, K.W., Kaupp, U.B., Solubilization and functional reconstitution of the cGMP-dependent cation channel from bovine rod outer segments. *J. Biol. Chem.*, 1986. **261**(36): 17033-17039.

23. Correa, A.M., Bezanilla, F., Latorre, R., Gating kinetics of batrachotoxin-modified Na+ channels in the squid giant axon. Voltage and temperature effects. *Biophys. J.*, 1992. **61**(5): 1332-1352.
24. Crary, J.L., Dean, D.M., Nguitragool, W., Kurshan, P.T., Zimmerman, A.L., Mechanism of inhibition of cyclic nucleotide-gated ion channels by diacylglycerol. *J. Gen. Physiol.*, 2000. **116**(6): 755-768.
25. Delgado, R., Hidalgo, P., Diaz, F., Latorre, R., Labarca, P., A cyclic AMP-activated K+ channel in Drosophila larval muscle is persistently activated in dunce. *Proc. Natl. Acad. Sci.* USA, 1991. **88**(2): 557-560.
26. Dhallan, S., Yau, K.-W., Schrader, K.A., Reed, R.R., Primary structure and functional expression of a cyclic nucleotide-activated channel from olfactory neurons. *Nature*, 1990. **347**(13): 184-187.
27. Distler, M., Biel, M., Flockerzi, V., Hofmann, F., Expression of cyclic nucleotide-gated cation channels in non-sensory tissues and cells. *Neuropharmacology*, 1994. **33**(11): 1275-1282.
28. Donaldson, P.L., Beam, K.G., Calcium currents in a fast-twitch skeletal muscle of the rat. *J. Gen. Physiol.*, 1983. **82**(4): 449-468.
29. Doyle, D.A., Morais, Cabral J., Pfuetzner, R.A., Kuo, A., Gulbis, J.M., Cohen, S.L., Chait, B.T., MacKinnon, R., The structure of the potassium channel: molecular basis of K+ conduction and selectivity. *Science*, 1998. **280**(5360): 69-77.
30. Dryer, S.E., Henderson, D., A cyclic GMP-activated channel in dissociated cells of the chick pineal gland. *Nature*, 1991. **353**(6346): 756-758.
31. Dryja, T.P., Finn, J.T., Peng, Y.W., McGee, T.L., Berson, E.L., Yau, K.W., Mutations in the gene encoding the alpha subunit of the rod cGMP-gated channel in autosomal recessive retinitis pigmentosa. *Proc. Natl. Acad. Sci.* USA, 1995. **92**(22): 10177-81.
32. Dzeja, C., Hagen, V., Kaupp, U.B., Frings, S., Ca2+ permeation in cyclic nucleotide-gated channels. *EMBO J.*, 1999. **18**(1): 131-144.
33. Fesenko, E.E., Kolesnikov, S.S., Lyubarsky, A.L., Induction by cyclic cGMP of cationic conductance in plasma membrane of retinal rod outer segment. *Nature*, 1985. **313**(6000): 310-313.
34. Finn, J., Grunwald, M.E., Yau, K.-W., Cyclic nucleotide-gated ion channels: An extended family with diverse functions. *Annu. Rev. Physiol.*, 1996. **58**: 395-426.

35. Flynn, G.E., Johnson Jr, J.P., Zagotta, W.N., Cyclic nucleotide-gated channels: shedding light on the opening of a channel pore. *Nat. Rev. Neurosci.*, 2001. **2**(9): 643-651.
36. Fodor, A.A., Black, K.D., Zagotta, W.N., Tetracaine reports a conformational change in the pore of cyclic nucleotide-gated channels. *J. Gen. Physiol.*, 1997. **110**(5): 591-600.
37. Frankenhaeuser, B., Moore, L.E., The effect of temperature on the sodium and potassium permeability changes in myelinated nerve fibres of Xenopus laevis. *J. Physiol.*, 1963. **169**: 431-437.
38. Frings, S., Lynch, J.W., Lindemann, B., Properties of cyclic nucleotide-gated channels mediating olfactory transduction. Activation, selectivity, and blockage. *J. Gen. Physiol.*, 1992. **100**(1): 45-67.
39. Gavazzo, P., Picco, C., Eismann, E., Kaupp ,U.B., Menini, A. A point mutation in the pore region alters gating, Ca(2+) blockage, and permeation of olfactory cyclic nucleotide-gated channels. *J. Gen. Physiol*., 2000. **6**(3): 311-326.
40. Giovannardi, S., Lando, L., Peres, P., Flash photolysis of caged compounds: Casting light on physiological processes. *News Physiol. Sci.*, 1998. **13**: 251-255.
41. Gold, G.H., Controversial issues in vertebrate olfactory transduction. *Annu. Rev. Physiol.*, 1999. **61**: 857-871. Review.
42. Goldin, A.L., Maintenance of Xenopus laevis and oocyte injection. *Methods Enzymol.*, 1992. **207**: 266-279.
43. Gordon, S.E., Zagotta, W.N., Localization of regions affecting an allosteric transition in cyclic nucleotide-activated channels. *Neuron*, 1995. **14**: 857-864.
44. Gordon, S.E., Varnum, M.D., Zagotta, W.N., Direct interaction between amino- and carboxyl-terminal domains of cyclic nucleotide-gated channels. *Neuron*, 1997. **19**(2): 431-441.
45. Goulding, E.H., Ngai, J., Kramer, R.H., Colicos, S., Axel, R., Siegelbaum, S.A., Chess, A., Molecular cloning and single-channel properties of the cyclic nucleotide-gated channel from catfish olfactory neurons. *Neuron*, 1992. **8**(1): 45-58.
46. Goulding, E.H., Tibbs, G.R., Siegelbaum, S.A., Molecular mechanism of cyclic-nucleotide-gated channel activation. *Nature*. 1994. **372**(6504): 369-374.
47. Hackos, D.H., Korenbrot, J.I., Divalent cation selectivity is a function of gating in native and recombinant cyclic nucleotide-gated ion channels from retinal photoreceptors. *J. Gen. Physiol.*, 1999.**113**(6): 799-818.

48. Hagen, V., Bendig, J., Frings, S., Eckardt, T., Helm, S., Reuter, D., Kaupp, U.B., Highly efficient and ultrafast phototriggers for cAMP and cGMP by using long-wavelength UV/Vis-activation. *Angew. Chem. Int. Ed.*, 2001. **40**(6): 1045-1048.
49. Hagen, V., Bendig, J., Frings, S., Wiesner, B., Schade, B., Helm, S., Lorenz, D., Kaupp, U.B., Synthesis, photochemistry and application of (7-methoxycoumarin-4-yl)methyl-caged 8-bromoadenosine cyclic 3',5'-monophosphate and 8-bromoguanosine cyclic 3',5'-monophosphate photolyzed in the nanosecond time region. *J. Photochem. Photobiol. B*, 1999. **53**(1-3): 91-102.
50. Hagen, V., Dzeja, C., Bendig, J., Baeger, J., Kaupp, U.B., Novel caged compounds of hydrolysis-resistant 8-Br-cAMP and 8-Br-cGMP: photolabile NPE esters. *J. Photochem. Photobiol. B*, 1998. **42**(1): 71-78.
51. Hagen, V., Dzeja, C., Frings, S., Bendig, J., Krause, E., Kaupp, U.B., Caged compounds of hydrolysis-resistant analogues of cAMP and cGMP: synthesis and application to cyclic nucleotide-gated channels. *Biochemistry*, 1996. **35**(24): 7762-71.
52. Hanke, W., Cook, N.J., Kaupp, U.B., cGMP-dependent channel protein from photoreceptor membranes: single-channel activity of the purified and reconstituted protein. *Proc. Natl. Acad. Sci.* USA, 1998. **85**(1): 94-98.
53. Haynes, L., Yau, K.W., Cyclic cGMP-sensitive conductance in outer segment membrane of catfish cones. *Nature*, 1985. **317**(6032): 61-64.
54. Henn, D.K., Baumann, A., Kaupp, U.B., Probing the transmembrane topology of cyclic nucleotide-gated ion channels with a gene fusion approach. *Pro.c Natl. Acad. Sci.* USA, 1995. **92**(16): 7425-7429.
55. Higgins, M.K., Weitz, D., Warne, T., Schertler, G.F.X., Kaupp, U.B., Molecular architecture of a retinal cGMP-gated channel: the arrangement of the cytoplasmic domains. *EMBO J.*, 2002. **21**(9): 2087-2094.
56. Hille, B., Ion channels of excitable membranes. 2nd Ed. Sunderland, Massachusetts, Sinauer Associates Inc.
57. Hodgkin, A.L., Huxley, A.F., Movement of sodium and potassium ions during nervous activity. Cold Spring Harb. Symp. Quant. Biol., 1952. **17**:43-52
58. Jiang, Y., Lee, A., Chen, J., Cadene, M., Chait, B.T., MacKinnon, R., The open pore conformation of potassium channels. *Nature*, 2002. **417**(6888): 523-526.
59. Kaplan, J.H., Somlyo, A.P., Flash photolysis of caged compounds: new tools for cellular physiology. *TINS*, 1989. **12**(2): 54-58.

60. Karpen, J.W., Zimmerman, A.L., Stryer, L., Baylor, D.A., Gating kinetics of the cyclic-GMP-activated channel of retinal rods: Flash photolysis and voltage-jump studies. *Proc. Natl. Acad. Sci.* USA, 1988. **85**(4): 1287-1291.
61. Kaupp, U.B., Altenhofen, W., Cyclic nucleotide-gated channels of vertebrate photoreceptor cells and olfactory epithelium. *Soc. Gen. Physiol. Ser.*, 1992. **47**: 133-150.
62. Kaupp, U.B., Niidome, T., Tanabe, T., Terada, S., Bönigk, W., Stühmer, W., Cook, N.J., Kanagawa, K., Matsuo, H., Hirose, T., Miyata, T., Numa, S., Primary structure and functional expression from complementary DNA of the rod photoreceptor cyclic GMP-gated channel. *Nature*, 1989. **342**: 762-766.
63. Kaupp, U.B., Seifert, R., Cyclic nucleotide-gated ion channels. *Physiol. Rev.*, 2002. **82**(3): 769-824.
64. Kohl, S., Baumann, B., Broghammer, M., Jagle, H., Sieving, P., Kellner, U., Spegal, R., Anastasi, M., Zrenner, E., Sharpe, L.T., Wissinger, B., Mutations in the CNGB3 gene encoding the beta-subunit of the cone photoreceptor cGMP-gated channel are responsible for achromatopsia (ACHM3) linked to chromosome 8q21. *Hum. Mol. Genet.*, 2000. **9**(14): 2107-2116.
65. Komatsu, H., Mori, I., Rhee, J.S., Akaike, N., Ohshima, Y., Mutations in a cyclic nucleotide-gated channel lead to abnormal thermosensation and chemosensation in C. elegans. *Neuron*, 1996. **17**(4): 707-718.
66. Korschen, H.G., Illing, M., Seifert, R., Sesti, F., Williams, A., Gotzes, S., Colville, C., Muller, F., Dose, A., Godde, M., et al., A 240 kDa protein represents the complete beta subunit of the cyclic nucleotide-gated channel from rod photoreceptor. *Neuron*, 1995 **15**(3): 627-636.
67. Korth, M., Reiman, V., Stimulus alternation and fast retinal potentials: photopic and scotopic contributions. *Acta Ophthalmol. (Copenh).*, 1979. **57**(3):369-381.
68. Koutalos, Y., Brown, J., Karpen, J.W., Yau, K.-W., Diffusion coefficient of the cyclic GMP analog 8-(Fluoresceinyl)Thioguanosine 3`, 5` Cyclic Monophosphate in the salamander rod outer segment. *Biophys. J.*, 1995. **69**(5): 2163-2167.
69. Kramer, R.H., Molokanova, E., Modulation of cyclic-nucleotide-gated channels and regulation of vertebrate phototransduction. *J. Exp. Biol.*, 2001. **204**(Pt 17): 2921-2931.
70. Kurahashi, T., Kaneko, A., Gating proprieties of the cAMP-gated channel in the toad olfactory receptor cells. *J. Physiol.*, 1993. **466**: 287-302.

71. Kusch, J., Ionen-, cGMP- und spannungsabhängiges Schaltverhalten von CNGA1-Kanälen. Dissertation, 2003.
72. Kusch, J., Nache, V., Benndorf, K., Effects of permeating ions and cGMP on gating and conductance of rod-type cyclic nucleotide-gated (CNGA1) channels. J. Physiol., 2004. **560** (Pt 3): 605-616.
73. Leng, Q., Mercier, R.W., Yao, W., Berkowitz, G.A., Cloning and first functional characterization of a plant cyclic nucleotide-gated cation channel. *Plant-Physiol.*, 1999. **121**(3): 753-761.
74. Li, J., Lester, H.A., Single-channel kinetics of the rat olfactory cyclic nucleotide-gated channel expressed in Xenopus oocytes. *Mol. Pharmacol.*, 1999. **55**(5): 883-893.
75. Li, J., Zagotta, W.N., Lester, H.A., Cyclic nucleotide-gated channels: structural basis of ligand efficacy and allosteric modulation. *Q. Rev. Biophys.*, 1997. **30**(2): 177-193.
76. Liman, E.R., Buck, L.B., A second subunit of the olfactory cyclic nucleotide-gated channel confers high sensitivity to cAMP. *Neuron*, 1994. **13**(3): 611-621.
77. Liu, D.T., Tibbs, G.R., Siegelbaum, S.A., Subunit stoichiometry of cyclic nucleotide-gated channels and effects of subunit order on channel function. *Neuron*, 1996. **16**(5): 983-990.
78. Liu, D.T., Tibbs, G.R., Paoletti, P., Siegelbaum, S.A., Constraining ligand binding site stoichiometry suggests that a cyclic nucleotide-gated channel is composed of two functional dimers. *Neuron*, 1998. **21**: 235-248.
79. Liu, D.T., Siegelbaum, S.A., Change of pore helix conformational state upon opening of cyclic nucleotide-gated channels. *Neuron*, 2000. **28**(3): 899-909.
80. Lowe, G.H., Gold, G.H., Contribution of the ciliary cyclic nucleotide-gated conductance to olfactory transduction in the salamander. *J. Physiol*., 1993. **462**: 175-196.
81. Lowe, G., Gold, G.H., Nonlinear amplification by calcium-dependent chloride channels in olfactory receptor cells. *Nature*, 1993. **366**(6452): 283-286.
82. Ludwig, J., Margalit, T., Eismann, E., Lancet, D., Kaupp, U.B., Primary structure of cAMP-gated channel from bovine olfactory epithelium. *FEBS Letters* 1990. **270**(1-2): 24-9.
83. Ludwig, J., Owen, D., Pongs, O., Carboxy-terminal domain mediates assembly of the voltage-gated rat ether-a-go-go potassium channel. *EMBO J.*, 1997. **16**(21): 6337-6345.

84. Mazzolini, M., Punta, M., Torre, V., Movement of the C-helix during the gating of cyclic nucleotide-gated channels. *Biophys. J.*, 2002. **83**(6): 3283-3295.
85. McCormack, K., Joiner, W.J., Heinemann, S.H., A characterization of the activating structural rearrangements in voltage-dependent Shaker K+ channels. *Neuron*, 1994. **12**(2): 301-315. Erratum in: Neuron 1994 Mar;12(3):706.
86. McKay, D.B., Steitz, T.A., Structure of catabolite gene activator protein at 2.9 A resolution suggests binding to left-handed B-DNA. *Nature*, 1981. **290**(5809): 744-749.
87. Methfessel, C., Witzemann, V., Takahashi, T., Mishina, M., Numa, M., Sakmann, B., Patch clamp measurements on Xenopus laevis oocytes: currents through endogenous channels and implanted acetylcholine receptor and sodium channels. *Pflugers Arch.*, 1986. **407**(6): 577-588.
88. Middendorf, T.R., Aldrich, R.W., Baylor, D.A., Modification of cyclic nucleotide-gated ion channels by ultraviolet light. *J. Gen. Physiol.*, 2000. **116**(2): 227-252.
89. Middendorf, T.R., Aldrich, R.W., Effects of ultraviolet modification on the gating energetics of cyclic nucleotide-gated channels. *J. Gen. Physiol.*, 2000. **116**(2): 253-282.
90. Molday, R.S., Molday, L.L., Dose, A., Clark-Lewis, I., Illing, M., Cook, N.J., Eismann, E., Kaupp, U.B., The cGMP gated channel of the rod photoreceptor cell characterization and orientation of the amino terminus. *J. Biol. Chem.*, 1991. **266** (32): 21917-22.
91. Monod, J., Wyman, J., Changeux, J.P., On the nature of allosteric transitions: a plausible model. *J. Mol.Biol.*, 1965. **12**:88-118.
92. Möttig, H., Spannungs- und cGMP-abhängiges Schalten an von cyclischen Nukleotiden gesteuerten Ionenkanälen. Dissertation, 2000.
93. Möttig, H., Kusch, J., Zimmer, T., Scholle, A., Benndorf, K., Molecular regions controlling the activity of CNG channels. *J. Gen. Physiol.*, 2001. **118**(2): 183-192.
94. Nakamura, T., Gold, G.H., A cyclic nucleotide-gated conductance in olfactory receptor cilia. *Nature*, 1987. **325**(6103): 442-444.
95. Nargeot, J., Nerbonne, J.M., Engels, J., Lester, H., Time course of the increase in the myocardial slow inward current after a photochemically generated concentration jump of intracellular cAMP. *Neurobiol.*, 1983. **80**: 2395-2399.

96. Nerbonne, J.M., Richard, S., Nargeot, J., Lester, H.A., New photoactivatable cyclic nucleotides produce intracellular jumps in cyclic AMP and cyclic GMP concentrations. *Nature*, 1984. **310**(5972): 74-76.

97. Ohyama, T., Hackos, D.H., Frings, S., Hagen, V., Kaupp, U.B., Korenbrot, J.I., Fraction of the dark current carried by Ca(2+) through cGMP-gated ion channels of intact rod and cone photoreceptors. *J. Gen. Physiol.*, 2000. **116**(6): 735-754.

98. Ottschytsch, N., Raes, A., Van Hoorick, D., Snyders, D.J., Obligatory heterotetramerization of three previously uncharacterized Kv channel alpha-subunits identified in the human genome. *Proc. Natl. Acad. Sci.* USA, 2002. **99**(12): 7986-7991.

99. Penner, R., A practical guide to patch clamping. In: Single-channel recording. B Sakmann and E. Neher, *Plenum Press*, New York, 1995.

100. Picco, C., Gavazzo, P., Menini, A., Co-expression of wild-type and mutant olfactory cyclic nucleotide-gated channels: restoration of the native sensitivity to Ca(2+) and Mg(2+) blockage. *Neuroreport*, 2001. **12**(11): 2363-2367.

101. Picones, A., Korenbrot, J.I., Spontaneous ligand-independent activity of the cGMP gated ion channels in cone photoreceptors in fish. *J. Physiol.*, 1995. **485**: 699-714.

102. Pusch, M., Ludewig, U., Jentsch, T.J., Temperature dependence of fast and slow gating relaxations of ClC-0 chloride channels. *J. Gen. Physiol.*, 1997. **109**(1): 105-16.

103. Richards, M., Gordon, S.E., Cooperativity and cooperation in cyclic nucleotide-gated ion channels. *Biochemistry*, 2000. **39**(46): 14003-14011.

104. Ruiz, M.L., Brown, R.L., He, Y., Haley, T.L., Karpen, J.W., The single-channel dose-response relation is consistently steep for rod cyclic nucleotide-gated channels: implications for the interpretation of macroscopic dose-response relations. *Biochemistry*, 1999. **38**(33): 10642-10648.

105. Ruiz, M.L., Karpen, J.W., Single cyclic nucleotide-gated channels locked in different ligand-bound states. *Nature*, 1997. **389**(6649): 389-392.

106. Ruiz, M.L., Karpen, J.W., Opening mechanism of a cyclic nucleotide-gated channel based on analysis of single channels locked in each liganded state. *J. Gen. Physiol.*, 1999. **113**(6): 873-895.

107. Sautter, A., Zong, F., Hofmann, F., Biel, M., An isoform of the rod photoreceptor cyclic nucleotide-gated channel β subunit expressed in olfactory neurons. *Proc. Natl. Acad. Sci.* USA, 1998. **95**: 4696-4701.

108. Seebohm, G., Lerche, C., Busch, A.E., Bachmann, A., Dependence of I(Ks) biophysical properties on the expression system. *Pflugers Arch.*, 2001. **442**(6): 891-895.
109. Sesti, F., Nizzari, M., Torre, V., Effect of changing temperature on the ionic permeation through the cyclic GMP-gated channel from vertebrate photoreceptors. *Biophys. J.*, 1996. **70**(6): 2616-2639.
110. Sesti, F., Straforini, M., Torre, V., Gating, selectivity and blockage of single channels activated by cyclic GMP in retinal rods of the tiger salamander. *J. Physiol.*, 1994. **474**.2: 203-221.
111. Shapiro, M.S., Zagotta, W.N., Stoichiometry and arrangement of heteromeric olfactory cyclic nucleotide-gated ion channels. *Proc. Natl. Acad. Sci.* USA, 1998. **95**(24): 14546-51.
112. Shapiro, M.S., Zagotta, W.N., Structural basis for ligand selectivity of heteromeric olfactory cyclic nucleotide-gated channels. *Biophys. J.*, 2000. **78**(5): 2307-2320.
113. Stryer, L., The molecules of visual excitation. *Sci. Am.*, 1987. **257**(1): 42-50.
114. Sun, Z.P., Akabas, M.H., Goulding, E.H., Karlin, A., Siegelbaum, S.A., Exposure of residues in the cyclic nucleotide-gated channel pore: P region structure and function in gating. *Neuron*, 1996. **16**(1): 141-9.
115. Takeuchi, H., Kurahashi, T., Photolysis of caged cyclic AMP in the ciliary cytoplasm of the newt olfactory receptor cell. *J. Physiol.*, 2002. **541**(Pt 3): 825-833.
116. Tibbs, G.R., Goulding, E.H., Leypold, B., Siegelbaum, S.A., Spontaneous opening of cyclic nucleotide-gated channels supports an allosteric model of activation. *Biophys. J.*, 1996. **70**: 137.
117. Tibbs, G.R., Goulding, E.H., Siegelbaum, S.A., Allosteric activation and tuning of ligand efficacy in cyclic-nucleotide-gated channels. *Nature*, 1997. **386**(6625): 612-615.
118. Trudeau, M.C., Zagotta, W.N., Calcium/calmodulin modulation of olfactory and rod cyclic nucleotide-gated ion channels. *J. Biol. Chem.*, 2003. **278**(21): 18705-18708.
119. Varnum, M.D., Black, K.D., Zagotta, W.N., Molecular mechanism for ligand discrimination of cyclic nucleotide-gated channels. *Neuron*, 1995. **15**(3): 619-625.
120. Varnum, M.D., Zagotta, W.N., Subunit interactions in the activation of cyclic nucleotide-gated ion channels. *Biophys. J.*, 1996. **70**(6): 2667-2679.
121. Weitz, D., Ficek, N., Kremmer, E., Bauer, P.J., Kaupp, U.B., Subunit stoichiometry of the CNG channel of rod photoreceptors. *Neuron*, 2002. **36**(5): 881-889.

122. Weyand, I., Godde, M., Frings, S., Weiner, J., Muller, F., Altenhofen, W., Hatt, H., Kaupp, U.B., Cloning and functional expression of a cyclic-nucleotide-gated channel from mammalian sperm. *Nature*, 1994. **368**(6474): 859-863.
123. Wohlfart, P., Haase, W., Molday, R.S., Cook, N.J., Antibodies against synthetic peptides used to determine the topology and site of glycosylation of the cGMP-gated channel from bovine rod photoreceptors. *J. Biol. Chem.*, 1992. **267**(1): 644-648.
124. Yau, K.-W., Baylor, D.A., Cyclic GMP-activated conductance of retinal photoreceptor cells. *Annu. Rev. Neurosci.,* 1989. **12**: 289-327.
125. Yau, K.W., Nakatani, K., Light-suppressible, cyclic GMP-sensitive conductance in the plasma membrane of a truncated rod outer segment. *Nature*, 1985. **317**(6034):252-255.
126. Yellen, G., The voltage-gated potassium channels and their relatives. *Nature*, 2002. **419**(6902): 35-42.
127. Zheng, J., Trudeau, M.C., Zagotta, W.N., Rod cyclic nucleotide-gated channels have a stoichiometry of three CNGA1 subunits and one CNGB1 subunit. *Neuron*, 2002. **36**(5): 891-896.
128. Zheng, J., Zagotta, W.N., Stoichiometry and assembly of olfactory cyclic nucleotide gated channels. *Neuron*, 2004. **42**(13): 411-421.
129. Zhong, H., Molday, L.L., Molday, R.S., Yau, K.-W., The heteromeric cyclic nucleotide-gated channel adopts a 3A:1B stoichiometry. *Nature*, 2002. **420**(6912): 193-198.
130. Zong, X., Zucker, H., Hofmann, F., Biel, M., Three amino acids in the C-linker are major determinants of gating in cyclic nucleotide-gated channels. *EMBO J*., 1998. **17**(2): 353-362.
131. Zimmerman, A.L., Karpen, J.W., Baylor, D.A., Hindered diffusion in excised membrane patches from retinal rod outer segments. *Biophys. J.*, 1988. **54**(2): 351-355.
132. Zufall, F., Hatt, H., Dual activation of a sex pheromone-dependent ion channel from insect olfactory dendrites by protein kinase C activators and cyclic GMP. *Proc. Natl. Acad. Sci.* USA, 1991. **88**(19): 8520-8524.
133. Zufall, F., Hatt, H., Firestein, S., Rapid application and removal of second messengers to cyclic nucleotide-gated channels from olfactory epithelium. *Proc. Natl. Acad. Sci.* USA, 1993. **90**(20): 9335-9339.

6. Appendix

6.1. Abbreviations

BCMCMcGMP	[6,7-bis(carboxymethoxy)coumarin-4-yl]methyl ester of cGMP
BCMACMcGMP	[7-bis(carboxymethylamino)coumarin-4-yl]methyl ester of cGMP
BCMACMcAMP	[7-bis(carboxymethylamino)coumarin-4-yl]methyl ester of cAMP
cAMP	3,5-cyclic adenosine monophosphate
CaM	calmodulin
CAP	*Escherichia coli* catabolite gene activator protein
CD-Model	Coupeld-Dimer Model
cGMP	3,5-cyclic guanosine monophosphate
CN	cyclic nucleotide
CNBD	cyclic nucleotide-binding domain
CNG channels	cyclic nucleotide-gated channels
CNGA1	subunit of the CNG channels from vertebrate rod photoreceptors
CNGA2/A4/B1b	CNGA2, CNGA4, CNGB1b subunits of the CNG channels from olfactory sensory neurons
cNMP	cyclic nucleoside monophosphate
cRNA	complementary RNA
DEACMcAMP	[7-(diethylamino)coumarin-4-yl]methyl ester of cAMP
DEACMcGMP	[7-(diethylamino)coumarin-4-yl]methyl ester of cGMP
DMSO	dimethyl sulfoxide
EAG channels	ether-a-gogo voltage activated K^+ channels
EC_{50}	concentration of the cyclic nucleotide that causes half-maximal activation (μM)
H	Hill coefficient
HCN channels	cyclic nucleotide gated pacemaker channels
HEPES	4-(2-hydroxyethyl)-1-piperazineethanesulfonic acid

HERG channels	human eag-related gene family of voltage activated K^+ channels
I	current (pA)
mM	Millimolar
MWC-Model	Monod-Wyman-Changeux Model
o1r	CNGA1 chimera with CNGA2 N-terminus
OSNs	olfactory sensory neurons
P_o	open probability
PDE	phosphodiesterase
PKG, PKA	cGMP- and cAMP-dependent protein kinases
r1o	CNGA2 chimera with CNGA1 N-terminus
V	voltage (mV)
τ_o	mean open time
τ_{fast}, τ_{slow}	concentration dependent activation time constant
τ_v	voltage dependent activation time constant

6.2. Curriculum Vitae

Name:	Nache Vasilica
Maiden name:	Borta
Place and Date of birth:	Bacau/Romania, 15.02.1978
Address:	07747 Jena, Schlegelstr. 8/203
Nationality:	Rumanian
Marital status:	married
E-mail:	Nache.Vasilica@mti.uni-jena.de
Telephone:	+49-(0)3641-934348

Training and studies:

1984 - 1992	Primary School, Bacau/Romania
1992 - 1996	"Gh. Vranceanu" Secondary School, Bacau/Romania
1996	Secondary School-ending examination
1996 - 2000	Biology Faculty, "Al.I.Cuza" University, Iasi/Romania First Specialty Biochemistry, Second Specialty Biology
1999	French - Rumanian Summer School in Biochemistry, Iasi/Romania
2000	Faculty final examination, Diploma - Biochemist, Note 9.3 (on a scale 1 to 10). Thema: "Megaloblastic anemia"
2000 - 2002	Specialization courses in Microbiological Technologies, "Al.I.Cuza" University, Iasi/Romania
2001 - 2002	Practical courses in Microbiology, Albert-Ludwigs-University Freiburg im Br., Germany, with a Socrates/Erasmus scholarship; Thema: "Acetate assimilation of *Rubibrivivax gelatinosus*"
2002 - 2005	Ph.D. student at the Institute of Physiology II, Friedrich Schiller University Jena, Germany; Thema: "Gating kinetics of CNG channels studied with cyclic nucleotide-concentration jumps"

6.3. Research and publications

Articles

Hagen V, Dekowski B, **Nache V**, Schmidt R, Geissler D, Lorenz D, Eichhorst J, Keller S, Kaneko H, Benndorf K, Wiesner B.
Coumarinylmethyl Esters for Ultrafast Release of High Concentrations of Cyclic Nucleotides upon One- and Two-Photon Photolysis.
Angew Chem Int Ed Engl. 2005 Nov 4

Nache V, Schulz E, Zimmer T, Kusch J, Biskup C, Koopmann R, Hagen V, Benndorf K.
Activation of olfactory-type cyclic nucleotide-gated channels is highly cooperative.
J Physiol. 2005 Nov 15;569(Pt 1):91-102.

Kusch J, **Nache V**, Benndorf K.
Effects of permeating ions and cGMP on gating and conductance of rod-type cyclic nucleotide-gated (CNGA1) channels.
J Physiol. 2004 Nov 1;560(Pt 3): 605-16.

Nache V, Kusch J, Hgen V., Benndorf K.
Gating of cyclic nucleotide-gated (CNGA1) channels by cGMP jumps and depolarising voltage steps - submitted for publication to The Journal of Biophysics

Posters/Abstracts:

2003 Nache, V., Kusch, J., Hagen, V., Benndorf, K. Gating kinetics of CNG channels studied with cGMP concentration jumps. Pflügers Arch. 445 (Suppl.1): 103.

Nache, V., Hagen, V., Benndorf, K. Gating kinetics of CNG channels studied with cGMP concentration jumps. 1st Meeting of the Joint Research Centers, Sonderforschungsbereich 604 and Graduiertenkolleg 768, Jena, 2003

2004 Nache, V., Hagen, V., Benndorf, K. Activation of CNGA2 channels by concentration jumps using flash photolysis. Pflügers Arch. 447 (Suppl.1): 127.

Nache, V., Hagen, V., Benndorf, K. Gating kinetics of CNG channels studied with cGMP concentration jumps. Biophysical Society Congress, Baltimore, USA, January 2004.

Schulz, E., Nache, V., Koopmann, R., Benndorf, K. Beschreibung der Schaltkinetiken von CNG-Ionenkanälen durch Markov-Modelle -Tag der Forschung, Fachhochschule Schmalkalden, April 2004.

2005 Nache, V., Schulz, E., Zimmer, T., Kusch, J., Biskup, C., Koopmann, R., Hagen, V., Benndorf, K., Activation of olfactory cyclic nucleotide-gated channels (A2) is highly cooperative. Pflügers Arch. 449 (Suppl.1): 114.

6.4. Acknowledgments

I would like to acknowledge those who have helped me during my Ph.D. study, especially those who encouraged and guided me to go for the intellectual pursuit through the whole study and also the rest of my career.

First, I would like to acknowledge Prof. Klaus Benndorf (Institut für Physiologie II, Klinikum Jena) for his invaluable support, help, and guidance. Every step of progress that I made, it is because of him. His suggestions frequently provided me the motivation to make things better.

I would like to thank Prof. Stefan Heinemann (AG Molekulare und Zelluläre Biophysik, Klinikum Jena), without him, this work wouldn't be possible. Our Graduiertenkolleg meetings were valuable times were we learned many things about the way of science.

In addition, I would like to thank Dr. Reinhard Wetzker (Arbeitsgruppe Molekulare Zellbiologie, Klinikum Jena) and Prof. Stephan Frings (Dept. of Molecular Physiology, University of Heidelberg) for the readiness in offering their expertise regarding this thesis.

I am thankful to Dr. Jana Kusch for the help she provided along all this years of my study, not only for her guidance when I was a novice in electrophysiology, and for the helpful discussions but also in understanding the German life-style and the German language.

I would like to thank all the former and actual colleagues in the group of Physiology II for their collaboration and solidarity. They encouraged and helped me to overcome the difficult periods of this thesis sharing laughs and good humor.

In addition, I want to thank Birgit Tietsch, Karin Schoknecht, Sonja Rabe and Sandra Bernhardt for excellent technical assistance.

Finally, I would like to express my sincere gratefulness to my friends for invaluable moral and logistic support, to Marius for his patience and understanding and last but not least, to my parents.

Selbständigkeitserklärung

Ich erkläre, dass ich die vorliegende Arbeit selbständig und nur unter Verwendung der angegebenen Hilfsmittel und Literatur angefertigt habe.

....

Ort, Datum Vasilica Nache

Erklärung zur Bewerbung

Hiermit erkläre ich, dass ich mich mit der vorliegenden Arbeit an keiner anderen Hochschule um den akademischen Grad Doctor rerum naturalium beworben habe und dass ich weder früher noch gegenwärtig die Eröffnung eines Verfahrens zum Erwerb des o.g. akademischen Grades an einer anderen Hochschule beantragt habe.

....

Ort, Datum Vasilica Nache